Plastic baseline (t_0) measurement in the scope Flemish Integral Action Plan on Marine Litter

Plastic t_0 study 2020-2021

Author(s) in alphabetical order		
Author	**Organisation**	**E-mail**
Prof. dr. ir. Jana Asselman (JA)	UGent	jana.asselman@ugent.be
MSc. Jan Bouwens (JB)	VLIZ	jan.bouwens@vliz.be
dr. Ana Catarino (AC)	VLIZ	ana.catarino@vliz.be
ir. Lisa Devriese (LD)	VLIZ	lisa.devriese@vliz.be
dr. ir. Gert Everaert (GE)	VLIZ	gert.everaert@vliz.be
Prof. dr. Colin Janssen (CJ)	UGent	colin.janssen@ugent.be
MSc. Nithin Achutha Shettigar (NAS)	KUL	nithinachutha.shettigar@kuleuven.be
MSc. Bert Teunkens (BT)	UA	bert.teunkens@uantwerpen.be
Prof. dr. ir. Erik Toorman (ET)	KUL	erik.toorman@kuleuven.be
Prof. dr. Stefan Van Damme (SVD)	UA	stefan.vandamme@uantwerpen.be
dr. Maaike Vercauteren (MV)	UGent	maaike.vercauteren@ugent.be

Document revision history			
Version	**Date**	**Modifications**	
		Modification reason	**Modified by**
V.1	20/10/'21	Agreement on content of report	GE, JB, AC, LD, JA, NAS, ET, MV, CJ
V.2	20/12/'21	Backbone created	GE
V.3	14/02/'22	Inclusion figures	JB, MV, BT, NAS, ET
V.4	15/02/'22	Definition of results and highlights	GE, JB, AC, LD, JA, NAS, ET, MV
V.5	28/02/'22	Revision round	GE, JB, AC, LD, JA, NAS, ET, MV
V.6	02/03/'22	Alignment and lay-out	GE
V.7	07/04/'22	Fine tuning Dutch summary	ET, NAS, LD, GE

Delivery date: 03/03/22
Commissioned by: OVAM & FostPlus

Suggested reference: Everaert, G., Asselman, J., Bouwens, J., Catarino, A.I., Janssen, C.R., Shettigar, N.A., Teunkens, B., Toorman, E., Van Damme, S., Vercauteren, M., Devriese, L. Plastic baseline (t_0) measurement in the scope Flemish Integral Action Plan on Marine Litter (OVAM). Plastic t_0 study 2020-2021. Flanders Marine Institute, Ostend, Belgium. https://dx.doi.org/10.48470/26

Table of Contents

List of Figures

List of Tables

List of Abbreviations

2DH	Two dimensional horizontal
BLS	Bed-Load Sampler
CA	Cellulose-acetate
CSA	Coordination and support actions
cSBO	cluster Strategic Basic Research
DW	Dry Weight
EU	European Union
EVA	Ethylene-vinyl-acetate
FTIR	Fourier Transform Infrared Spectroscopy
JPI	Joint Programming Initiative
MDA	Marine Data Archive
PAM	Polyacrylamide
PB	Polybutadiene
PE	Polyethylene
PET	Polyethylene Terephthalate
PLUXIN	Plastic Flux for Innovation and Business Opportunities in Flanders
PP	Polypropylene
PS	Polystyrene
PTFE	Polytetrafluoroethylene (teflon)
PU	Polyurethane
QA	Quality Assurance
QC	Quality Control
RV	Research Vessel
RIB	Rigid Inflatable Boat
SS	Suspension Sampler
STEM	Science Technology Engineering Mathematics
t_0	baseline measurement

Extended Dutch summary
Uitgebreide Nederlandstalige samenvatting

Doelstelling 9 van het Vlaams Actieplan Marien Zwerfvuil (OVAM) stelt dat **voor Vlaanderen tegen 2025 de instroom van plastic afval naar het mariene milieu met 75% verminderd zal zijn**. Een objectieve manier om het behalen van deze doelstelling te evalueren is door zowel een nulmeting (t_0-waarde in 2020 en 2021) als een een evaluatiemeting (in 2024-2025) uit te voeren. Vergelijking van de plastic flux in 2025 met deze t_0- waarde is één van de belangrijke stappen om te beoordelen of de doelstelling werd gehaald. Het bepalen van de t_0-waarde, om een eerste inzicht te krijgen over de hoeveelheid plastic die naar zee stroomt, werd door de OVAM als prioritaire actie aangeduid.

Om dit te realiseren werden de krachten gebundeld met het PLUXIN consortium (cSBO project van de Blauwe Cluster, VLAIO). Voor deze unieke en omvangrijke studie werden **gedurende twee jaar 346 staalnames uitgevoerd op twintig locaties** in directe verbinding met de Noordzee! Zowel de in situ staalnames als laboratoriumanalyses gebeurden via gestandaardiseerde methodes. Alle data en protocollen werden gearchiveerd in het Marien Data Archief (MDA). In het PLUXIN project wordt een model ontwikkeld waarmee de t0-waarde voor de plastic flux vanuit Vlaanderen richting Noordzee vervolgens gekwantificeerd kan worden. Dit hydrodynamisch en sedimentologisch verspreidingsmodel moet gevoed worden met data om accurate voorspellingen te kunnen maken. Onderliggend rapport presenteert de informatie over de bemonstering, locatie-specifieke concentraties van plastic, de principes van de modellering, de berekening van de plastic t_0 flux en de vooruitzichten in de context van de opvolging van plastic in het milieu.

Om voldoende **ruimtelijke spreiding** te voorzien, werden plastics bemonsterd op twintig locaties: vier locaties in de Schelde (Zeeschelde stroomafwaarts van Temsebrug), drie locaties in de IJzer (stroomafwaarts van de Ganzepoot in Nieuwpoort), drie locaties in de haven van Oostende, zes locaties in het Vlaamse deel van het kanaal Gent-Terneuzen en in North Sea Port en vier locaties in de haven van Antwerpen. Om tegemoet te komen aan de **seizoensgebonden variatie** werden zowel getijdencyclus metingen als seizoensgebonden campagnes uitgevoerd, naast de steekproefsgewijze bemonsteringscampagnes.
De belangrijkste resultaten en bevindingen over de plastic vervuiling in deze studie zijn:

- **Plastics zijn abundant aanwezig op alle onderzochte locaties**, en de hoeveelheden variëren sterk tussen de locaties. Kleinere plastic deeltjes zijn veel abundanter dan de grotere plastic stukken.
- Hoogste microplastic concentraties in oppervlaktewater zijn gevonden in de Schelde rivier: gemiddeld 42,9 deeltjes microplastic/m^3.
- De microplastic concentraties in sediment zijn hoog, wat erop wijst dat **microplastics accumuleren in het sediment**. Gemiddelde microplastic concentraties van 2758 microplastics kg DW^{-1} in de rivier de Schelde, 4058 microplastics kg DW^{-1} in Oostende en 2825 microplastics kg DW^{-1} in Nieuwpoort werden geobserveerd.

- De hoogste macroplastic concentraties werden aangetroffen in het oppervlaktewater van de haven van Antwerpen en in het kanaal Gent-Terneuzen, gemiddeld respectievelijk 727 g macroplastic/1000 m^3 en 841 g macroplastic/1000 m^3. Het oppervlaktewater van de Schelde, Oostende en Nieuwpoort bevat kleinere hoeveelheden macroplastics.

Een volgende stap om het gedrag en transport van plastic beter te begrijpen bestaat erin om die **locatie-specifieke massa-gebaseerde plastic concentraties om te zetten in een plastic flux en stroomrichting**. Drie simulaties met het hydrodynamisch plastic verspreidingsmodel werden gebruikt om inzicht te krijgen in de beweging van plastic deeltjes in en naar het estuarium:

- Scenario 1: waarbij gebruikt gemaakt wordt van een initiële uniforme concentratie voor het volledig gebied dat men naar een quasi-evenwicht laat evolueren;
- Scenario 2: waarbij een constante flux van deeltjes toegepast wordt als puntbron op verschillende plaatsen in het estuarium;
- Scenario 3: waarbij een concentratie opgelegd wordt langs de open zeegrens waarmee inzicht wordt verkregen op wat er met plastic van mariene oorsprong gebeurt.

Op basis van deze scenario's werd vastgesteld dat een grote meerderheid van plastic in het estuarium blijft en door eb en vloed heen en weer beweegt over een gemiddelde afstand van ca. 20 km. Een zeer **kleine landinwaartse netto flux** werd berekend:

- Voor elke kg plastic die passeert in het Schelde estuarium ter hoogte van het Kanaal Gent-Terneuzen, zal 5 g plastic de Schelde monding bereiken (flux van 0,5%).
- Voor elke kg plastic die passeert in het Schelde estuarium ter hoogte van Bath, zal nog slechts 0,5 g plastic de Schelde monding bereiken (flux van 0,05%, en dus één grootte-orde midner dan in bovenstaand geval).
- Voor elke kg plastic die passeert in het Schelde estuarium ter hoogte van Bath, zal 5 g plastic terechtkomen aan de Belgisch-Nederlandse grens (flux van 0,5% landinwaarts).

Dit vernieuwend inzicht over het gedrag van plastic in de waterlopen onthult enkele zeer interessante patronen:

- **Het estuarium is als het ware een groot reservoir voor plastic.** Plastic deeltjes bewegen stroomopwaarts en stroomafwaarts in het estuarium, en deze beweging is getij afhankelijk. Bijvoorbeeld, plastic deeltjes die in het estuarium gedetecteerd worden in de zone Terneuzen bereiken de monding van het estuarium, maar worden bij de volgende vloed terug landinwaarts gevoerd. Het merendeel (> 99%) van de plastic deeltjes die voorkomen stroomopwaarts van de Nederlands-Belgische grens passeert de Scheldemonding niet, en bereikt de Noordzee niet.
- Plastic deeltjes hebben een grotere neiging om te **accumuleren in het intertidale gebied en oeverzones.** Dit suggereert dat stranding een belangrijk proces is, en misschien zelfs belangrijker dan accumulatie op de rivierbedding. Deze resultaten dienen verdere bevestiging, want de in situ metingen geven aan dat ook in het sediment plastics worden teruggevonden.

Op basis van het model beweegt het meeste plastic op en neer volgens de getijdencycli, en bezinkt vaak binnen een straal van ongeveer 20 km van zijn puntbron. Door de asymmetrische getijdencyclus verplaatsen plastic deeltjes afkomstig van het mariene milieu zich netto landwaarts. De berekende t0-flux van plastic moet gezien worden als een eerste momentopname, en **het is noodzakelijk om de evolutie van de plastic flux op te volgen op het evaluatiemoment in 2024-2025.** In tegenstelling tot de veronderstelling van de laatste jaren, waarbij gesteld wordt dat waterlopen een grote bron van plastic naar zee zijn, is nu preliminair wetenschappelijk aangetoond dat het plastic uit de waterlopen (zeker de specifieke Vlaamse context met laaglandrivieren met een kleine verhouding tussen het zoetwaterafvoervolume en het getijdevolume) veel dichter bij huis blijft. **Het plastic dat in onze waterlopen terecht komt, blijft als het ware gevangen in het stroombekken en kan mogelijks negatieve invloed hebben op het functioneren van de ecologische systemen**. Ten gevolge van de asymmetrische getijdenwerking kan een estuarium plastic uit zee verzamelen. Model-technisch is het in deze context belangrijk te vermelden dat enkele biologische en hydrodynamische processen die het gedrag van plastic beïnvloeden, zoals golfregimes, biofouling en de aggregatie van klein plastic met cohesieve sedimentaggregaten ontbreken nog in het huidig model. Integratie van deze processen kunnen in de toekomst de gesimuleerde patronen van de plastic flux nog verfijnen. In de analyse werd geopteerd voor de Scheldemonding als arbitraire grens tussen het mariene en estuariene milieu.

De ontwikkelde methodes, de verkregen resultaten en de met het hydrodynamisch model gemaakte simulaties zijn transparant en maken een eerlijke evaluatie mogelijk van de flux op het evaluatiemoment in 2024-2025. Dergelijke opvolgstudie zal belangrijk blijken om na te gaan of de netto fluxen die nu werden berekend ter hoogte van de Belgisch-Nederlandse grens in het Schelde-estuarium en ter hoogte van de Scheldemonding wijzigen ten opzichte van de referentiejaren 2020-2021. Bovendien, nu blijkt dat het plastic zich opstapelt in gebieden die dichterbij gelegen zijn dan verwacht is verdere opvolging een prioriteit. De verwachting is dat, zolang er puntbronnen aanwezig zijn in de stroombekkens, de concentraties aan plastic gradueel zullen verhogen tot op niveaus die mogelijks ecologische effecten en effecten op de menselijke gezondheid kunnen veroorzaken. Om de risico's van plastic vervuiling voor mens en milieu te kunnen inschatten is verder wetenschappelijk nodig. Opvolging van de graad van vervuiling in het estuarium, dat potentieel kan fungeren als plastic reservoirs, is hierbij noodzakelijk.

Chapter 1
Introduction and background

On 12 May 2021, the European Commission adopted the EU Action Plan: "Towards a Zero Pollution for Air, Water and Soil" - a key deliverable of the European Green Deal. The zero pollution vision for 2050 is for air, water and soil pollution to be reduced to levels no longer considered harmful to health and natural ecosystems, that respect the boundaries with which our planet can cope, thereby creating a toxic-free environment. This is translated into key 2030 targets to speed up reducing pollution at source. These targets include, among five others, one for plastic litter and microplastics stating: improving water quality by reducing waste, plastic litter at sea (by 50%) and microplastics released into the environment (by 30%). The SOS-ZEROPOL2030 (HorizonEurope CSA) project, with VLIZ as Belgian partner, aims at developing a holistic zero pollution framework that will guide the EU towards achieving zero pollution in European seas by 2030.

Fig. 1 Towards a Zero Pollution for Air, Water and Soil is a key deliverable of the European Green Deal

At the Flemisch level, the objective no. 9 of the Flemish Action Plan for Marine Litter states that "by 2025, the influx of litter from Flanders into the marine environment will have been reduced by 75%". This requires a baseline measurement, a t_0 value, which has been designated by OVAM as a priority action. In order to quantify the plastic baseline measurement in the framework of the Flemish Integral Action Plan Marine Litter, OVAM, and FostPlus reached out to the PLUXIN-consortium in 2020 and 2021.

In 2020, a key task of the project was to define suitable sampling methodologies and laboratory analytical techniques for quantifying the micro- and macroplastic litter concentrations at the water surface, in the water column, and in and on the sediment. This has resulted in effective and accurate protocols, ready to be implemented when the outcomes of the Flemish Action Plan for Marine Litter are to be evaluated in 2024 and 2025. Still in 2020, a second key task was taking initial micro- and macroplastics samples at different locations (the port of Ostend, the river Yser in Nieuwpoort, and in the river Scheldt), and processing these samples in a standardised way. As the overall aim was to quantify the riverine plastic flux toward the North Sea, all sampling locations had a direct link with and were in the vicinity of the North Sea. The initial sampling campaigns have resulted in first insights about the plastic concentrations, polymer types and sizes observed at the selected sampling locations. For detailed results, the project consortium would like to refer to the 2020 report of the plastic baseline (t_0) measurement (https://www.vliz.be/en/imis?module=ref&refid=338341).

In 2021, relying on the insights of the 2020 campaigns, the sampling area was broadened compared to the previous year. Indeed, in the 2021 report also plastic concentrations, polymer compositions, and size frequency distributions are being integrated for the Ghent-Terneuzen canal (only macroplastic), and the port of Antwerp (only macroplastic). As the tidal regime was being considered an important factor for the plastic flux, efforts for tidal cycle measurements were increased. All data of the sampling campaigns of June 2020 and to July 2021, 346 samples in total, were integrated in a hydrodynamic model. Finally, the plastic flux towards the marine environment was quantified.

In this report for the year 2021, the consortium presents the:

- sampling locations and timing;
- quantified concentrations of plastics at the water surface, and in/on the sediment;
- principles of the hydrodynamic model;
- plastic flux towards the marine environment;
- highlights and perspectives.

Chapter 2
Plastic sampling, identification, and quantification

1. Content

In this section, we list and describe:

- the sampling strategy;
- the sampling locations;
- the sampling frequency.

Detailed information about the sampling methodology and laboratory analytics is shared in the 2020 report to ensure that the evaluation measurements, most likely organized in 2024 and 2025, can make use of the same sampling locations, sampling protocols, and laboratory analysis. By doing so, a fair and honest comparison can be made with the 2020 and 2021 data, and the resulting plastic flux.

2. Sampling strategy

The aim of this project was to collect data on plastic concentrations in selected locations to establish baseline information of the plastic flux from Flemish rivers and canals to the coastal and marine environment. Due to the lack of quality-controlled existing data, in situ data needed to be collected at predefined locations. Hence, a sampling plan with specific locations, timing, and infrastructure needed was drafted, and shiptime requested. It was agreed that the focus should not only be on meso-, macro-, and mega-sized plastic debris (> 5 mm), but that also information on microplastic pollution (100 µm - 5 mm) needed to be integrated in order to provide a full picture of the current plastic pollution situation. As the fate of plastic in the aquatic environment depends on the polymer type, we considered the acquisition of polymer-specific information via FTIR analysis. Since the behaviour and flux of the plastic depends on the polymer type, which impacts density and bouyancy, we acquired samples at the water surface, water column, and on sediment surface and in the sediment (up to 15-20 cm depth). We considered potential seasonal variations in plastic accumulation as well as the impact of tidal cycles on the plastic flux and distribution. The sampling protocols developed in 2020 align with the consortiums' expertise from other nationally funded (e.g. PLUXIN) and European projects (e.g. JPI Andromeda, JPI Baseman, JPI Weather-Mic).

3. Sampling locations

The consortium aims to obtain polymer-specific information on the flux of microplastics (100 µm – 5 mm) and macroplastics (> 5 mm) from the river Scheldt (Zeeschelde), the river Yser (Nieuwpoort), the Ghent-Terneuzen canal, port of Antwerp and the port of Ostend towards the North Sea (Belgium; Figures 2-6). The sampling campaigns on the river Scheldt took place on board of the RV Simon Stevin and the RV Veremans, while the sampling campaigns in the river Yser and the port of Ostend took place on board of the RIB Zeekat (Table 1). For taking samples in the Ghent-Terneuzen canal, the vessel HT-1 was used. Details of the sampling locations are available here - https://bit.ly/3CamYfK.

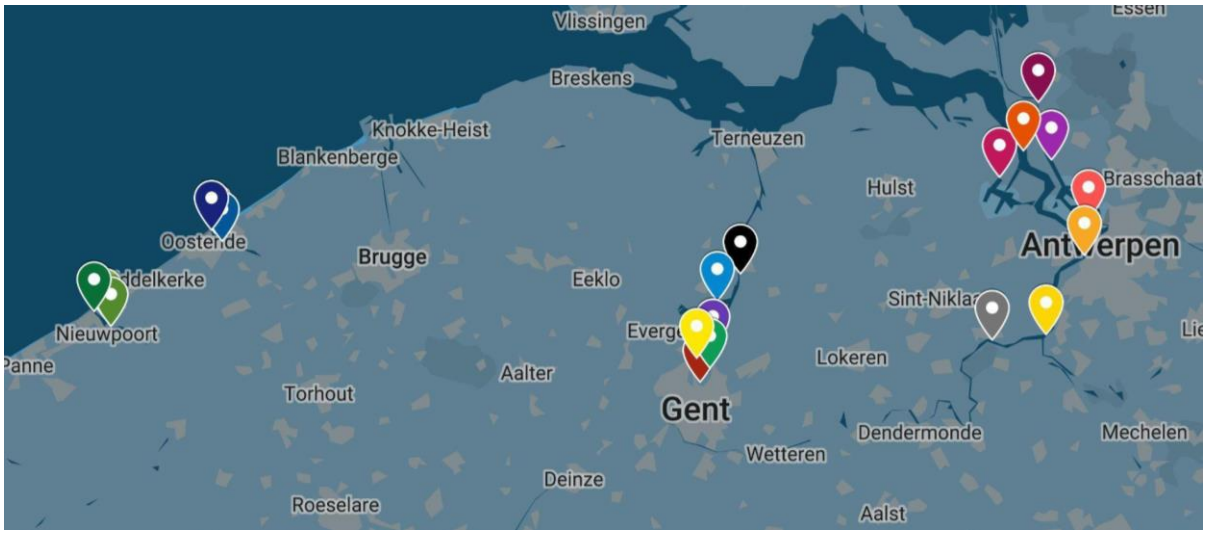

Fig. 2 Sampling locations in 2020-2021 for the plastic t_0 measurement in Nieuwpoort (details in Fig. 3), in Ostend (details in Fig. 4), Ghent-Ternezuen canal (details in Fig. 5), in the river Scheldt (details in Fig. 6), and port of Antwerp (details in Fig. 6).

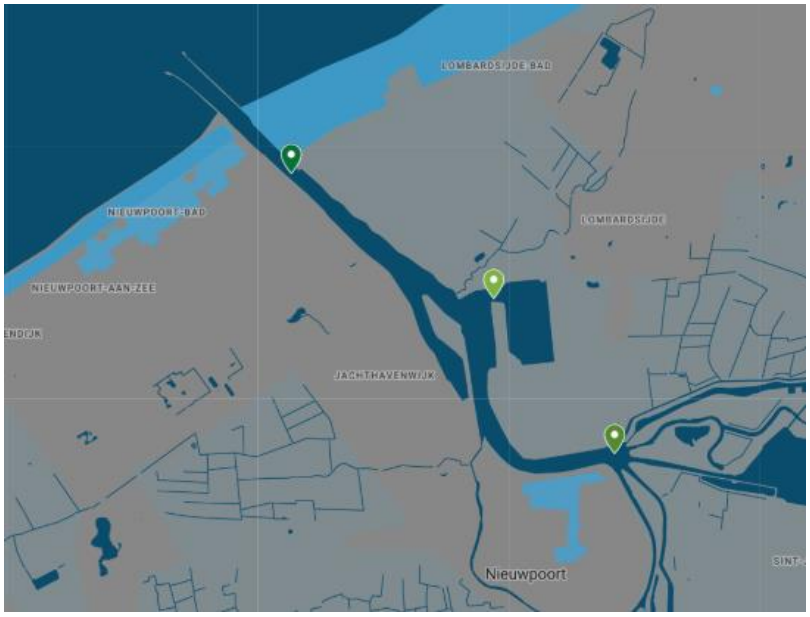

Fig. 3 Detailed sampling locations in the river Yser in Nieuwpoort along an inland-coastal gradient (with sampling locations Ganzepoot, Portus Novus, Havenmond).

Fig. 4 Detailed sampling locations in the port of Ostend along an inland-coastal gradient (with sampling stations Ryco, Tijdok, Havenmond)

Fig. 5 Detailed sampling locations in the Ghent-Terneuzen canal (with sampling stations Grootdok, Kluizendok, Mercatordok, Ringvaart, Sifferdok, Zelzate Insteekdok)

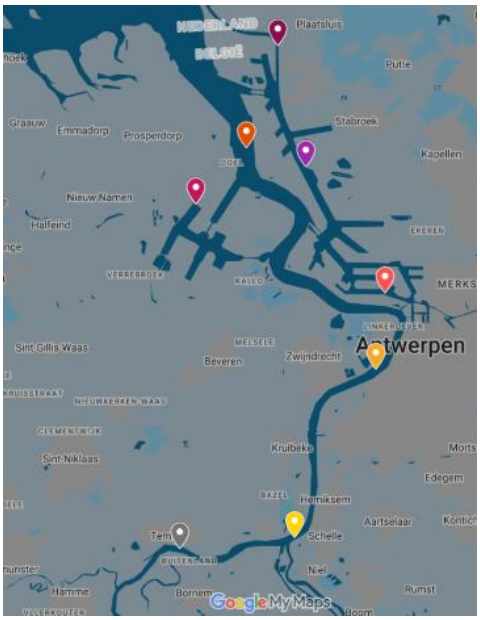

Fig. 6 Detailed sampling locations in the river Scheldt and port of Antwerp (with sampling stations Antwerpen (Scheldt), Doel (Scheldt), Temse (Scheldt), Wintam (Scheldt), Doeldok (PoA), Kanaaldok (PoA), Schelde-Rijn kanaal (PoA), Vijfde havendok (PoA)).

4. Sampling frequency

The sampling strategy included different types of campaigns to account for the spatial and temporal variation of plastics concentrations in various environmental compartments:

- Seasonal multi-day sampling campaigns are carried out on the river Scheldt, where VLIZ and UAntwerp simultaneously sample micro- and macroplastics in the water column and sediment at three different locations on the Zeeschelde (near Doel, Antwerp, Wintam, and Temse).
- Tidal cycle measurements are performed in the port of Ostend, the river Yser in Nieuwpoort and on the river Scheldt downstream from Wintam, near Antwerp, to account for the effect of the tides on the concentrations of micro- and macroplastics sampled.
- Bimonthly spot-sampling campaigns are performed in the port of Ostend and the river Yser in Nieuwpoort at three different locations within the port, spread along the inland-sea gradient. Yearly spotsampling campaigns are performed in the port of Antwerp and North Sea Port (canal Ghent-Terneuzen) at, respectively, four and six different locations within the port.

Table 1 Overview of the different types of plastic sampling campaigns

Type of campaign	Ship	Frequency	Location
Seasonal (multi-day campaign)	RV Simon Stevin/ RV Veremans	Seasonal (four times per year)	River Scheldt
Tidal cycle measurement (13h campaign)	RV Simon Stevin/ RV Veremans	Seasonal (four times per year)	River Scheldt
	RIB Zeekat	Yearly	Port of Ostend
	RIB Zeekat	Yearly	River Yser/ Nieuwpoort
Spot-sampling (day campaigns)	RIB Zeekat	Bimonthly	Port of Ostend
	RIB Zeekat	Bimonthly	River Yser/ Nieuwpoort
	RIB Zeekat	Yearly	Port of Antwerp
	HT-1	Yearly	North Sea Port (canal Ghent-Terneuzen)

For the 2021 report, plastic sampling campaigns took place between July 2020 and July 2021 at the selected sampling locations. In total, we collected 346 samples in 31 sampling days distributed over 26 sampling campaigns. We performed four seasonal campaigns, eighteen spot sampling campaigns, and four tidal cycle campaigns (Table 2 & Annex A).

The seasonal campaigns are three-day campaigns including spot sampling and tidal cycle measurements on the Scheldt near Wintam, Antwerpen and Doel. These were performed on the 14-16 October 2020, 8-10 December 2020, 26-28 January 2021, 20-22 April 2021.

The bimonthly spot sampling campaigns and tidal cycle measurement campaigns in port of Ostend, port of Nieuwpoort (Yser), Temse (river Scheldt), port of Antwerp and North Sea Port (canal Ghent-Terneuzen) were organized as separate day campaigns. These sampling campaigns were performed on 9-10 July 2020, 22-24 September 2020, 7 October 2020, 17-19 November 2020, 3 February 2021, 15 February 2021, 12 March 2021, 31 March 2021, 27-28 April 2021, 17-18 May 2021, 15-16 June 2021 and 28-30 June 2021. A full overview of all samples taken, is provided in Annex A about the cruise planning.

Table 2 Number of samples acquired according to location, compartment, and sampling technique

Type	Sampling stations	Sampling methodology					Total
		Bed-load sampler	Suspension sampler	Bongonet	Mantanet	Van Veen grab	
Sediment	River Scheldt (Antwerpen)	--	--	--	--	5	5
	River Scheldt (Doel)	--	--	--	--	5	5
	River Scheldt (Wintam)	--	--	--	--	2	2
	River Scheldt (Temse)	--	--	--	--	1	1
	Port of Ostend (A, B, C)	--	--	--	--	18	18
	Port of Nieuwpoort (river Yser) (A, B, C)	--	--	--	--	20	20
	Port of Antwerp	--	--	--	--	4	4
	North Sea Port	--	--	--	--	6	6
Water	River Scheldt (Antwerpen)	7	15	14	28	--	64
	River Scheldt (Doel)	4	8	3	8	--	23
	River Scheldt (Wintam)	6	12	3	15	--	36
	River Scheldt (Temse)	--	--	--	2	--	2
	Port of Ostend	--	--	6	64	--	70

	(A, B, C)						
	Port of Nieuwpoort (river Yser) (A, B, C)	--	--	2	64	--	66
	Port of Antwerp	--	--	4	8	--	12
	North Sea Port	--	--	6	6	--	12
Grand Total		17	35	38	195	61	346

Chapter 3
Plastic concentrations, polymer composition, and size frequency distribution

1. Samples taken, processed and reported

For an overview of the samples collected between July 2020 and June 2021, we refer to Table 2 and Annex A. Microplastic concentrations were reported in the number of particles (100 µm-5mm) detected per volumetric unit (i.e. # particles/m³). Macroplastic concentrations were reported in mass of plastic detected per volumetric unit (i.e. g macroplastics/1000 m³). To enable integration in the model (see Chapter 4), the microplastic concentrations were changed to mass-based units based on the size dimensions, shape and polymer type of the particle under consideration.

2. Plastic concentrations

Based on samples taken between July 2020 and June 2021 (Table 2), we calculated location-specific average micro- and macroplastic concentrations. The results of each individual sample are available in a dedicated folder in the Marine Data Archive. In the microplastics analyzes, no data from the tidal campaigns was included, more information on the tidal fluctuations of microplastic concentrations can be found at the end of this chapter. One extreme concentration of 349.2 microplastics/m³ was observed in the surface water at Wintam (River Scheldt); this observation was removed for analysis.

River Scheldt

All water samples collected along the river Scheldt contained microplastics. In the river stretch between Temse and Doel, on average a microplastic concentration of 42.9 ± 70.6 microplastics/m³ were observed (Table 3a). The maximum concentration of 273.7 microplastics/m³ was observed in Wintam. Generally, the spatial and temporal variation in terms of microplastic pollution in the surface waters of the river Scheldt was quite large. No clear concentration gradient can be observed from more upstream towards more downstream locations. The location upstream (Temse) showed very low microplastic concentrations but only one sample was collected, therefore, making conclusions is not recommended.

In the sediment along the river Scheldt, on average 2757.7 ± 3559.7 particles kg DW^{-1} were observed (Table 3a). All sediment samples that were analyzed did contain microplastics. For these measurements, a spatial concentration gradient was present. The sampling location of Wintam was observed to be more polluted than the downstream sampling location Antwerp and Doel (i.e. 4301.6 ± 4926.8 particles kg DW^{-1} versus 1599.1 ± 899.8 particles kg DW^{-1} and 1214.7 ± 849.9 particles kg DW^{-1}, respectively). Important to mention is that the high number of microplastics in Wintam is mainly attributable to one sample with elevated microplastic concentrations (13 816.1 particles kg DW^{-1}).

All samples taken with the Suspension Sampler and Bed-load Sampler contained macroplastics. On average in the surface water of the river Scheldt 11.04 ± 24.65 g macroplastic per 1000 m^3 was observed. The minimum plastic load was detected in the most downstream sampling in location Doel (i.e. 0.009 g/1000m³). The highest macroplastic concentrations are to be expected at the water surface, i.e. the mass of macroplastic at the water surface is a 10-fold to a 40-fold higher than the mass of plastic observed in the water column (Table 3b). The average mass of macroplastic collected on the river bed between Wintam and Doel is 318.00 ± 1290.28 g macroplastic/1000 m³ (Table 3b). The maximum concentration of macroplastic of 5324.9 g/1000 m³ water was observed at sampling location 'Antwerpen'. The lowest

concentration of macroplastics are observed in the most downstream location (Doel) (Table 3b). The mass of macroplastic observed in 2021 at the water surface and in the water column is in line with the concentrations reported for the year 2020. At the riverbed however, the concentration of the year 2020 (i.e. 2.9 ± 5.2 g macroplastic/1000 m^3) is remarkably lower than the concentration observed in 2021 (Table 3b).

Table 3a Microplastic concentrations in the river Scheldt with the number of samples between brackets. The sediment measurements represent an average value over 3 replicate measurements.

Microplastic	Temse	Wintam	Antwerpen Schelde	Antwerpen Port	Doel	Scheldt average
Water surface (# part./m^3	6.9 (n=1)	87.3 ± 101.8 (n=10)	20.6 ± 22.3 (n=8)	3.1 ± 3.4 (n=4)	25.8 ± 12.6 (n=4)	42.9 ± 70.6
Sediment # part. kg DW^{-1})	/	4301.6 ± 4926.8 (n=2)	1599.1 ± 899.8 (n=2)	/	1214.7 ± 849.9 (n=1)	2757.7 ± 3559.7

Table 3b Average macroplastic concentrations, collected with the Suspension Sampler, Bed-Load Sampler, Mantanet and Bongonet in the river Scheldt (with the number of samples between brackets).

Macroplastics (g/1000 m^3)	Wintam	Antwerpen	Doel	Scheldt (Average
Water Surface Depth: 0m - 0.5m	16.51 ± 28.94 (n=13)	17.36 ± 74.47 (n=37)	1.05 ± 1.91 (n=11)	14.24 ± 59.45 (n=61)
Water Column Depth: 1.80m - 2.30m	0,73 ± 0,33 (n=3)	0.16 ± 0.08 (n=4)	0.08 ± 0.05 (n=2)	0.33 ± 0.34 (n=9)
Water Column Depth: 3.80m - 4.30m	0.65 ± 0.21 (n=3)	0.19 ± 0.09 (n=4)	0.04 ± 0.01 (n=2)	0.31 ± 0.29 (n=9)
Bed-Load Depth: Riverbed	1.52 ± 0.21 (n=6)	769.55 ± 2000.76 (n=7)	2.53 ± 3.50 (n=4)	318.00 ± 1290.28 (n=17)

Port of Ostend

In the port of Ostend, microplastics plastics were detected in all water samples (Table 4a). The average microplastics concentration in surface water is 8.6 ± 13.2 microplastics/m³ (Table 4a), with a minimum concentration of 0.04 microplastics/m³ and a maximum of 47.1 microplastics/m³. The sampling location in the Tijdok had the highest microplastic concentrations. There is no gradual decrease of concentrations from the inner port towards the North Sea, based on the microplastic data. All sediment samples from the port of Ostend did contain microplastics. The average concentration of microplastics observed in the samples was 4058.1 ± 6590.4 particles kg DW^{-1} (Table 4a).

The microplastic concentrations observed in the port of Ostend for this reporting year are higher than for the year 2020. In 2020, we observed on average 1.7 ± 2.2 microplastics/m³ in the water surface. Indeed, at the three sampling location, the 2021 microplastic concentrations (Table 4a) are 4-fold to 20-fold higher than the concentrations reported in 2020. The microplastic sediment concentrations in the Tijdok remained equal between 2020 (= 4104 ± 3090 particles kg DW^{-1}) and 2021(= 4058.1 ± 6590.4 particles kg DW^{-1}).

The average macroplastic concentration in the surface water of the port of Ostend was 8.8 ± 35.2 microplastics/m³ (Table 4b). The highest concentrations were detected at the harbour mouth and the lowest concentrations in the inner harbor at sampling location 'RYCO'. No conclusions about a potential spatial gradient can be taken, because last year, the apparent spatial gradient was in the other direction. It is very likely that the tidal cycle plays a much more important role than the vicinity of the coastline, especially in this port where the estuarium only goes landinwards for a few kilometers.

Table 4a Microplastic concentrations in the port of Ostend with the number of samples between brackets. The sediment measurements represent an average value over 3 replicate measurements per sample.

Microplastic	Location A Harbour mouth	Location B Tijdok	Location C RYCO	Ostend average
Water surface (# part./m³)	2.7 ± 1.6 (n=5)	11.1 ± 15.9 (n=19)	5.6 ± 5.7 (n=6)	8.6 ± 13.2
Sediment (# part. kg DW^{-1})	/	4058.1 ± 6590.4 (n=4)	/	4058.1 ± 6590.4

Table 4b Macroplastic concentrations in the port of Ostend with the number of samples between brackets. The average macroplastic concentration in the water surface includes data from six bongonet samples, collected over a trajectory at the Harbor mouth, in the Tijdok and close to RYCO.

Macroplastic	Unit	Location A Harbour mouth	Location B Tijdok	Location C RYCO	Ostend average
Water surface	g/1000 m³	39± 87.4 (n=6)	3.8 ± 7 (n=20)	3.7 ± 5.8 (n=6)	8.8 ± 35.2 (n=38)

River Yser/Nieuwpoort

In the river Yser, downstream from the locks and spillways of the Ganzepoot, microplastics were detected in the surface water with an average concentration of 6.8 ± 7.5 microplastics/m³ (Table 5a). Two of the samples collected in the surface water of the river Yser did not contain microplastics in the 100 µm to 5 mm range. The maximum observed microplastic concentration was 28.9 microplastics/m³, and was collected near Portus Novus. At the harbor mouth, an average concentration of 2.8 microplastics/m³ was detected. A concentration gradient can be distinguished with increasing concentrations when moving from the North Sea towards the inner port (Table 5a). All sediment samples from the port of Nieuwpoort did contain microplastics. The average concentration of microplastics observed in the samples was 2824.8 ± 5660.5 particles kg DW^{-1}, based on four samples (Table 5a).

The number of microplastics detected in 2021 (i.e. 6.8 ± 7.5 microplastics/m³) confirms the concentrations mentioned in the report of 2020 (i.e. 5.9 ± 7.9 microplastics/m³). The spatial gradient observed in 2021 is opposite to the one observed in 2020. This indicates that results of individual spot samples that are not integrated in a hydrodynamic model may be not be extrapolated in order to infer estuarine wide conclusions about the plastic flux. Indeed, integration of the data in a hydrodynamic model that considers tidal regimes is crucial to make relevant conclusions about the plastic flux and the direction of this flux. The microplastic sediment concentrations reported here are a factor three higher than in the year 2020 (954 ± 338 microplastics/m³), but also the variability of the average concentration was a lot higher (i.e. 5660.5 microplastics/m³ in 2021 versus 338 microplastics/m³ in 2020).

The average mass-based concentration of macroplastics at the water surface in the river Yser downstream of the Ganzepoot was 0.6 ± 2.4 g/1000 m³ (Table 5b). The macroplastic concentrations was highest in the harbor mouth of Nieuwpoort (i.e. 2.4 ± 5.4 g/1000 m³). The reported concentrations in 2021 align with those of 2020.

Table 5a Microplastic concentrations in the river Yser close to the port of Nieuwpoort with the number of samples between brackets. The sediment measurements represent an average value over 3 replicate measurements per sample.

Microplastic	Location A	Location B	Location C	Nieuwpoort average
Water surface (# part./m^3	2.8 ± 2.9 (n=5)	7.3 ± 7.0 (n=19)	9.0 ± 11.8 (n=5)	6.8 ± 7.5
Sediment (# part. kg DW^{-1})	/	2824.8 ± 5660.5 (n=4)	/	2824.8 ± 5660.5

Table 5b Macroplastic concentrations in the port of Nieuwpoort with the number of samples between brackets. The average macroplastic concentration in the water surface includes data from 2 bongonet samples, collected over a trajectory at the Harbor mouth, Portus Novus and close to Ganzepoot.

Macroplastic	Unit	Location A Harbor mouth	Location B Portus Novus	Location C Ganzepoot	Nieuwpoort average
Water surface	g/1000 m^3	2.4 ± 5.4 (n=6)	0.3 ± 1.1 (n=20)	0.1 ± 0.2 (n=6)	0.6 ± 2.4 (n=34)

Port of Antwerp

Compared to the 2020 report, macroplastic concentrations observed via spot sampling campaigns at four locations in the port of Antwerp are newly reported. On average, we detected macroplastic concentrations at the water surface of 727 ± 2056 g/1000 m³. However, large spatial differences are were found. Of the four selection sampling locations, the sampling location 'Vijfde Havendok' had the highest number of plastic items (i.e. 2908 ± 4112 g/1000 m³ (Table 6). The second highest macroplastic concentration was observed along the transect in the Doeldok, but is about four orders of magnitude lower than the sampling location with the highest number of items in the port of Antwerp. Two other sampling locations, at the Schelde-Rhine kanaal, and in the Kanaaldok, relatively low concentrations of macroplastics were observed compared to other sampling locations in the port of Antwerp (Table 6). The results for microplastic will be integrated in the PLUXIN hydrodynamic plastic model.

Table 6 Macroplastic concentrations in the port of Antwerp with the number of samples between brackets.

Macroplastic	Unit	Schelde Rijn kanaal	Kanaaldok	Vijfde Havendok	Doeldok	Port of Antwerp average
Water surface	g/1000 m³	0.02 ± 0.03 (n=2)	0.05 ± 0.07 (n=2)	2908 ± 4112 (n=2)	0.2 ± 0.3 (n=2)	727 ± 2056 (n=8)

Ghent-Terneuzen canal/ North Sea Port

In 2021, the Flemish part of the Ghent-Terneuzen canal and North Sea Port has been sampled for macroplastics at six sampling locations. The average concentration of macroplastic detected in North Sea Port was 841 ± 2440 g/1000 m³ (Table 7). Large spatial differences were observed. For example, in the Insteekdok in Zelzate no macroplastic have been retrieved during the transect, while large masses of plastics were detected close to the connection with the Ringvaart (824 ± 1166 g/1000 m³) and in the Sifferdok (4221 ± 5969 g/1000 m³). The results for microplastic will be integrated in the PLUXIN hydrodynamic plastic model.

Table 7 Macroplastic concentrations in North Sea Port with the number of samples between brackets.

Macro-plastic	Unit	Groot-dok	Ring-vaart	Siffer-dok	Mercator-dok	Insteek-dok (Zelzate)	Kluizen-dok	North Sea Port average
Water surface	g per 1000 m3	0.003 ± 0.004 (n=2)	824 ± 1166 (n=2)	4221 ± 5969 (n=2)	0.001 ± 0.001 (n=2)	0 ± 0 (n=2)	0.0002 ± 0.0003 (n=2)	841 ± 2440 (n=12)

3. Polymer composition microplastic in the water phase

Besides quantifying the plastic concentrations, we identified the polyer type of each of the plastic items that was observed. Below, we compiled the information about the polymer composition in the water phase at each of the sampling sites. Detailed information about the polymer type of each individual particle is available in the data achieved in the MDA of VLIZ. Overall, for microplastics at the water surface, polypropylene (PP) and polystyrene (PS) are the most prevalent in the surface water with observed fractions of 47 % and 29 %, respectively. In the sediment, PS (40%), PET (21%) and PAM (26%) are most prevalent.

PAM is a non-trivial polymer that was not on the anticipated list of polymers to be detected in the study area. PAM is often used in agriculture, contact lenses and thickener for paints. The FTIR-spectrum of PAM is quite difficult to differentiate from the spectrum of water due to a broad peak between 3500 cm^{-1} and 2500 cm^{-1} (Fig. 10). The signal of water has a similar peak in that wavelength region. As such, it may be possible that some plastic particles (e.g. being of PP, PS or PP nature) that were still wet may have been misidentified as being PAM. This broad peak, either from water or PAM, is quite prominent and can cause mis-identification of particles. Therefore, the results on PAM should be interpreted with caution, and it requires further investigation whether PAM is indeed a polymer present in the samples. The fact that there is no consistent fraction of the plastic items errornously be identified as PAM, is an argument that the PAM identifications are correct. Also, the river basin Yser mainly is situated in agricultural field, whereas in the Scheldt estuary there is a mix of land use.

River Scheldt

In the river Scheldt, the two most prevalent polymer types in the water surface are PS (47 %) and PP (41 %). In the specific locations along the river, composition slightly shifts with PP being more prevalent at sampling location 'Temse', at sampling location 'the port of Antwerp' and Doel and PS being more prevalent in Wintam and Antwerp (Fig. 7). PE was present in all locations except for Temse, PET was present in all locations albeit in lower frequencies (2-9%; Fig. 7). These results align with the results of the 2020 report.

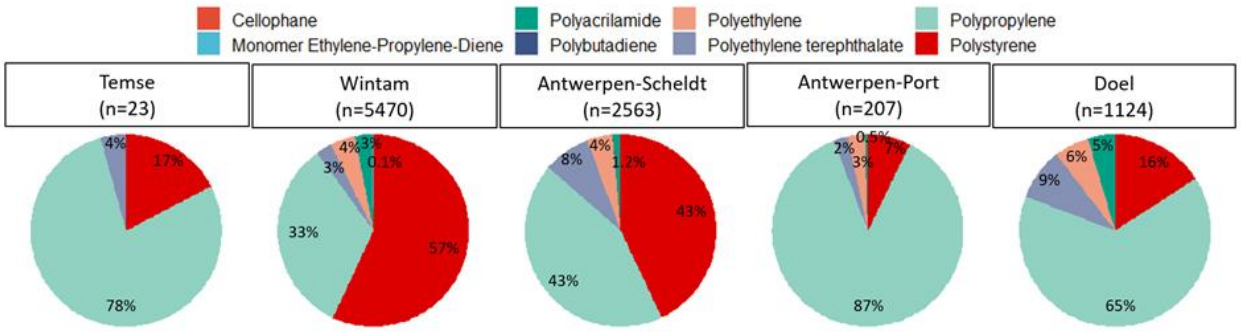

Fig. 7 Polymer composition of the microplastics detected in the water at different sampling locations along in the river Scheldt. The number of particles (n) per location is indicated between brackets.

Port of Oostende

In the port of Ostend, 62 % of the plastic observed were PP, 20 % were PS. Other polymer types like PAM, PE and PET were also present but in lower amounts. At sampling location A, in the harbor mouth and closest to the North Sea, PP was predominant in the sample with prevalence of 67%, followed by PS (13%), and PAM (8 %, Fig. 8). In the region of the passenger ferry at the eastern bank (Location B, Tijdok), 56 % of the plastics observed were PP, 25% were PS. PAM was the third prominent polymer type (7%). PET and PE were also observed in lower amounts, 5 % and 6 %, respectively. In location C, more land inwards close to RYCO, PP was the most prominent comprising 77 % of the particles in the sample. In 2020, the relative number of particles for which the polymer type was identified was limited, but the spectrum of polymers present was as broad as observed in 2021. Overall, the water mass in the port of Ostend can be considered well mixed.

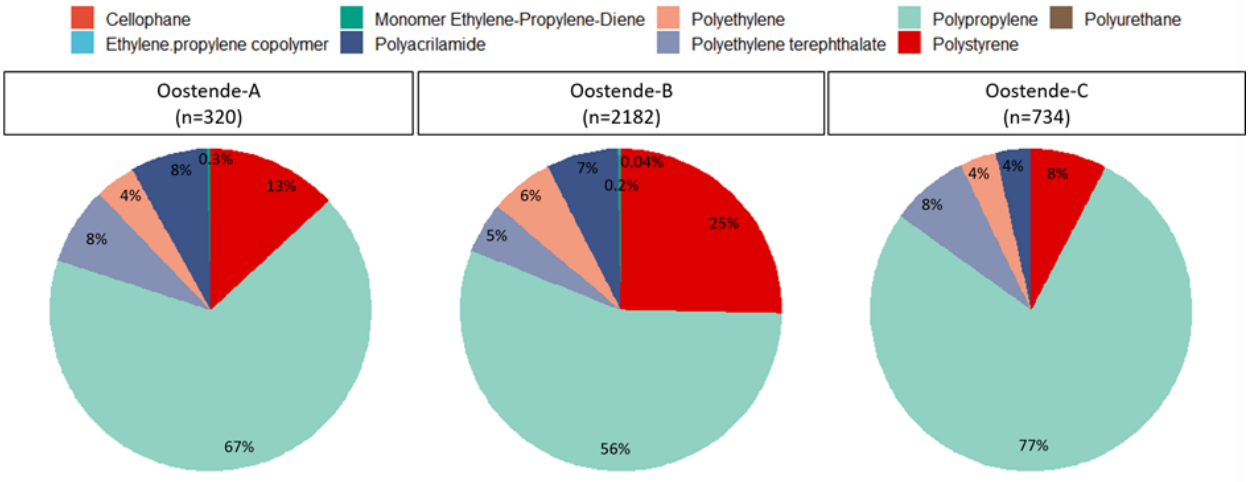

Fig. 8 Polymer composition of the microplastics detected in the water at different sampling locations in the port of Ostend; location A = Harbour mouth, location B = Tijdok, location C = RYCO (Table 9). The number of particles (n) per location is indicated between brackets.

River Yser in Nieuwpoort

In the river Yser, close to the port of Nieuwpoort, PAM was most prominently present (34%), followed by PP (30 %). Closest to the North Sea in the harbour mouth (Location A), PP (42 %) and PAM (36 %) were most prominent, followed by PS (9%), PET(6%) and PE (6%, Fig. 9). In the neighborhood of the marinas, location B, PAM was most often detected (30 %) followed by PP (27%). More land inwards (Location C), 51 % of the microplastics observed were made of PAM, 42 % of PP. In line with the results of 2020, PAM and PP seem to be quite prevalent in river Yser downstream from the Ganzepoot.

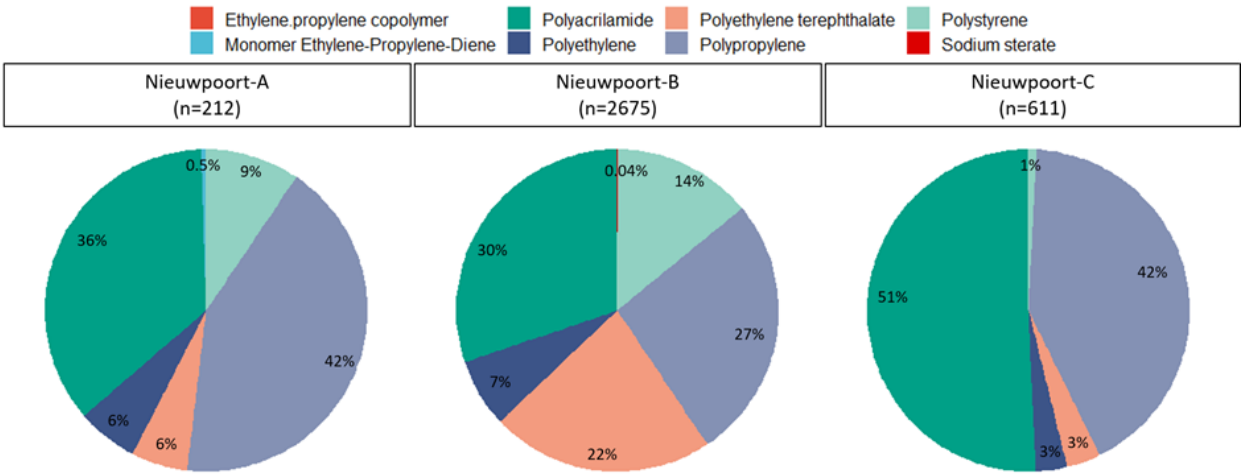

Fig. 9 Polymer composition of the microplastics detected in the water at different sampling locations along in the river Yser, close to the port of Nieuwpoort; location A = Harbour mouth, location B = Portus Novus, location C = Ganzepoot (Table 9). The number of particles (n) per location is indicated between brackets.

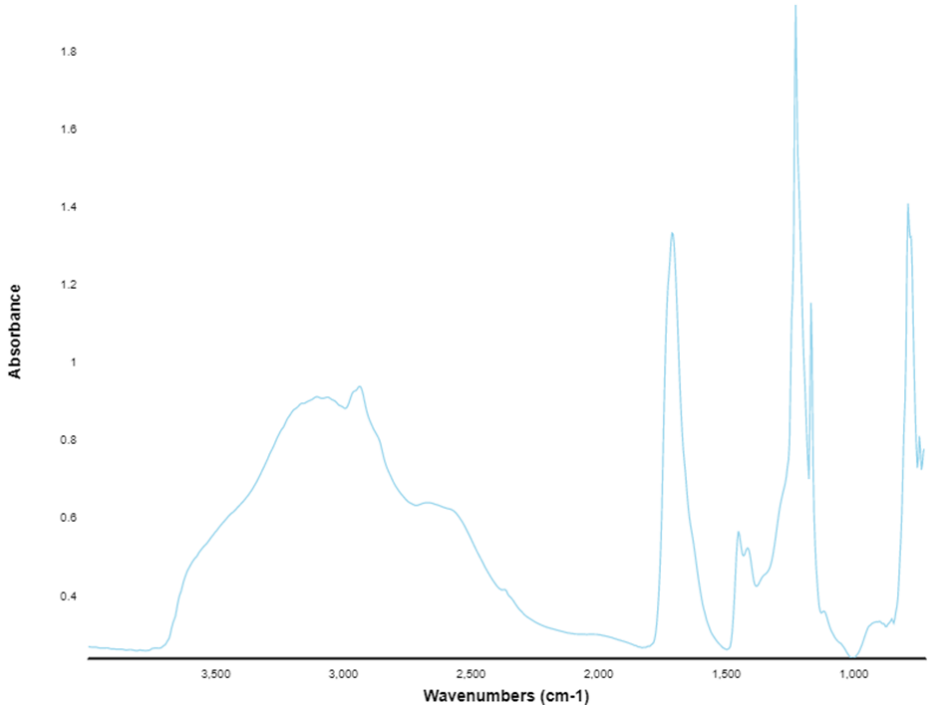

Fig. 10 FTIR spectrum for polyacrylamide (PAM) on a PTFE filter.

4. Polymer composition macroplastic in the water phase

The polymer composition of the macroplastic corroborates with the polymer composition of the microplastic (Table 8). PP, PE, and PS together were responsible for >90% of the polymer types observed. In some rare occasions EVA, CA, PU, PB have been identified. Compared to microplastics, no PAM has been identified as being part of the macroplastic (Table 8).

Table 8 Polymer composition of macroplastic expressed as the relative abundance of a polymer type for each sampling station (expressed in %).

Polymer type	PP	PE	PS	EVA	CA	PU	PB
Port of Ostend	65	30	3	1	1		
River Yser	33	58	8				
River Scheldt - Wintam	54	39	5	2			
River Scheldt - Antwerp	53	41	5	1		1	
River Scheldt - Doel	48	48	4				
Port of Antwerp	34	23	36			8	
Ghent-Terneuzen canal	64	35				1	1

5. Polymer composition in the sediment

Below, we compiled the information about the polymer composition in the sediment at each of the sampling sites. Overall based on FTIR analysis for microplastics, PS (49%), PAM (22%) and PET (18%) are most prevalent in the sediment.

River Scheldt

In the river Scheldt, PET was most abundant with a prevalence of 37 %. Along the river Scheldt, from upstream to downstream, a difference is apparent with more PP in the sediment in Wintam (45%) towards more PET in the sediment in Antwerp (48%) and Doel (85%) (Fig 11). PAM was prominently present in Wintam (28%) and Antwerp (32%), but less in Doel (7%).

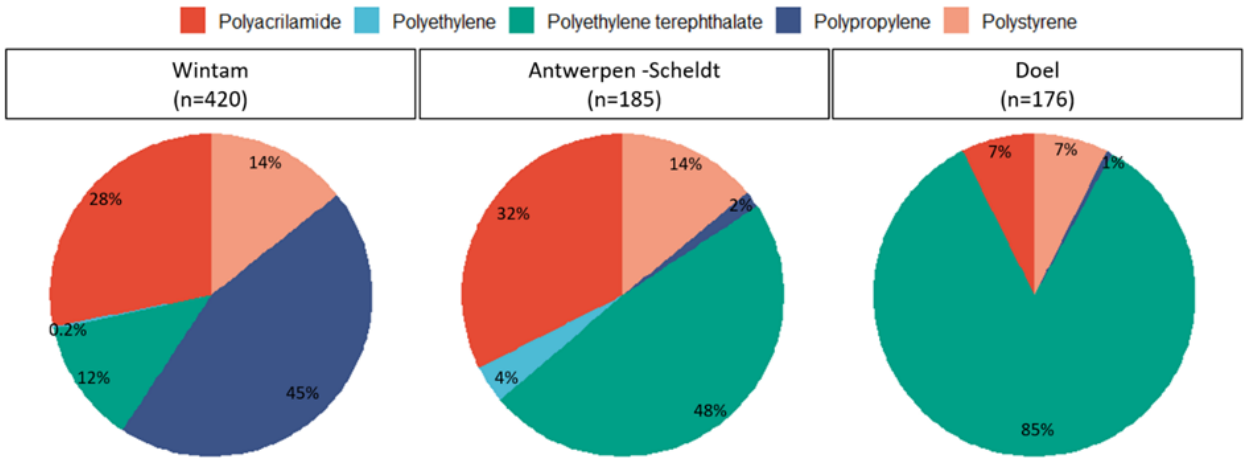

Fig. 11 Polymer composition of the microplastics detected in the sediment at different sampling locations along the river Scheldt. The number of particles (n) per location is indicated between brackets.

Port of Oostende

In the sediment of Location B in Ostend, PS was the most prevalent polymer type with a frequency of 71 %, followed by PAM (17%), PET (8%) and PP (4%) (Fig 12).

River Yser in Nieuwpoort

In the Yser river, 67 % of the plastics were identified as PAM, 25 % as PS and 6% as PET (Fig. 13).

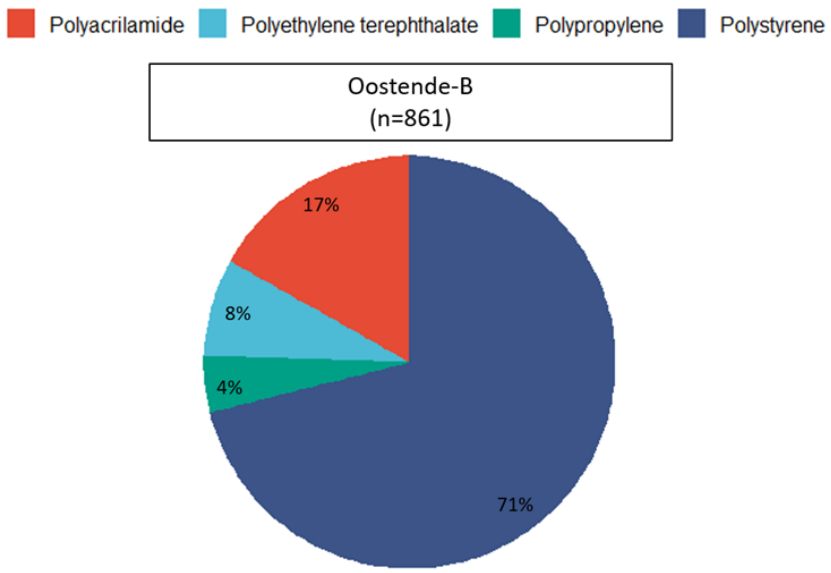

Fig. 12 Polymer composition of the microplastics detected in the sediment in the port of Oostende. The number of particles (n) per location is indicated between brackets.

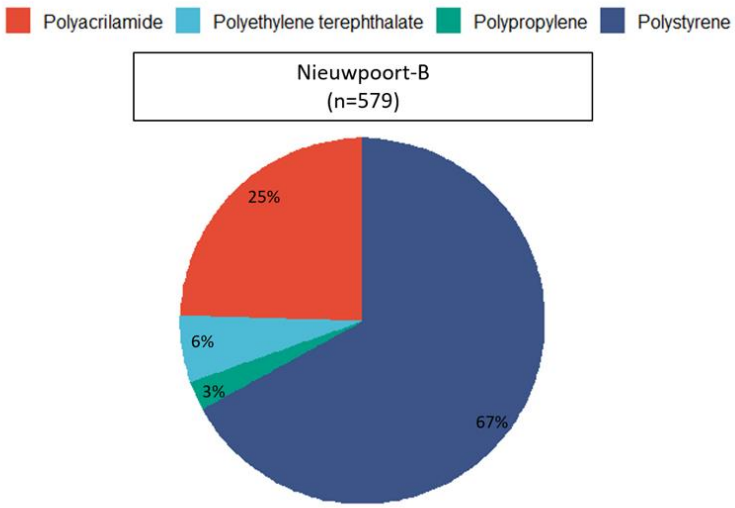

Fig. 13 Polymer composition of the microplastics detected in the sediment in the river Yser, close to the port of Nieuwpoort. The number of particles (n) per location is indicated between brackets.

6. Size frequency distributions

Based on the size frequency distributions, small-sized particles are more abundant than larger particles. This trend was detected at each of the sampling locations in the water compartment and in the sediment (Fig. 14 - 16), and for micro- and macroplastic (Fig. 17). In the surface water, the size category 100 µm – 300 µm was always most abundant and usually represents 46 -67 % of the microplastics observed. About 26 – 48 % of the particles were in size category 300 µm – 1mm. Particles larger than 1mm are less frequently detected. The shape of this size distribution was very consistent over the sampling locations, i.e. river Scheldt (Fig. 14), the port of Ostend (Fig. 15), and river Yser in Nieuwpoort (Fig. 16). In the sediment, the size category 100 µm – 300 µm was always most abundant and usually represents 63 – 84 %, particles of 300 µm - 1 mm were less frequently detected with prevalence between 15 % and 36 %. Particles larger than 5 mm were not present in any of the samples (Fig 14 - 16). Figures have been normalized based on the total number of particles observed at one specific location. Also in the macroplastic samples the smaller-sized particles are more abundant than larger particles, and this at all locations (Fig. 17 - 19).

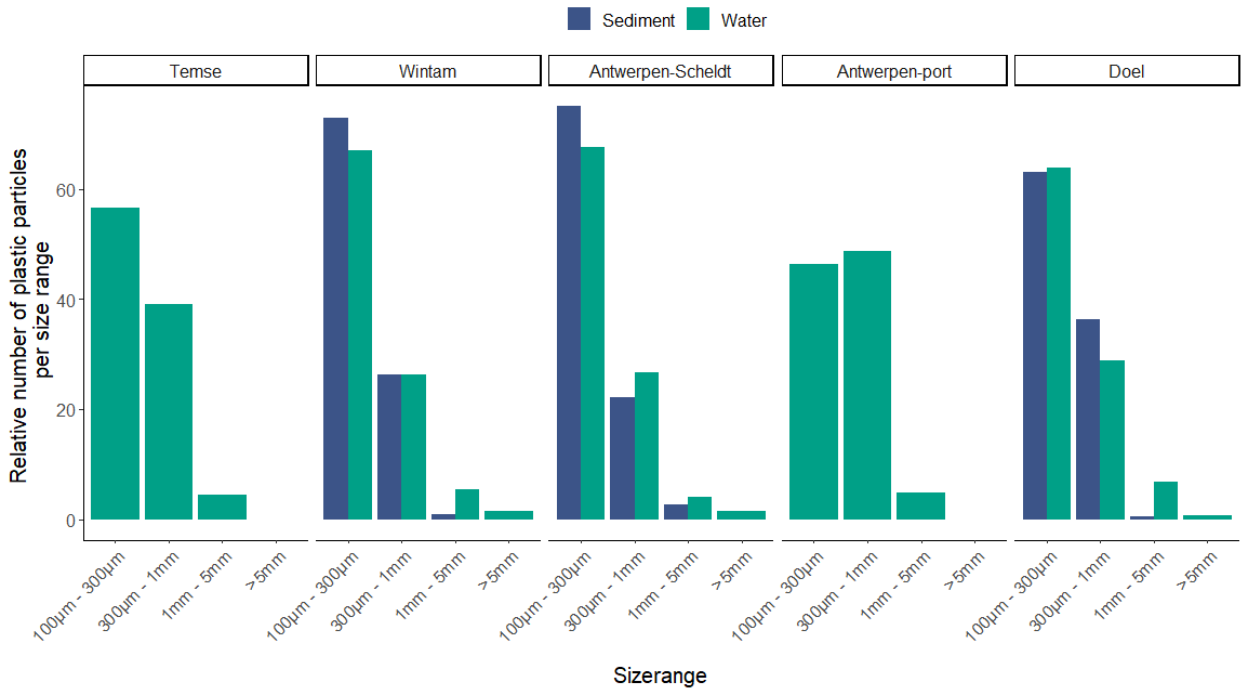

Fig. 14 Size frequency distribution of microplastics detected in the sediment (blue) and the water surface (green) in the river Scheldt at four sampling locations. The y-axis reports the relative numbers of particles for each size category. The number of particles per sample can be found in the graphs of the polymer composition.

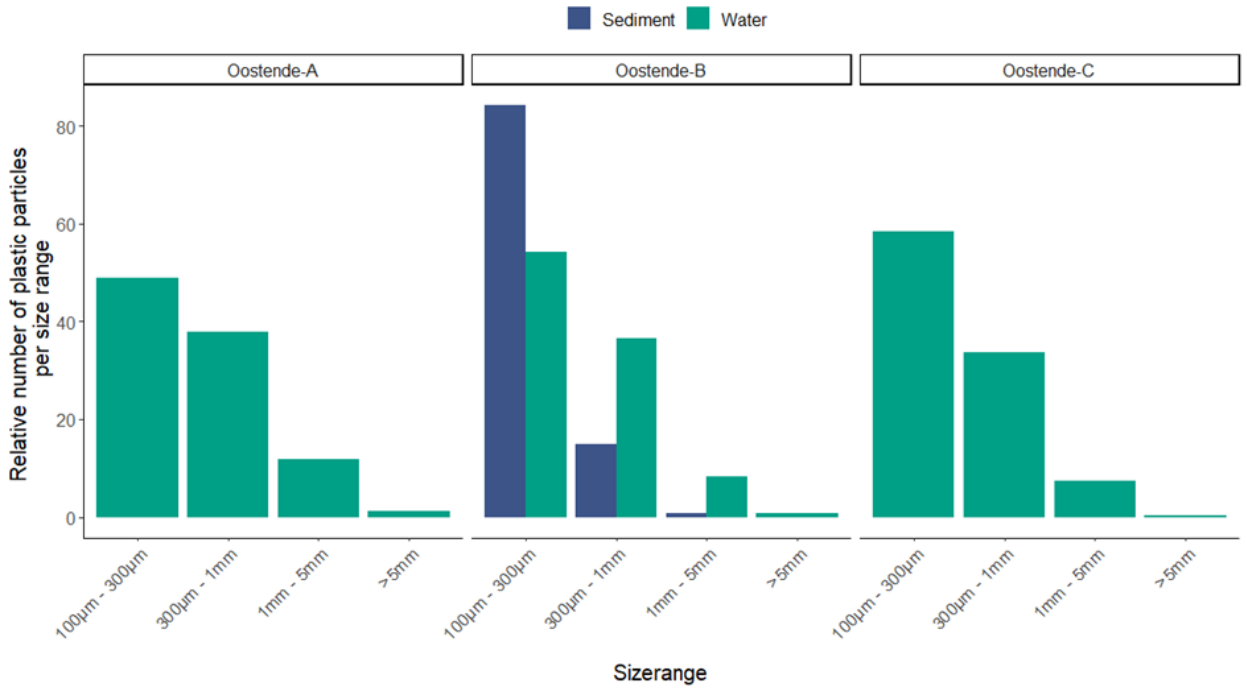

Fig. 15 Size frequency distribution of microplastics detected in the sediment (blue) and the water surface (green) in the port of Ostend at three sampling locations. The y-axis reports the relative numbers of particles for each size category. The number of particles per sample can be found in the graphs of the polymer composition.

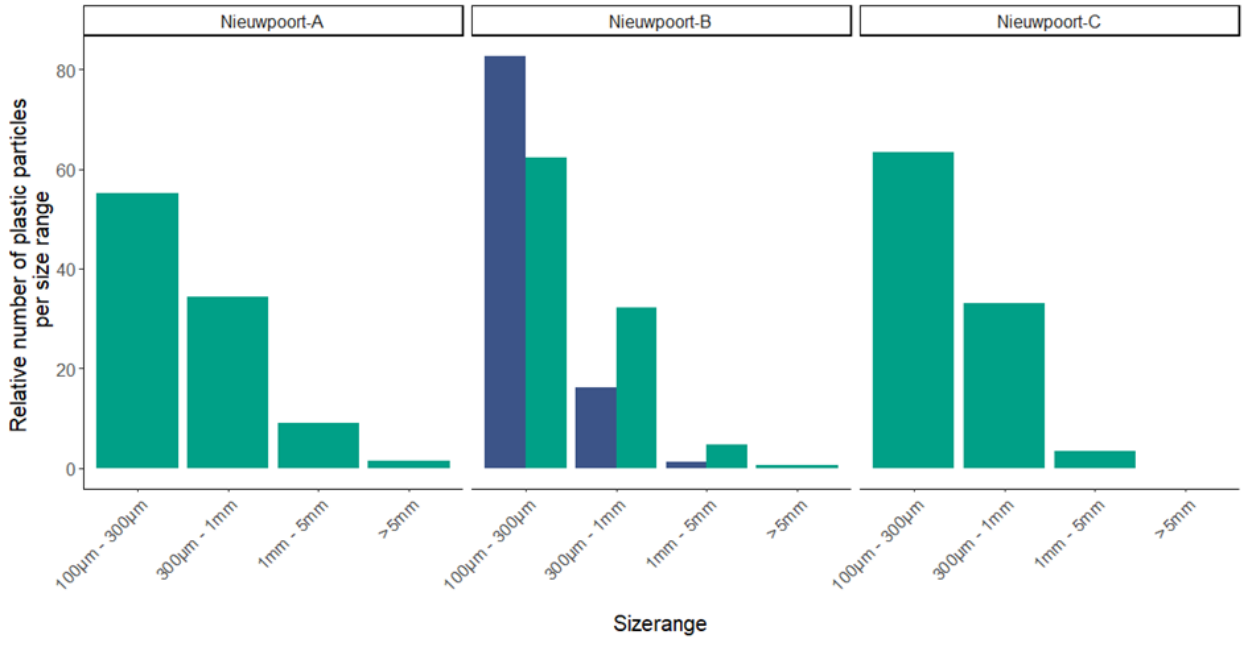

Fig. 16 Size frequency distribution of microplastics detected in the sediment (blue) and the water surface (green) at three sampling locations in the port of Nieuwpoort, along the river Yser. The y-axis reports the relative numbers of particles for each size category. The number of particles per sample can be found in the graphs of the polymer composition.

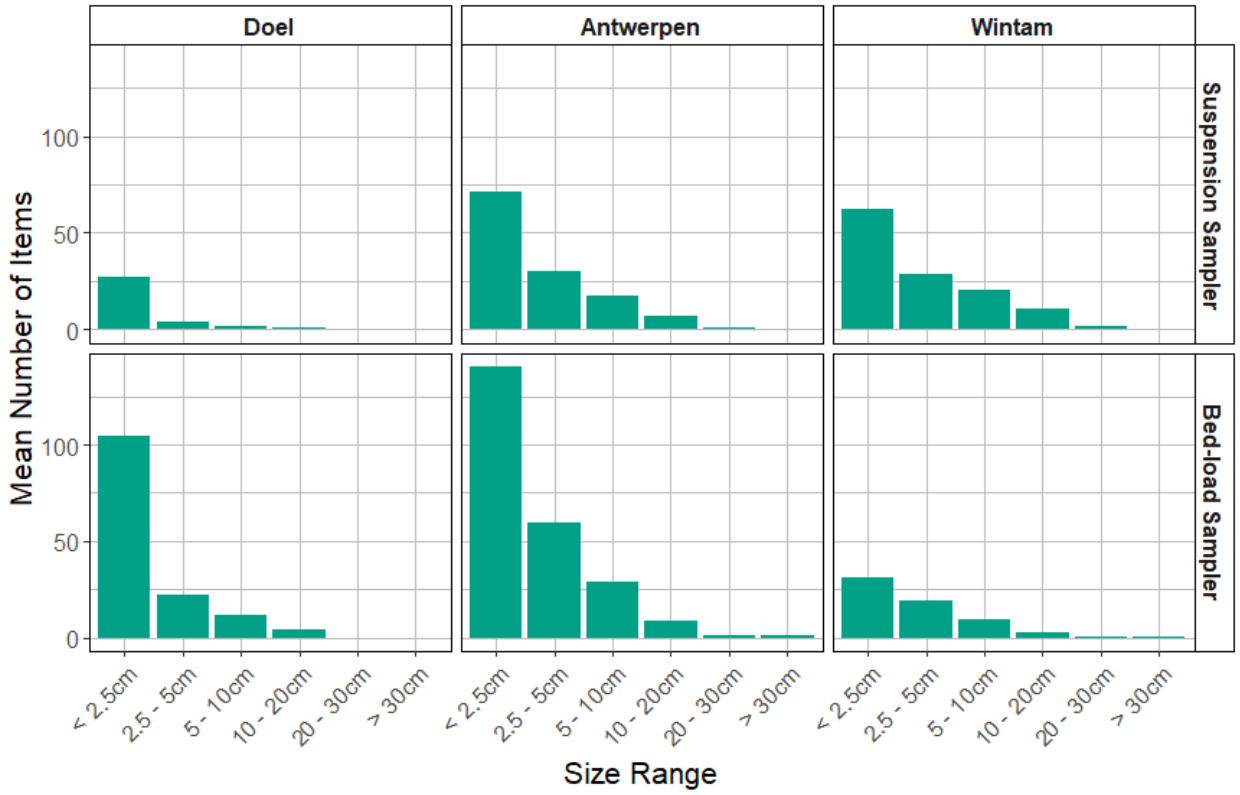

Fig. 17 Absolute size frequency distribution of macroplastic foils collected with the Suspension Sampler and the Bed-load Sampler in Doel, Antwerpen and Wintam during 4 sampling campaigns. Note that the y-axis is in absolute numbers, so has no correction for unbalanced sampling efforts.

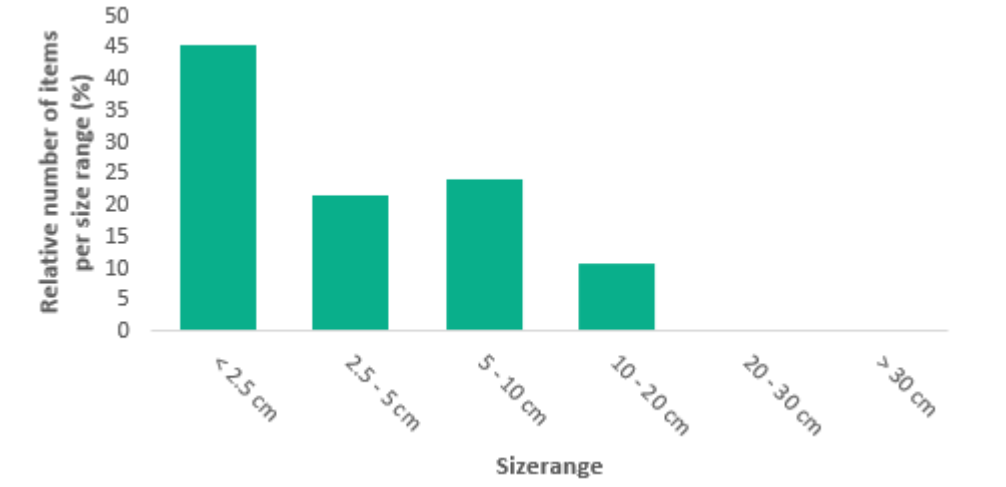

Fig. 18 Relative size frequency distribution of macroplastic in the water surface of Ghent-Terneuzen canal

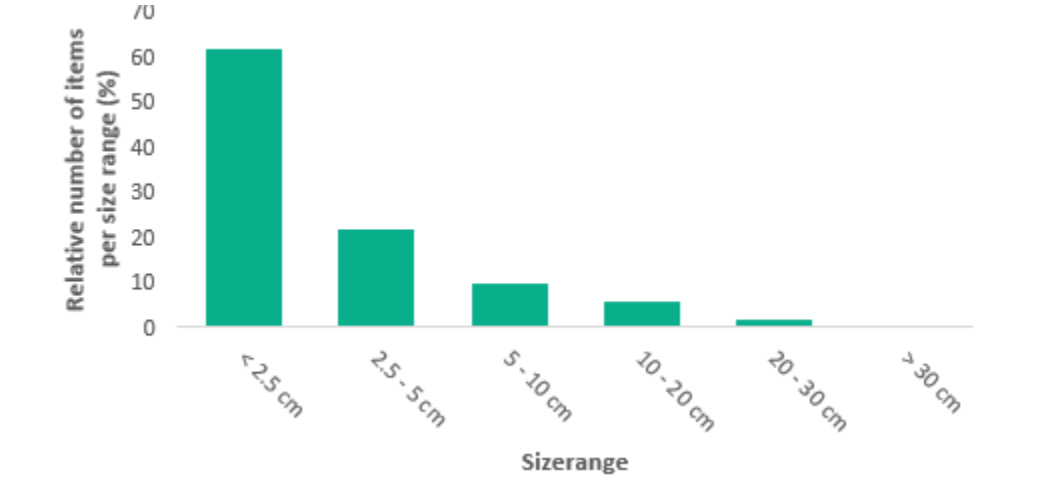

Fig. 19 Relative size frequency distribution of macroplastic in the water surface of the port of Antwerp

7. Tidal cycle influence on plastic concentration

The tidal cycle measurement was carried out by stationing the research vessel at the same location for 13 hours. During this 13h cycle, a full tidal cyle passed and a sample was taken every 2h. Despite the fact that the measurements were carried out at exactly the same location and within a time window of 13h, remarkable differences in the number of plastic items have been observed (Fig. 20-22). This variation is likely to be explained by the tidal cycle and its effect on the plastic concentration. From the raw data, it is difficult to distill a general pattern, but the variation indicated the importance of integrating the tidal cycle when determining and quantifying the plastic flux towards the marine environment.

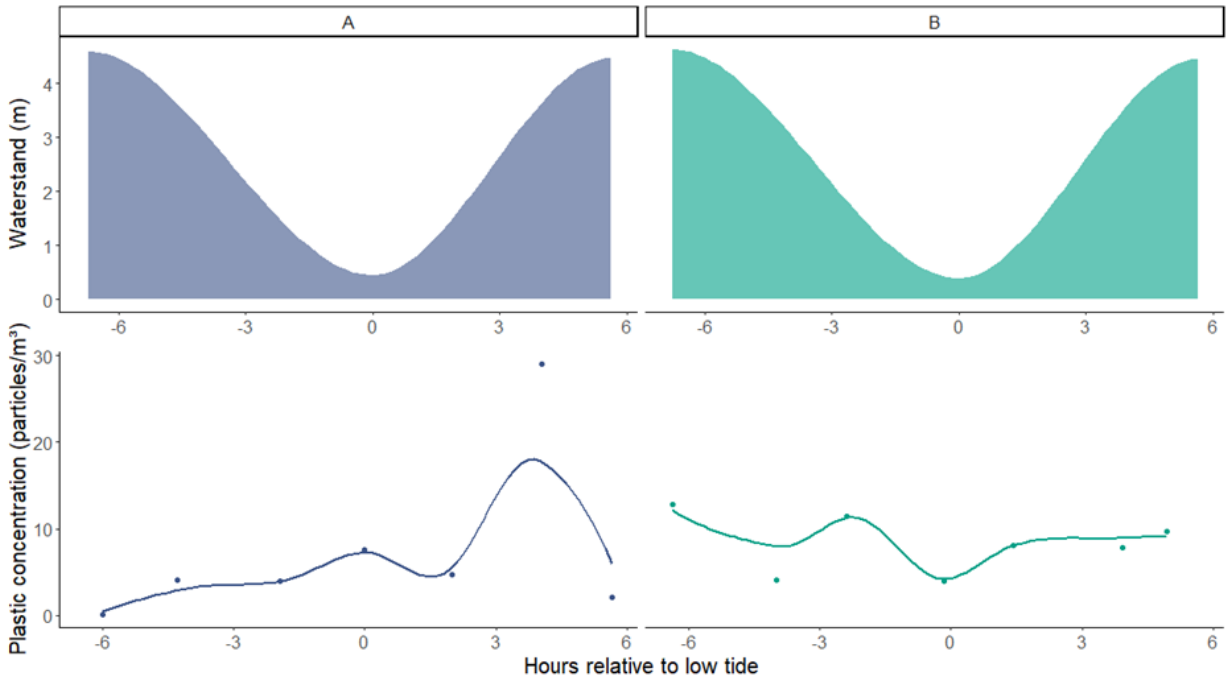

Fig. 20 Link between tidal cycle (relative to TAW) and microplastic concentration in port of Nieuwpoort in two replicate samples

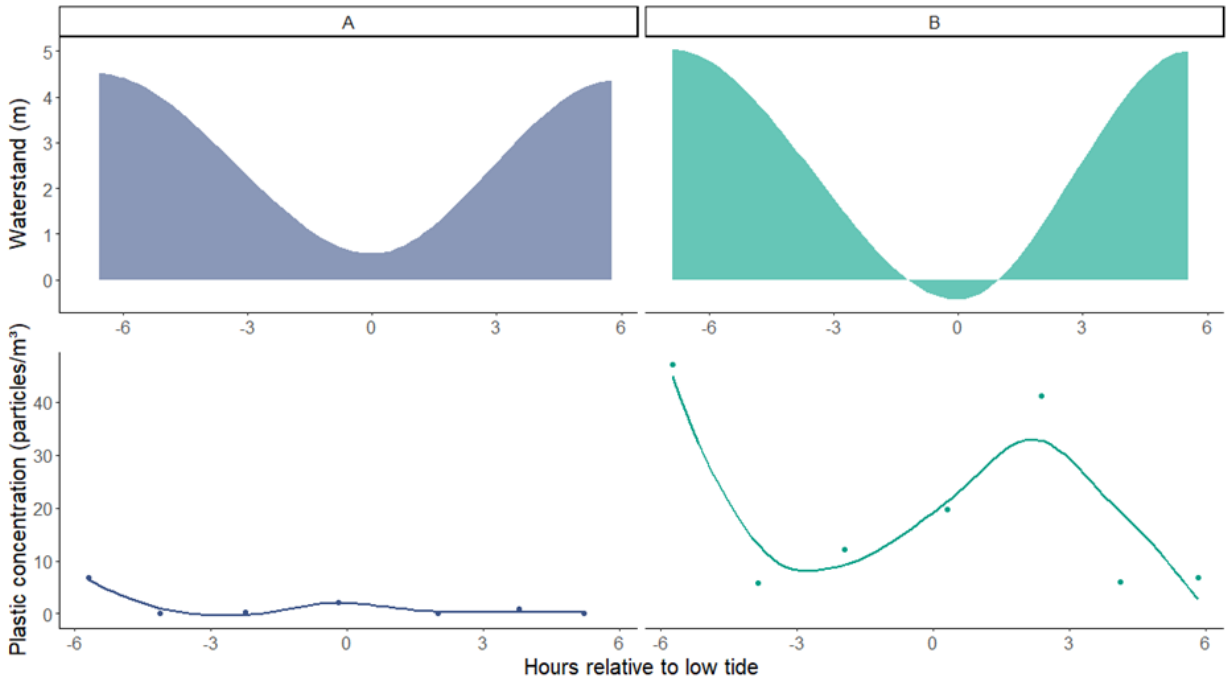

Fig. 21 Link between tidal cycle (relative to TAW) and microplastic concentration in port of Ostend in two replicate samples

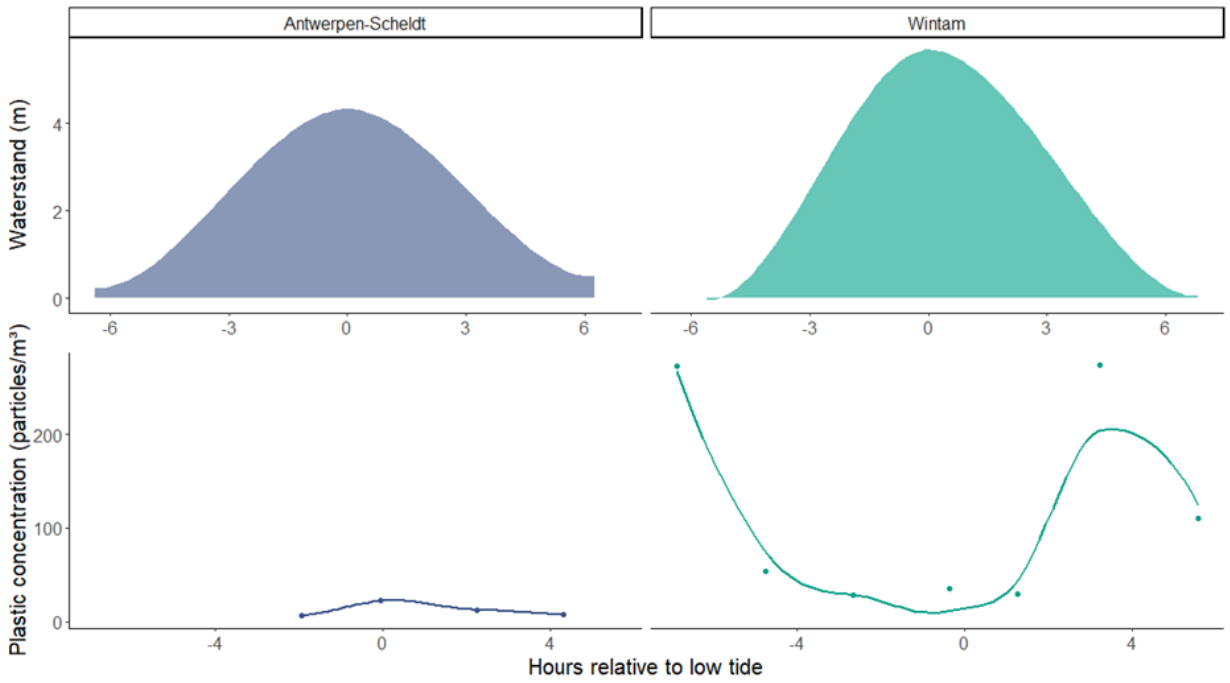

Fig. 22 Link between tidal cycle (relative to TAW) and microplastic concentration in River Scheldt in two locations; Antwerp and Wintam

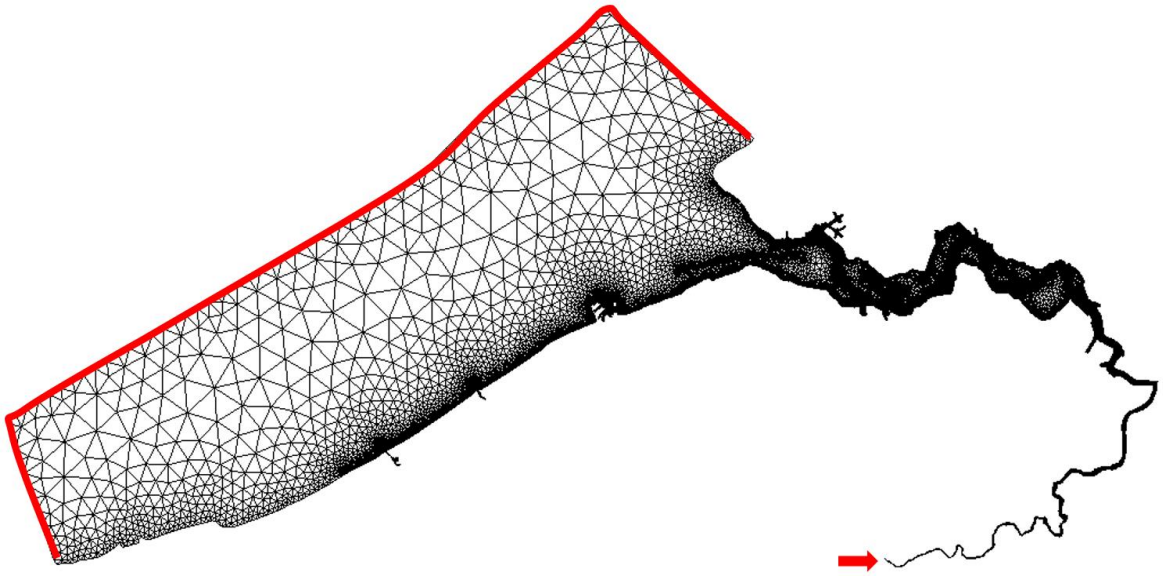

Chapter 4
Modelling the plastic flux

1. Introduction

For the quantification of the plastic flux, the spatial and temporal variation of the plastic concentrations as quantified based on field sampling can be used in different ways in the modelling process.

The first way is by helping to define the initial state of the mass of plastic in each grid cell of the study area. This can be achieved by the field data collected at the sampling locations, and for those grid cells not covered in the field campaigns, an interpolation method could be applied if the field data would cover enough area of the computational domain. Unfortunately, the latter condition is not fulfilled in this campaign, and, considering the long samples processing time, is also not realistically feasible.

The second method used the sampling data to calibrate and validate the model. After these important steps, the model result itself will generate a space-covering t_0 reference condition for the entire study area, which can be used for future scenario analysis. This ultimately is the main goal of the current modelling study.

In this section, the following aspects are discussed:

- Dominant physical process affecting the fate of the plastic debris in the estuarine system;
- The modelling approach intended to be followed;
- The data requirements and challenges to be addressed in order to develop effective plastic dispersion model;
- Scenario analysis in order to make sense of the datasets collected and generate model outputs that serve as input for future analysis;
- Results from the current model.

2. Physical processes

Particles in water constitute a so-called two-phase medium. Depending on the relative volumetric contribution, the two–phase medium behaves either as a fluid (when water dominates) or as a solid (when the particles dominate and form a 3D interconnected network or skeleton). The fluid phase is called a suspension and the solid phase a porous medium. The entire modelling framework relies on the fundamental laws of mechanics, i.e. the three basic equations for conservation of respectively mass, momentum and energy. They are applied to both the water phase and the solid phase of the particles, or can be applied immediately to the combination by the so-called mixture theory.

To understand the fate of plastic particles in an aquatic environment, one has to zoom in at the scale of a single particle in water (Fig. 23). This allows the construction of process models, primarily studied by considering the force balance (i.e. momentum conservation) for the single particle. One considers the motion of the particle relative to that of the ambient water, according to the following forces:

- inertia (i.e. change of momentum due to acceleration or deceleration);
- gravity;
- fluid pressure, consisting of the hydrostatic pressure (a response to gravity) and the dynamic pressure (a response to dilatation following ac- or deceleration);
- fluid stress (a response to the viscous shear between adjacent streamlines with different velocities).

Shear with the particle surface (i.e., skin friction) and displacement of water when pushed aside by the passing particle (i.e., form friction) both generate forces on the particle. The net force, obtained by integration of the disturbed pressure field and shear stresses over the particle surface, in the flow direction is the drag force; the net force perpendicular to this direction is the lift force.

When the relative motion between particle and fluid increases, the shear flow along the surface becomes unstable, generating a turbulent boundary layer, which eventually will separate downstream the particle where a turbulent wake is formed. The drag force then increases significantly.

Sedimentation: A particle in still water, subject to gravity, eventually will reach a steady velocity, governed by a balance between all vertical forces, i.e. buoyant weight (= gravity - Archimedes force) is in equilibrium with the drag force[1]. This velocity is called the *(terminal) settling or fall velocity*. Its value is determined by the particle characteristics (size, shape, surface roughness, stiffness and density) and the ambient fluid properties density and molecular viscosity. Since the diversity of plastic particles is so large, it is impossible to characterize it by a single value of settling velocity. It is currently not possible to consider this huge variability. This problem is one of the key knowledge gaps that will be further investigated in the PLUXIN-project.

Turbulent drift: The value of the fall velocity that is often used in sediment transport models to account for sedimentation and deposition, i.e. the flux towards the bottom. However, the conditions in natural water usually imply that water is most of the time and in most places in motion, and even turbulent motion[2]. This implies that the particle in addition is subject to additional forces caused by the motion of the fluid around it. The water motion exerts additional drag and lift and this can go in all directions. Moreover, turbulence constantly generates small eddies[3] which toss particles in different directions, superimposed on the drag and lift by the mean current. The time-averaged motion by the turbulent fluctuations is called turbulent drift. Turbulence may oppose the settling of particles in flowing waters, or enhance it. In particular, for low-density plastics, with densities close to that of water, this drift may be more important than the effect of gravity. The net effect of turbulence on sedimentation is still not well understood, but it can explain why the theoretical value of the settling velocity usually does not produce the real sedimentation rates observed in the field. This is an important knowledge gap, which will be investigated in the PLUXIN-project.

Wave drift: Similarly, waves, time-averaged, also generate a drift on particles in the wave direction, which may have completely different directions than the mean current. This wave drift, also known as Stoles drift, is very important to understand why plastics are driven towards shorelines and riverbanks. This drift can be caused by *wind waves* as well as *ship waves*. The latter is important along navigable waterways, like the Scheldt, as well as in the harbours.

[1] drag force = the hydrodynamic resistance from the surrounding water due to the relative difference in speed.
[2] turbulent motion = (apparently) arbitrary fluctuations of the fluid molecules, on top of their time-averaged current speed, which become more intense with increasing shear between adjacent streamlines.
[3] eddy = a very small vortex (rotating motion).

Wind drag: Also, the wind may push big enough floating particles in its direction by direct drag, depending on its strength relative to the resistance by adhesion of water to the particle and the resulting shear force.

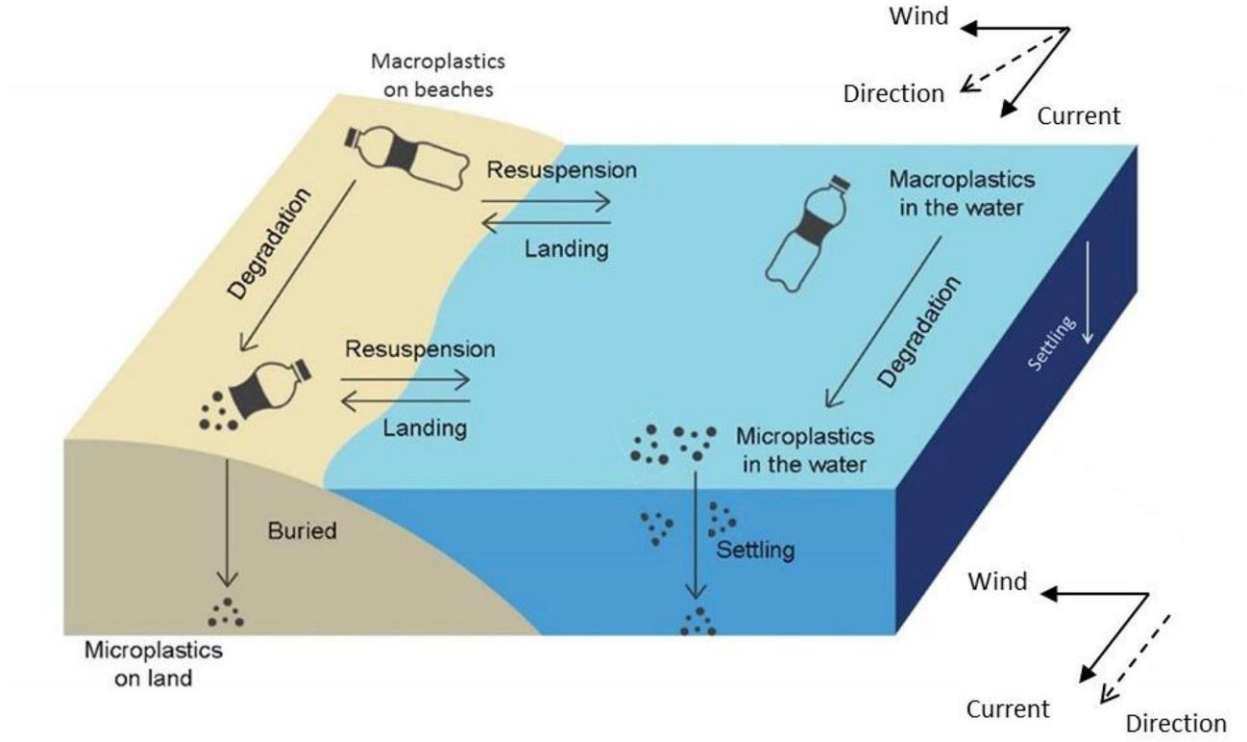

Fig. 23 Schematic representation of the various processes that plastic in a water system undergoes. Source: (Critchell & Lambrechts, 2016)

Beaching (called "landing" in Fig. 23): When plastic is pushed against a shoreline by any of the drift forces (wind, waves or tide), the balance between its momentum, buoyant weight and the shear with the bottom will determine whether the particle will beach (or land) or be driven back.

Backwash: Likewise, a beached particle may be picked up again by another wave or tide and resuspended into the main water body.

Burial: Particles deposited on the bottom or on a shore may be buried by sediment if the conditions are favourable for sedimentation.

Exposure, erosion & resuspension: When opposite conditions prevail that wash away the sediments, buried plastic particles may become exposed again to the shear forces of water and be eroded and subsequently resuspended.

Bioturbation: The activity of benthic fauna in sediment bottoms may enhance both burial and exposure, depending on the net direction of the bioturbated sediments. The modelling of this process can only be done in a heuristic way (e.g. approximating it as a diffusive process) and has a very low priority.

Trophic transfer: animals often mistake plastic particles as food. Microplastics are swallowed together with the much more abundant organic matter, which is an important source of food for smaller aquatic animals. The fate of swallowed plastics can vary from (1) death of the animal by obstruction in the digestive system, (2) the animal being eaten by a higher trophic level animal (and thus the particle migrating within a food chain), or (3) being extruded in faecal pellets, compact aggregates that settle relatively fast to the bottom. These mechanisms of plastic transport are called trophic transfer (e.g. Carbery et al., 2018; Nelms et al., 2018). The resulting sink of plastic is extremely difficult to be taken into account in the models, and will not be considered within the PLUXIN-project.

3. Modelling approach

The majority of modelling approaches for marine litter are based on the principle of so-called Lagrangean particle tracking. This method simply assumes that a particle follows the direction of the mean velocity in each point and its distance is then simply computed as the product of this velocity with a chosen time step. This methodology is suitable as a first approximation to determine the major pathways of floating particles, but it cannot account for multiple other processes that can drift the particle away from this streamline path. It evidently finds back the big gyres (i.e., large vortex flows) in the oceans as potential accumulation points (i.e., the famous garbage patches), but cannot determine the much more visible and abundant beaching of plastics in the surroundings of river mouths, neither can it determine the plastic accumulation on the bottom. Therefore, this popular method is not suitable to predict the relative distribution of beached, deposited, suspended and floating plastics.

As a Lagrangean particle tracking method is not suitable for the aim of the present study, we will adopt the Eulerian modelling strategy[4] that is commonly used for sediment particles. Such sediment particles in the aquatic environment are much more abundant than plastics. In an Eulerian model a mass balance equation is solved by computing all mass fluxes of all particles passing through (i.e. entering and leaving) the surfaces of a given volume (determined by the mesh cells of the computational grid). The net flux is then outbalanced by the change in mass concentration within.

The plastic dispersion model used to quantify the plastic flux towards the North Seal is built on the foundation of an Eulerian hydrodynamics-wave-sediment model. In this model, it is essential to incorporate all the physical processes that affect the fate of plastic in aquatic environments as described in the previous section. With existing knowledge of the sediment dynamics and incorporation of physical processes relevant to the plastic debris, a novel plastic dispersion model will be developed. In the following sections, a more detailed description of the Hydrodynamic-wave-sediment model is presented.

[4] In an Eulerian approach the focus is on computing fluxes that pass in fixed locations, which allows the quantification in terms of masses.

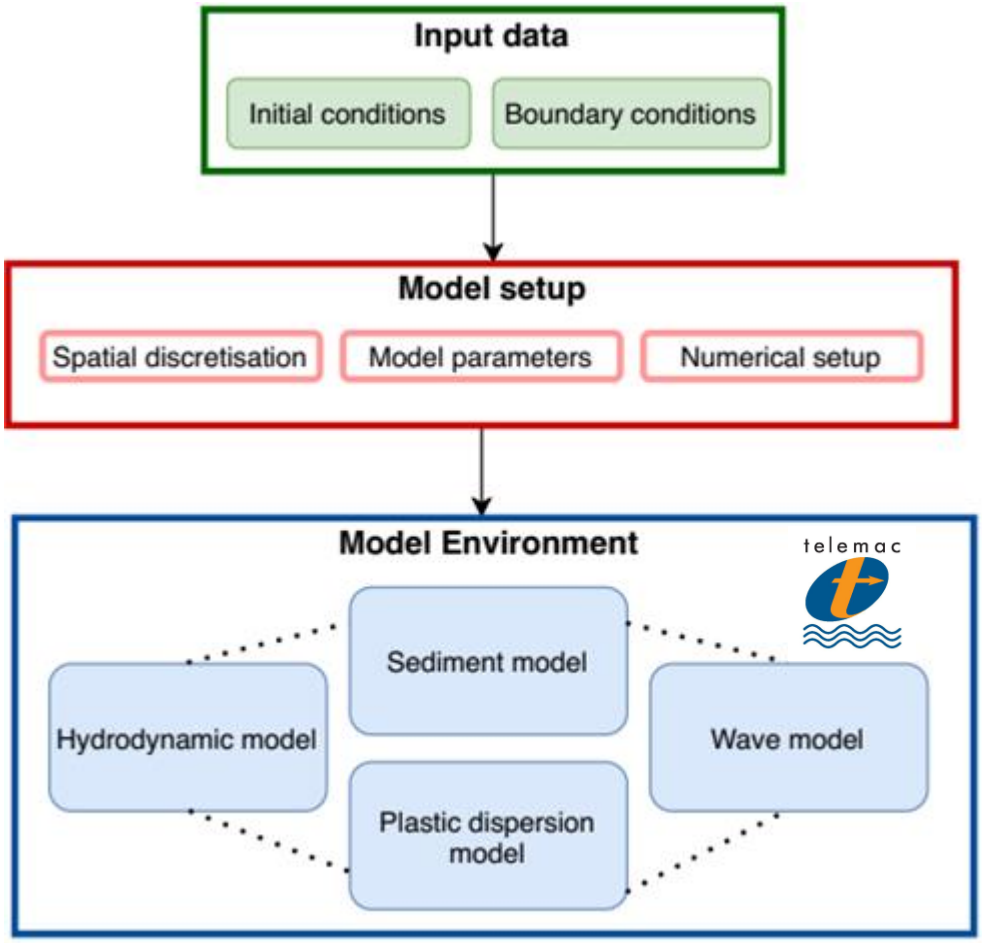

Fig. 24 Schematic representation of the modelling efforts

The open-source TELEMAC-MASCARET modelling environment (www.openTELEMAC.org) will be used for building the plastic dispersion model that will be used to quantify the plastic flux towards the North Sea. Three modules will be combined and are coupled: 1) a hydrodynamic model on currents (including a salinity correction); 2) a hydrodynamic model on waves; and 3) a sediment transport module, where plastics can be defined as a second particle fraction (Fig. 24). More technical details about these three modules can be found in the paragraphs below.

Hydrodynamics: Currents

The flow of water is determined by solving the depth-averaged continuity equation (mass conservation for an incompressible fluid) with the depth-averaged momentum conservation equation (Saint-Venant equations) in two orthogonal horizontal directions, chosen following latitude and easting coordinates (Toorman et al., 2021). These equations are solved in the TELEMAC-2D module and accounts for several of the most important phenomena, i.e. bed friction, Coriolis force, meteorological forces, turbulence,

different flow conditions, influence of temperature and salinity gradients, among others. This model will be the fundamental basis for other modules, i.e. for waves, salinity, sediment transport and plastic dispersion.

Hydrodynamics: Waves

Because wind wave dimensions (height and length) are much smaller than the mesh size of the model, they cannot be resolved by TELEMAC-2D. Therefore, another method has to be used to take into account wave effects. TELEMAC offers a spectral wave-modelling environment called TOMAWAC. TOMAWAC models the changes of the power spectrum of wind-driven waves and wave agitation for applications in the oceanic domain, in the intracontinental seas as well as in the coastal zone (Toorman et al., 2021). This model is particularly important for a plastic dispersion model as it helps to address beaching and resuspension/backwash of plastics that depends on the wave model outputs.

Salinity

Dealing with an estuary implies gradients in salinity with subsequent density variations of the water that need to be taken into account, even more in the case of plastics, since some polymers have densities close to that of water. Since salt occurs in a dissolved state, its distribution can be solved with a standard transport (i.e. advection-diffusion equation), which is available in the TELEMAC module.

The importance of salinity on fine sediment transport along the Belgian coast has recently been demonstrated by Vanlede (2022). Therefore, it is expected that it is important for plastics as well, and needs to be taken into account in the future model extensions.

Sediment / Particle transport

The complex processes of the sediment distribution and morphodynamics in the estuary as well as in the coast is modelled with an Eurlerian particle transport model. It can account for the spatial and temporal variability of the various classes of sediment (i.e. uniform, graded or mixed), properties of the sediment (i.e. cohesive and non-cohesive) and the transport modes (i.e. suspended and bedload) (Toorman et al., 2021). We use the GAIA particle transport module of the TELEMAC model environment. Sediment transport modes are grouped as bedload, suspended load or total load, with an extensive library of predictors for sediment transport carrying capacity. It is applicable to non-cohesive sediments that can be uniform (single-sized) or non-uniform (graded), cohesive sediments, as well as sand-mud mixtures. Furthermore, vertical stratification of sediments in the bed can be considered via a multi-layer model.

GAIA allows the definition of different particle classes whose transport equations are solved simultaneously. Originally, this is designed for taking into account different size fractions of sediments, but it can be extended to plastic particles, defining this as a new class. This modification will be realized in the PLUXIN project.

4. Remaining model challenges

The plastic dispersal model that will be used to quantify the plastic flux towards the North Sea is not available off the shelf and requires some specific attention. A tailor-made model will be developed in the PLUXIN project and the KU Leuven team is composed of experts in the field and will overcome some of

the hurdles initially detected. For example, a primary challenge is a good *drying/flooding algorithm*, necessary for the prediction of beaching. Due to the tide, the water level goes up and down, during which cells at the shoreline get inundated during flood and dry up again during ebb. Numerical models cannot handle a partially wet cell exactly. The standard methods require an inundation threshold, which for the Scheldt model needs a value of a few decimetres. Bi & Toorman (2015) removed this limitation by introducing a generalized friction law which spans all friction regimes (from hydraulic rough, over hydraulics smooth to laminar), but this new method still needs some further improvements (Vereecke, 2018).

5. Data needs

Numerical models that solve partial differential equations approximately by a discretization method (in this case finite elements) and the assumption of a specific simple (usual linear) interpolation function for the variation of the solved parameters in between adjacent nodes of the computational grid need various types of data. The basic data for most of the model set-up, i.e. for hydrodynamics, waves and sediments is available from previous studies by KU Leuven and Flanders Hydraulics Research (FHR). Bathymetric data and sediment composition (i.e. sand-mud ratio) maps for the area have been generated by combining survey and sampling data from various sources. Boundary conditions for the open sea boundary (water levels and wave data) are either obtained from online databases with results from ocean models, or by a coarse grid TELEMAC-TOMAWAC North Sea model. River discharge data are available from FHR. Details on these data can be found in a detailed model description report (Toorman et al., 2021).

Figure 25 illustrates that the model performs quite well for sediment transport applications after calibration for specific locations. However, comparison of spatial SPM patterns with satellite images still show discrepancies, which are still under investigation (Escobar, 2022). However, the necessary basic data for plastics are *not* readily available and raise several challenges, which are discussed in more detail in the following section.

6. Data challenges

The Scheldt Estuary-Belgian Coast plastics flux model needs input data on the plastics. These input data are at first instance obtained from the field sampling campaigns, but in case that certain variables are not or only limited available, the model will make use of literature knowledge or expert insight. At this stage, based on the data needs (cfr. above), we define four challenges to be solved: 1) spatial resolution of the data available; 2) characterization of the individual particles; 3) dealing with the uncertainty on the data (e.g., the repeated sampling data show a variance of the same order of magnitude as the mean value); 4) dealing with the heterogeneity of the particle properties.

To make the model spatially explicit, the study area is divided into multiple triangular cells, connecting 3 corner nodes where the actual calculations are done. In the ideal case, the presence of plastics should be known for every node at the beginning of each run. Since the model computes as a primary variable the amount of plastics in terms of mass concentration, one should know these concentrations in each node at the water surface, in suspension, right above the bottom and in the sediment (ideally even its variation

deeper within the sediment). For sediments, these data can approximately be generated because the variability of sediments is much smaller and sufficient field data has been gathered over the past decades. Unfortunately, for plastics few data is available. The present report actually is an important step to start generating data that in the long run should allow to create such an initial state map for the entire study domain.

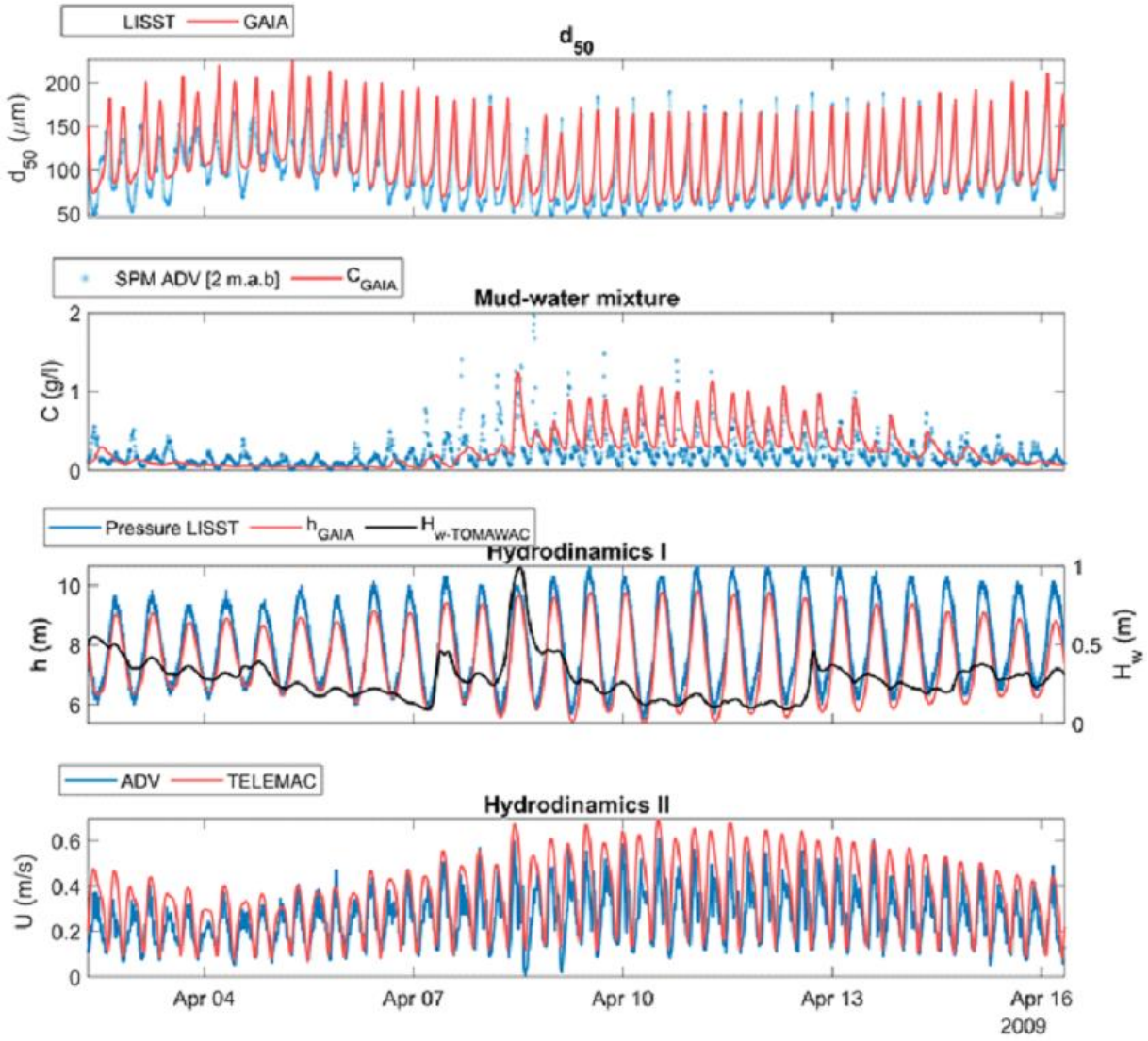

Fig. 25 Example of model validation for flow velocity (lower panel), water level (3rd panel), SPM concentration (2nd panel) and floc size (upper panel) for location MOW1, located NW of the Port of Zeebrugge where RBINS has a permanent measuring station (a bottom tripod) (Escobar, 2022).

There is a large variability between plastic particles, in terms of their polymer composition, their properties and the total mass per unit sampling volume. The data collected at the selected sampling locations aims to reveal part of this 'natural' variability, hence the model will be able to cope with this

variability. There are four more issues that are dealt with in the overarching PLUXIN project that may influence the plastic flux: 1) the age of the plastic; 2) the particles' residence time; 3) biofilm formation; and 4) aggregation. In terms of the age of the plastics, it is known that plastics weather once they are out in the environment. However, so far the rate of degradation and what characteristics exactly change over time have not been determined. It is generally accepted that plastics become brittle and break up in smaller fragments. The time scales at which this happens are only roughly determined, but it is clear that the weathering process often does not happen linearly in time. In addition, it is currently impossible to determine how long a particle or fibre has already been in the aquatic system at a particular location (especially for plastics on beaches and in sediments). This period is called the *particle residence time*. Besides, *biofilm*s grow on plastics and change the mechanical properties, since they alter size, shape and density, and thus settling velocity. To date, there is insufficient research, which hinders quantifying these changes in time. Therefore, this is also one of the research goals of the current PLUXIN project. Biofouled plastics are more prone to stick to each other and can cause *aggregation*. Usually, plastic concentrations in the water column are low. In the Scheldt and along the Belgian coast, the presence of sediment and organic matter particles is much more abundant. It is therefore hypothesized that it is more likely that microplastic particles get caught into cohesive sediment flocs and/or algae. In marine waters, near the bed, such flocs are usually called marine snow. This is one of the hypotheses that PLUXIN also would like to investigate by model scenarios.

These uncertainties also have consequences for the data collection from the samples. Ideally, for each sample, for each particle all properties should be determined (including polymer type, density, weight, the three primary sizes, shape parameters, biofilm thickness and density), as well as the weight of all the particles in one sample together, and the volume of the sample. The characterisation of each individual plastic particle is labour intensive and time consuming, but will be provided (cfr. identification and characterisation of plastic). If certain data are not available, assumptions based on expert and literature knowledge will be used. For instance, based on initial results presented here, it is expected that the number of particles per sample will be too low to apply statistical methods. Hence, it will be assumed, in analogy to sediment particles, that all parameters are lognormal distributed. The labour intensity of the sample processing limits the number of samples that can be handled and subsequently the number of locations where samples are taken. This leaves us with considerable gaps in the data available needed to generate an initial map. Therefore, interpolation methods are needed.

For now, the focus of the sampling campaigns of the project was at the border of the marine environment, as the minimum required information should be collected here. In second order, additional information about the plastic load in rivers and canals in the hinterland would be a valuable complement. At this stage, assumptions have been made about plastic fluxes at the different boundaries, i.e. the upstream river boundary, the inflow from tributaries, from sewer overflow discharges, the open sea boundaries, but also blown by the wind, washed into the river by rainfall or thrown overboard from ships.

Once initial and boundary condition data are available, the model needs to be validated. For this again a new large data set from field samples, in the same locations as the t_0 sampling campaign is needed in order to test whether the model is able to predict the changes since the initial state of the system.

7. Scenario analysis

The model is in principle completed after calibration and validation. Subsequently, the model can be used to analyse different scenarios. However, since it is to be expected that the available sampling data (and later complemented with remote sensing data) will remain insufficient for both calibration and validation, it will be necessary to run the model already for many different scenarios to fill the data gaps in the field observations.

Many possible scenarios are to be investigated. Each particular scenario can already address a list of questions. An example:

- What happens to a specified cloud of particles (of one type of plastic) released in one particular location over time (at least one spring-neap cycle)? Where will these particles be found? Does this simulation reveal potential hotspots for beaching or deposition? (The latter could then be verified with a dedicated sampling or drone image at this location).
- What is the residence time for these plastics before they leave the domain into the open sea? (This may require a long-term simulation of multiple spring-neap cycles). Which fraction remains trapped in the system (and where?).

This could be repeated for different plastics, and different types of objects (e.g. plastic bags, PET bottles, microplastics, etc.). The results from these scenarios can subsequently be used to try to fill the data gaps on plastic distribution over the entire domain for the t_0 reference. However, this is an iterative process. Since we do not know how long plastics are already in the system, and where they have entered the system, it may take a very large number of simulations before we understand the observations. It is only after this phase that we can use the model for very long-term simulations to make future projections of how the environment may be affected over the next decades.

8. Plastic flux model set-up

The plastic flux model is based on the available KU Leuven Scheldt & Belgian Coast sediment transport model in TELEMAC, which can deal with both sand and mud fractions. Bi & Toorman (2015) built the first version. Subsequently, a closer collaboration has been established with Flanders Hydraulics Research. The current KU Leuven version (Escobar, 2022) has many aspects in common with the Scaldis-Coast model of Flanders Hydraulics Research (De Maerschalck et al., 2020).

Model grid and bathymetry

The model domain encompasses the Belgian part of the North Sea, the Western Scheldt and the Upper Scheldt (from Rupelmonde upto Melle). Thanks to the irregular and flexible mesh generation, the model computational domain is refined in the areas with rapid bathymetric changes as well as in the areas of interest. As a result the computational grids at their coarsest refinement have edge length approximately 6000 metres and at their finest refinement approximately 20 metres. Most of the coarser refinement is done for the offshore area whereas the finest refinement is done for the deep channels along the Western Scheldt (Fig. 26). The geographic reference system of the grid is EPSG: 32631 WGS 84 31N. The grid consists of 31,714 nodes and 55,689 elements. The computational grid is then imposed with bathymetric

data at each node. The bathymetric data is the same as in the Scaldis-Coast model of Flanders Hydraulic Research (De Maerschalck et al., 2020). We use vertical reference of mean sea level at Ostend for the bed levels (Fig. 27). With the refinement adapted in the grid, the major bathymetric changes in the estuary are captured (with exception of the Flemish Banks).

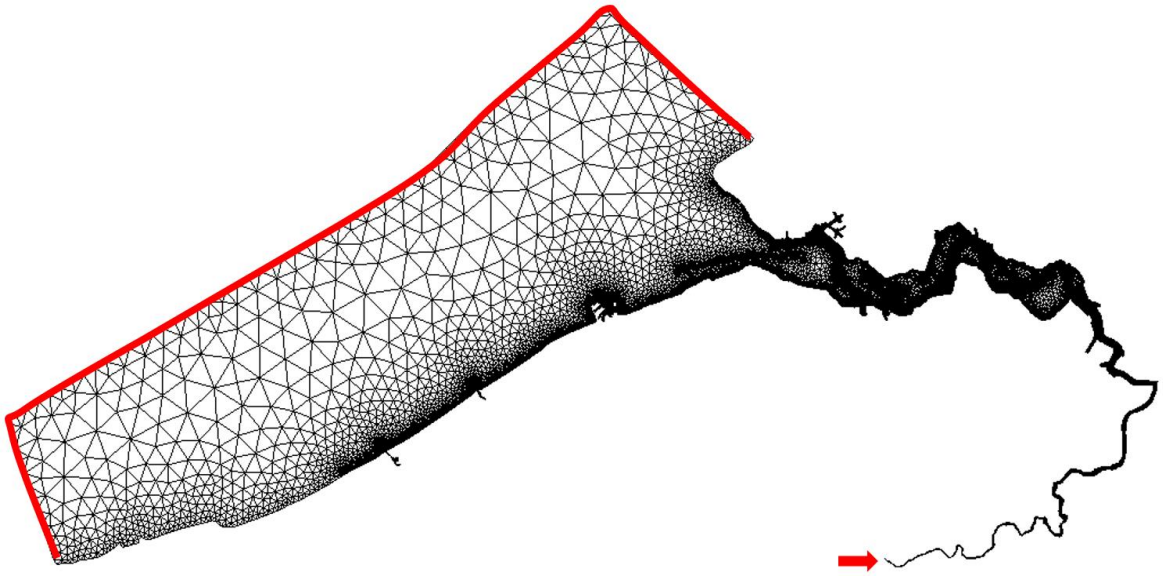

Fig. 26 Computational grid of the model. Red arrow and red line indicating the upstream (Melle) and off-shore sea boundary of the model respectively.

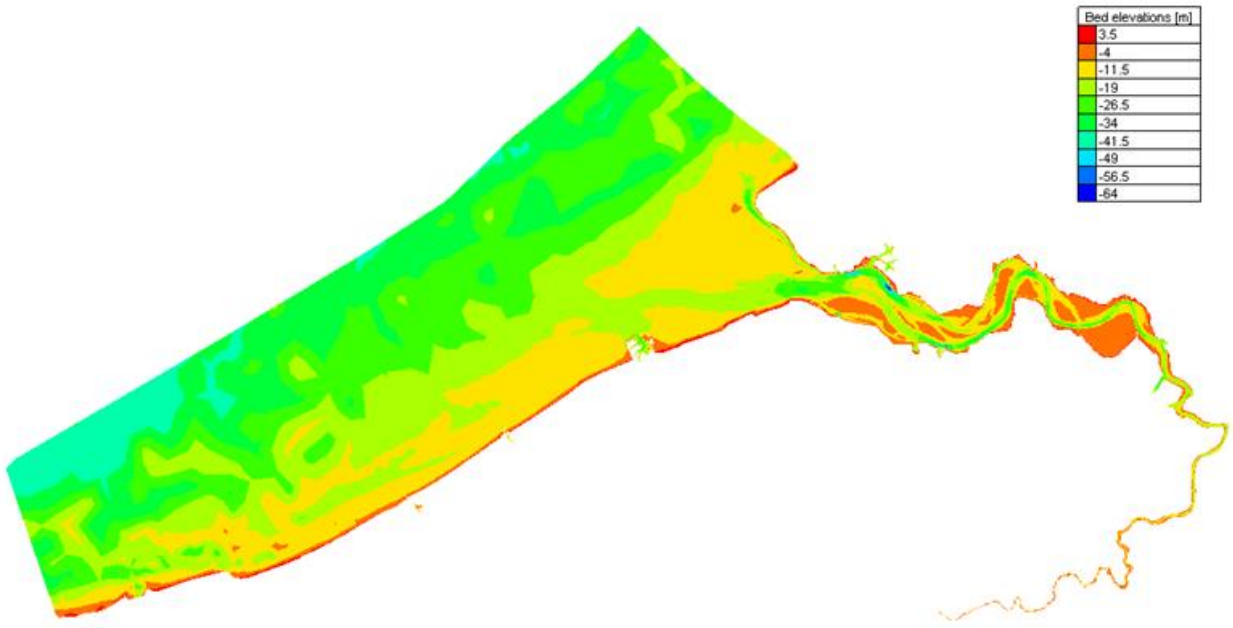

Fig. 27 Computational grid imposed with bathymetry.

Forcing of the model

Forcing of the model: Offshore boundary condition

The hydrodynamic forcings, such as free surface elevations and flow velocities, are imposed on the offshore boundaries of the model grid (Fig. 26). For this purpose the TPXO9 atlas dataset is used (https://www.tpxo.net/global), which computes the tidal motion of the oceans. The TPXO9 atlas has a fully global solution with 1/30 degree resolution. The TPXO models include complex amplitudes of Mean Sea Level - relative sea-surface elevations and transports/currents for eight primary (M2, S2, N2, K2, K1, O1, P1, Q1), two long period (Mf, Mm) and 3 non-linear (M4, MS4, MN4) harmonic constituents (plus 2N2 and S1 for TPXO9 only)[5]. Storm effects are not accounted for in the TPXO data. Therefore, in the future model setup, the boundary conditions will be generated with a larger model, covering the entire continental shelf of the North Sea. This will allow the introduction of (storm) surges by coupling with meteorological data to allow inclusion of the effects of wind shear over the water surface.

Forcing of the model: Upstream boundary condition

Upstream of the model domain is fixed at Melle (Fig. 26). Here the time varying discharge values are specified with a temporal resolution of 5 minutes (Fig. 28). The discharge data is sourced from waterinfo.be[6].

Forcing of the model: Waves

The computational cost for solving the wave field in sufficient detail (i.e. a sufficient number of directions and frequencies) is roughly one order of magnitude higher than for hydrodynamics and particle transport. However, since the wave field does not vary so much in space and time, the cost can be reduced by solving the wave energy equation over a coarser mesh, using the TEL2TOM interface, developed by IMDC (Breugem et al., 2019). However, in the current version of the model waves have not been taken into account, but should be added for future simulations, when the model has been extended with other missing processes (like beaching).

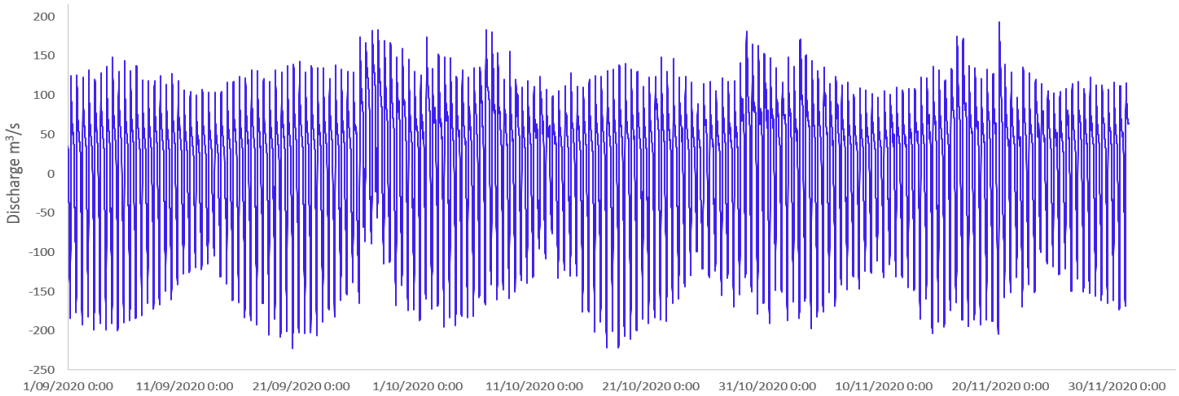

Fig. 28 Discharge boundary condition imposed at Melle

[5] https://www.tpxo.net/global/tpxo9-atlas
[6] https://www.waterinfo.be/station/04zes57a-1066

Simulation period

Different simulation periods are considered for different scenarios of modelling. These scenarios are explained in section 4.7. For scenario 1 with initially imposed plastic concentration, the model simulation period is from 01 September 2020 till 29 April 2021, a total of eight months. This period is selected particularly to compare the tidal measurements of plastic concentration available for Scheldt at two different locations i.e. Wintam and Antwerp for October 2020 and April 2021 respectively. This helps to understand the time evolution of the initially imposed concentration of plastic. The other two model scenarios 2 and 3, have been run for a simulation period of three months duration starting on 01 September 2020 until 30 November 2020. These two scenarios deal with the constant flux of plastic. The scope of these two scenarios is to analyze the transport routes and times scales of transport. This can be qualitatively be achieved in the 3-month simulation. It is good modelling practice, to run the model for at least one or two spring-neap cycles, as a warmup period prior to the time period of interest. Therefore, the results from the first month (September 2020) are not considered in the analysis.

Model hydrodynamic and particle transport set up

Hydrodynamic Parameter	**Value**
TELEMAC version	v8p1r2
Time step	15 seconds
Graphic printout period	15 minutes
Initial condition	Previous computation results (Hotstart)
Bed friction model	Physics based bottom friction law (Bi & Toorman 2015)
Roughness length	0.03 m
Option for treatment of tidal flats	1: tidal flats are detected and free surface gradient correction
Treatment of negative depths	2: flux control
Horizontal turbulence model	4: Smagorinski model
Velocity diffusivity	$1x10^{-6}$ m^2/s
Option for liquid boundaries	Suggested at upstream; imposed at downstream
Particle transport Parameter	Value
Type of sediment	Cohesive
Critical shear stress of deposition	0.06 Pa
Critical erosion shear stress	0.1 Pa
Partheniades constant	$1x10^{-6}$

Model validation

The model has been validated against several measured datasets for hydrodynamic variable - free surface elevation. This validation shows the model performs reasonably well for the purpose of use. The validation of free surface elevation has been carried out at 5 locations namely A2 measuring pile, Bol Van Heist, Scheur Wielingen, Wandelaar, Westhinder[7]. The correlation coefficient (r) and root-mean-square error (RMSE) calculated between measured and modelled result range between r = [0.965 - 0.980] and RMSE = [0.276 m - 0.353 m]. However, the model needs to be calibrated better for the most upstream part from Dendermonde to Melle. As we are focusing on the estuary region and the off-shore region in the current case for plastic dispersion scenarios, the model's performance is considered satisfactory with above mentioned validation metrics. The details of validation can be found in (Escobar, 2022).

Analysis methods

Analysis methods: Ensemble analysis

The principle behind this method is to compare a set of results against the field data instead of one single model result. This allows capturing some of the uncertainties that exist in the model results. The model results are grouped as spring, average and neap tides based on the amplitude of the flood-ebb cycles. All the flood-ebb cycles with amplitude more than 66th percentile (~5.0 m) are classified as spring tides, less than 33rd percentile (~4.3 m) are classified as neap tides and the rest are classified as average tides. If the classification is carried out for a long enough time period, each category of the tide will have a large enough number of flood-ebb cycles to perform statistical analysis.

Analysis methods: Flood-ebb cycle analysis

The time evolution of the plastic concentration can be understood with analysis of the behaviour during flooding and ebbing. The flow conditions during the entire flood-ebb cycles are the driving force towards the transport of plastic. Therefore we divide the entire flood-ebb cycle (12 hours) into four quarters (Q) of 3 hours each. The results of plastic concentration (from which plastic number concentration can be derived) for each such quarter are then averaged. Therefore Q1, Q2, Q3 and Q4 represent the early flood, late flood, early ebb and late ebb periods.

Analysis methods: Flux analysis

The model results of plastic concentrations C [kg/m^3] are converted to plastic flux f [kg/s]. This conversion helps in understanding the total quantity of material flowing across any giver point or cross-section. The conversion is performed as follows.

$$f\ [kg/s/m] = C\ [kg/m^3] * velocity\ [m/s]\ * depth\ [m]$$

The flux is then integrated over any given cross-section to get the flux in units of [kg/s]

Analysis methods: Residual mass flux analysis

[7] https://meetnetvlaamsebanken.be/Map

The plastic concentration alone does not give indication towards the direction of flows at a given point in time. This can be overcome by analyzing the concentration with velocity vectors. Here, we take the product of the *x* and *y* components of velocity (*u* and *v*) with plastic concentration individually over a specific period (for example, a spring-neap cycle). These u^*C [kg/m^2/s] and v^*C [kg/m^2/s] can then be averaged over a time period to derive a general circulation pattern of the plastic transport.

9. Plastic dispersion scenarios

After calibration and validation of the hydrodynamic model, the model has been run for non-buoyant spherical plastic with density - 1131 kg/m^3, diameter - 5 mm, characterized by a settling velocity - 127 mm/s (Khatmullina and Isachenko 2017). We use three different scenarios for plastic dispersion. The model is initiated in three distinctly different ways:

1) An initial uniform particle concentration (1 particle/m^3) is given for the entire domain at t = 0 hr.
2) A constant flux of particles (1 particle/s) is imposed as a point source at four selected locations in the estuary throughout the simulation period.
3) A concentration of particles/m^3 is imposed along the off-shore sea boundary throughout the simulation period

The purpose of these model scenarios is to understand the whereabouts of these particles in time and space. Each scenario helps us understand transport rates, timescales of transport and areas of accumulations, in relation to the initial state of plastics and the fluxes that enter the domain at a constant rate from sources.

10. Results

Results: Scenario 1

An initial uniform particle concentration (1 particle/m^3 = 74 x 10^{-6} kg/m^3 for the chosen particle size and density) is assigned at each node at t = 0 hr. Analysis has been carried out related to the time evolution of the plastic concentration. In Fig. 29a, the ensemble analysis includes results of the month October 2020, which includes 60 flood-ebb cycles. The classification yielded 21 spring tides, 19 neap tides and 20 average tides. In Fig. 29b, the ensemble analysis includes results of the month April 2021, which includes 60 flood-ebb cycles. The classification yielded 26 spring tides, 21 neap tides and 13 average tides. These sets of flood-ebb cycles are statistically analysed. We calculate the median (solid red line), 10th and 90th percentile (shaded red area; Fig. 29). The measured plastic concentration at Wintam and Antwerpen on the Scheldt river is compared with model results. The measured concentrations at Wintam are collected from 14-10-2020 20:55 to 15-10-2020 09:30, during which the average amplitude tide occurs. The measured concentrations at Antwerpen are collected from 21-04-2021 09:05 to 21-04-2021 15:32, during which the neap amplitude tide occurs (as per our classification explained further).

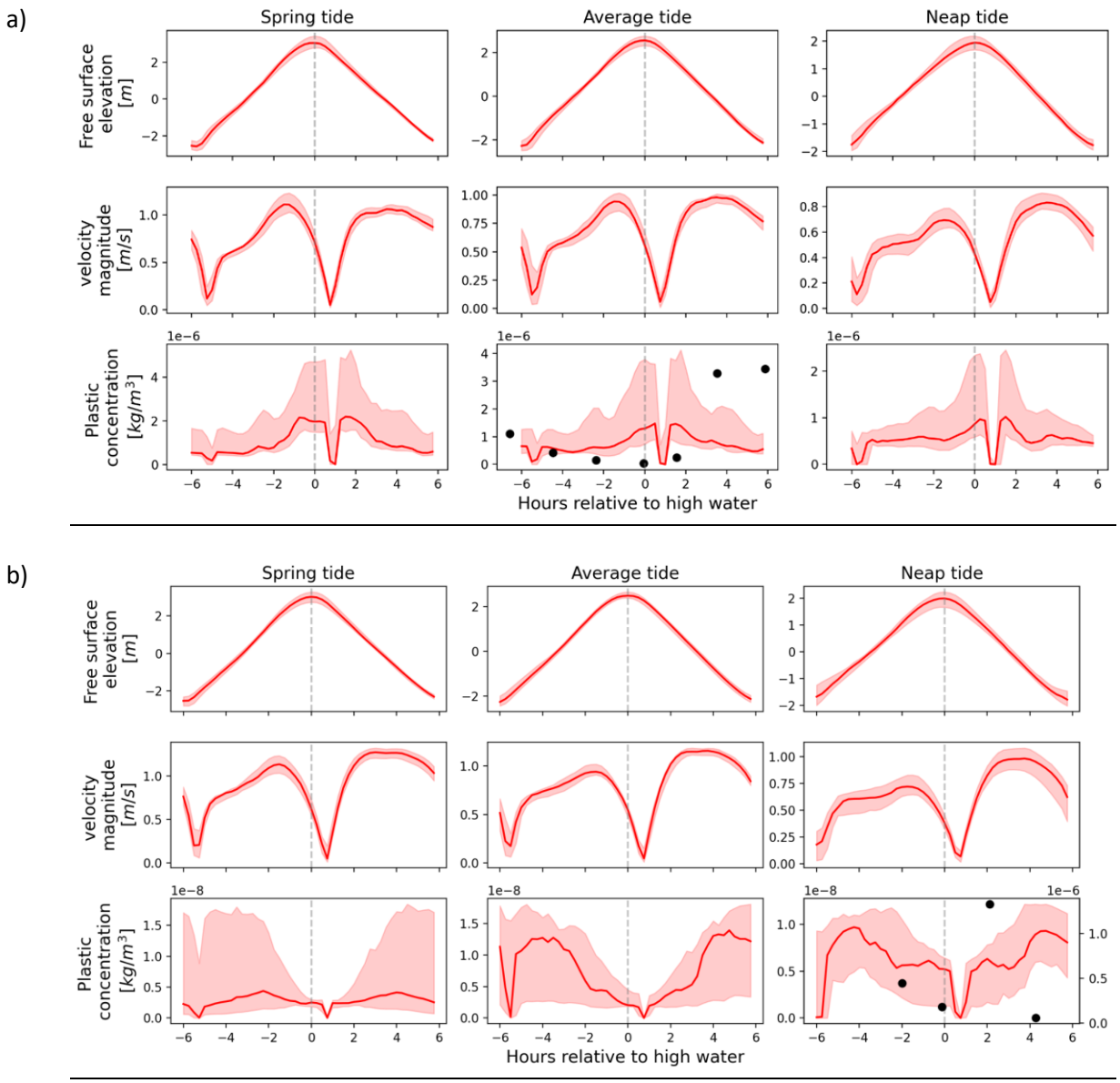

Fig. 29 Ensemble model results at the a) Wintam and b) Antwerpen tidal plastic measurement location, over the months of October 2020 and April 2021 respectively. The red solid line indicates median and the red shade indicates the uncertainty band between percentile 10 and 90 of the model result. Black dots represent the measured data (in 4b, refer to the secondary *y*-axis). Model run with initially imposed plastic concentration of 1 particle/m^3.

The model data shows that there is a rapid decline in plastic concentration soon after the peak water level is reached and the flow velocities are at their lowest. This likely facilitates the settling of particles and therefore results in lesser particles in the water column. This condition only lasts for a few minutes after which the suspension concentration increases again. It is also important to note the differences in the magnitude of plastic concentration between spring, average and neap tides. The peak magnitudes are around 5.5x10^{-6} kg/m^3, 4x10^{-6} kg/m^3 and 3x10^{-6} kg/m^3 for the three tidal conditions at Wintam. Similar

differences are also observed at Antwerpen. This also indicates the major role of tidal conditions on the suspended plastic concentration. The order of magnitude of plastic concentration is the same for the measured and modelled data for October 2020 (figure 4a). However, the concentration variation over the tidal period by the model deviates from the measurements. It is difficult to point out the exact reason but a few possible explanations are large uncertainty in the measurement data (only one sample per moment) and low time resolution of the collected data. Ideally, replicate measurements should be carried out in order to confirm the trend and to know the band-width of the variability of the concentration measurement. Also, the missing physical processes in the model could be a reason as well. The comparison of data from April 2021 (Fig. 29b), do not show the same order of magnitude of plastic concentration unlike in October 2020. Note that the measured data is plotted on a secondary *y*-axis for this campaign. The modelled plastic concentration is 100 times lower than that of measured values. This is the result of having no additional input of plastic in the model during the model run period.

a)

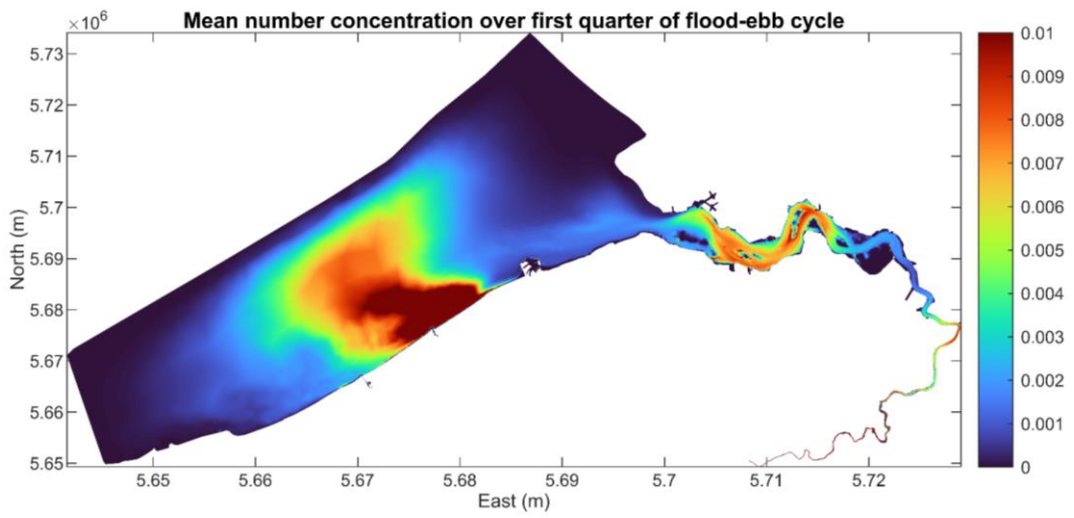

b)

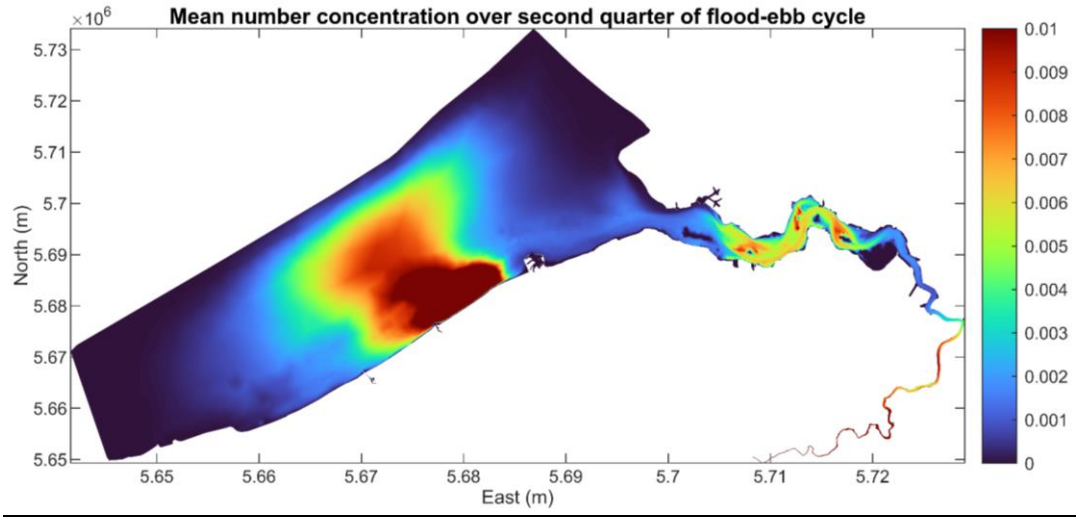

c)

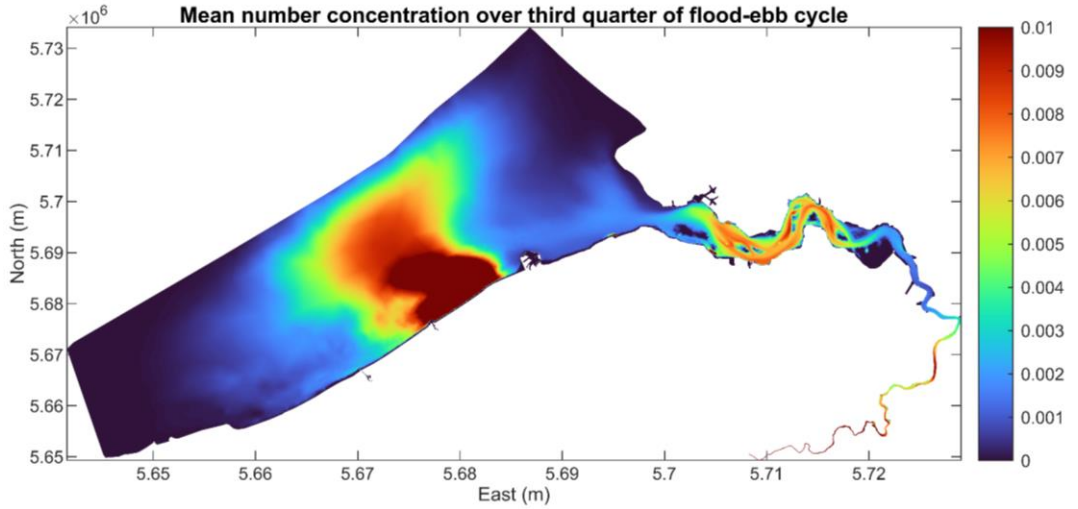

d)

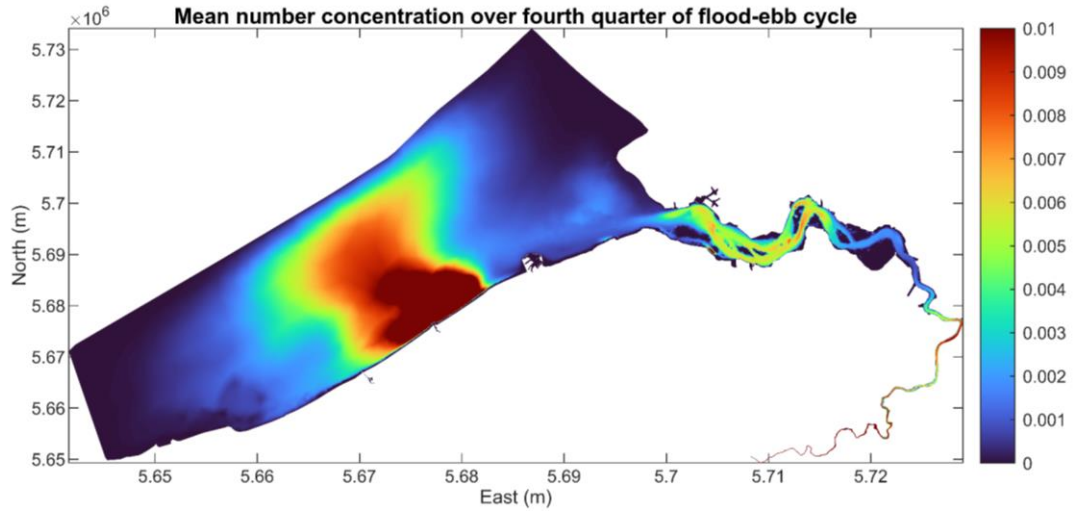

Fig. 30 Mean number concentration of the plastic particles for the model run with initially imposed plastic concentration = 1 particle /m^3 Figures show the average number concentration over 4 quarters (3 hours each) of a flood-ebb cycle (from 29 Nov 08:45 to 29 Nov 20:45) of model result.

In Fig. 30, the mean number concentration of the plastic particles is shown for four quarters of the last flood-ebb cycle of the model result (from 29 Nov 08:45 to 29 Nov 20:45). The order of magnitude of concentration is 0.01 particle/m^3. This is 100 times lower than the initially prescribed uniform concentration of 1 particle/m^3 over the entire domain. This indicates the loss of particles from the water column, either losing the particles to the bottom or out of the model domain. The highest persistent concentration is between the port of Ostend and Zeebrugge. Here the concentration of plastic stays above 0.01 particle/m^3. This is one of the major accumulation zones for plastic particles.

It is observed that there are three distinct zones with higher concentrations i.e., at the Ostend- Zeebrugge shore, intertidal area between Vlissingen & Bath and upstream of Antwerp. Only these areas show a

persistent higher concentration in comparison to their surrounding area, but the concentration in the Ostend-Zeebrugge shore is much higher than the other two regions. The water levels in the intertidal areas drop from a few centimeters to a few millimeters. In these conditions, microplastics may have a tendency to settle down- significantly on the intertidal areas. However, this physical phenomenon is not accounted for in the current model. Therefore intertidal areas could be an interesting zone to investigate the beaching mechanism in future models.

Fig. 31 shows the residual mass flux during the last 15days spring neap cycle, which is from 15-11-2020 to 30-11-2020. This is a useful way to visualise the transport routes that are predominant in the estaurian areas. We notice plastic transported towards sea are following the ebb channels and the plastic transported towards upstream are following the flood channels. These facts are in good agreement with the previous studies of the region concerning sediment transport. There are several small scale circulation patterns observed which suggest that a certain proportion of the particles could be trapped within these circulations and could not leave the estuarine region.

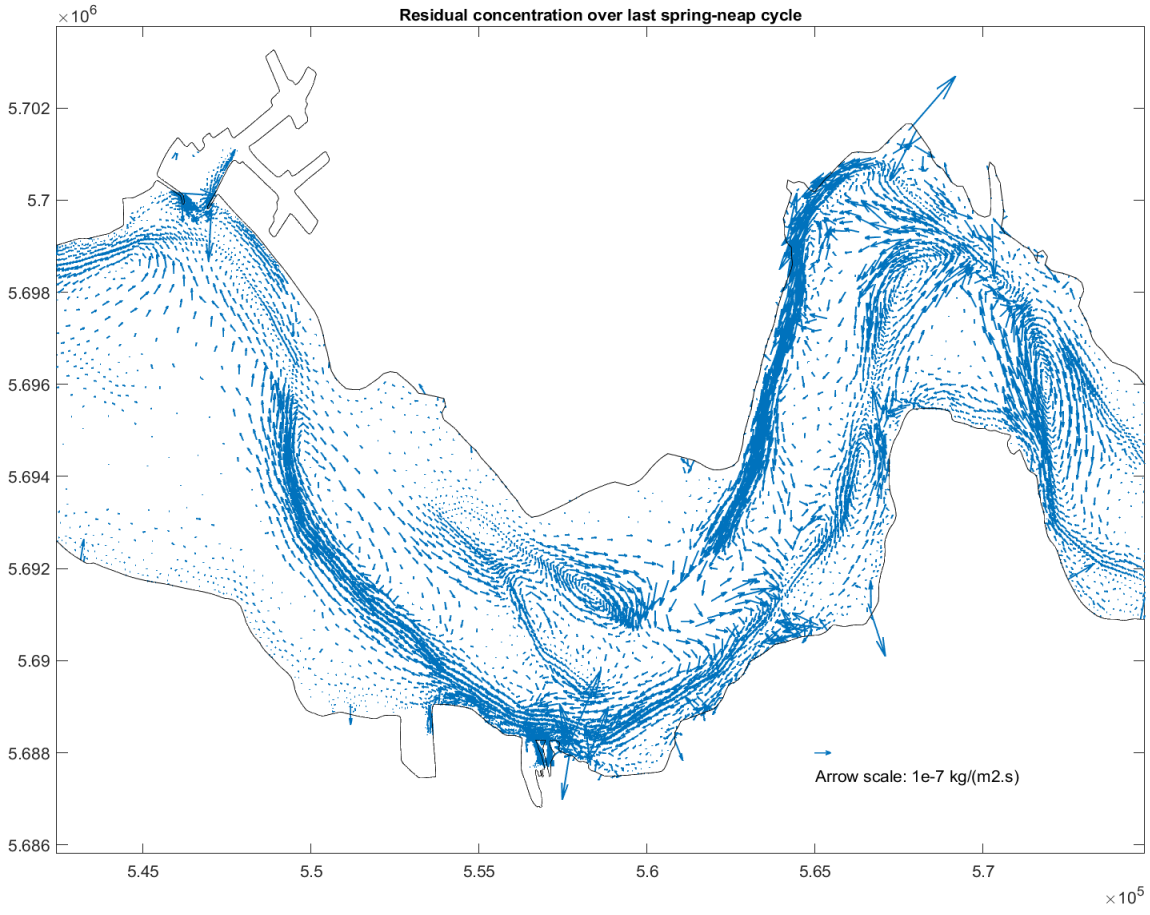

Fig. 31 Residual plastic mass flux [kg/m^2/s] for the last spring-neap cycle of the model run, focused on the Western Scheldt region.

In Fig. 32 the bed evolution [m] i.e., the increase in the bed elevation due to net erosion-deposition is shown for the last time step of the model (on 30-11-2020 00:00). The plastic particles settle to the bottom when the bed shear stress is below a critical value described as critical shear stress of deposition. But it is possible, these settled particles are eroded again when bed shear stress increases. But on a large timescale, one of the processes might be dominant in certain areas and lead to net erosion or net deposition. We notice bed evolution is highest in the areas shown in figure 7 and significantly lower elsewhere. Among these areas, Port of Ostend shows the highest bed evolution, implying the flow condition there is most favourable for deposition to occur. However, it should be noted these areas could have totally different flow conditions from inland (canals, locks, etc.) as compared to the model since they are heavily flow-controlled areas.

a)

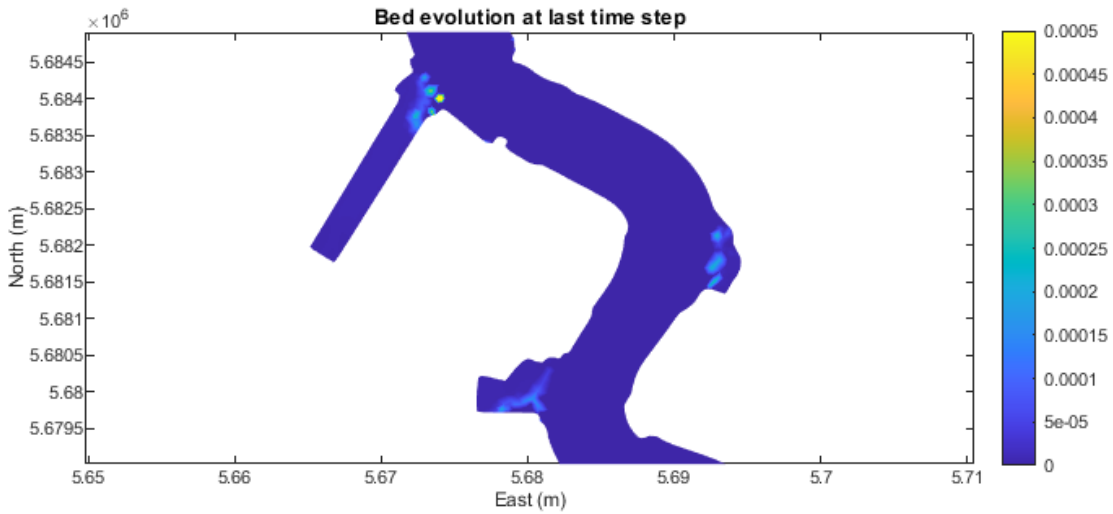

b)

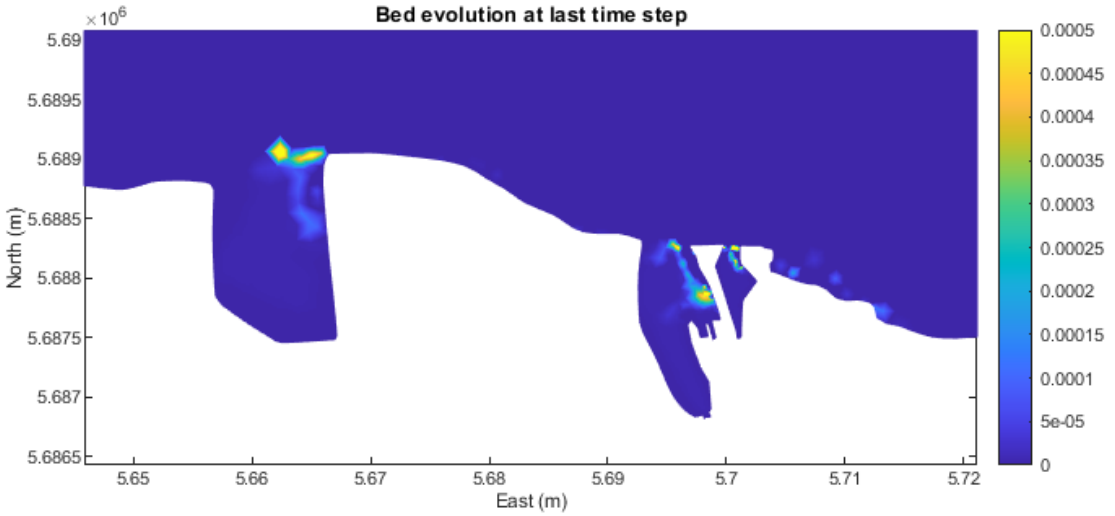

c)

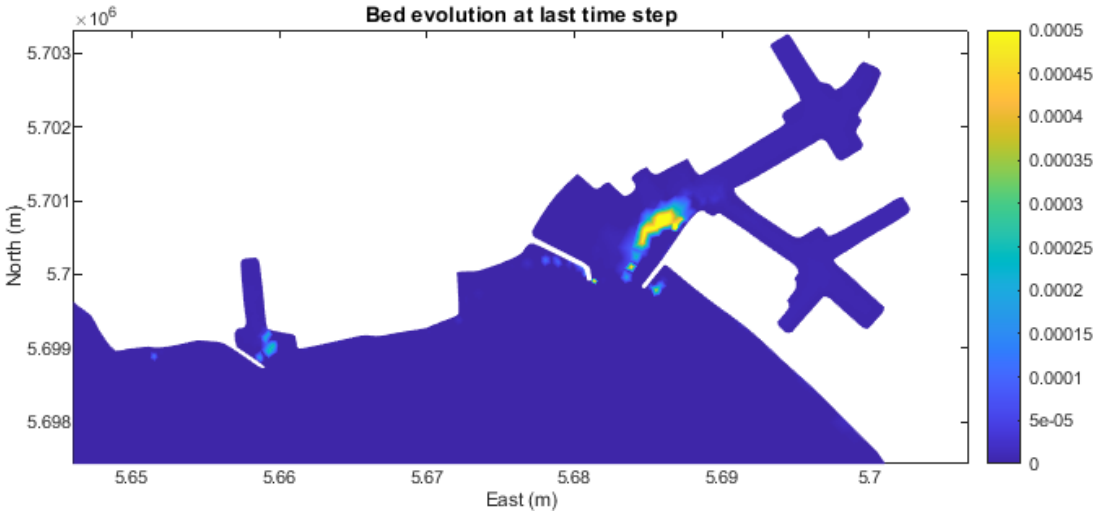
Bed evolution at last time step
×10^6
5.703
5.702
5.701
5.7
5.699
5.698
North (m)
5.65
5.66
5.67
5.68
5.69
5.7
East (m)
0.0005
0.00045
0.0004
0.00035
0.0003
0.00025
0.0002
0.00015
0.0001
5e-05
0

d)

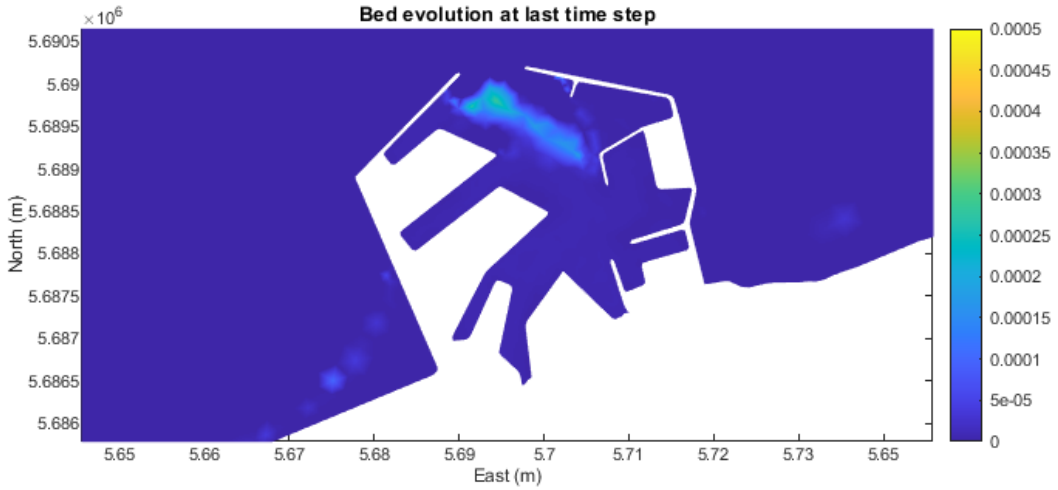
Bed evolution at last time step
×10^6
5.6905
5.69
5.6895
5.689
5.6885
5.688
5.6875
5.687
5.6865
5.686
North (m)
5.65
5.66
5.67
5.68
5.69
5.7
5.71
5.72
5.73
5.65
East (m)
0.0005
0.00045
0.0004
0.00035
0.0003
0.00025
0.0002
0.00015
0.0001
5e-05
0

e)

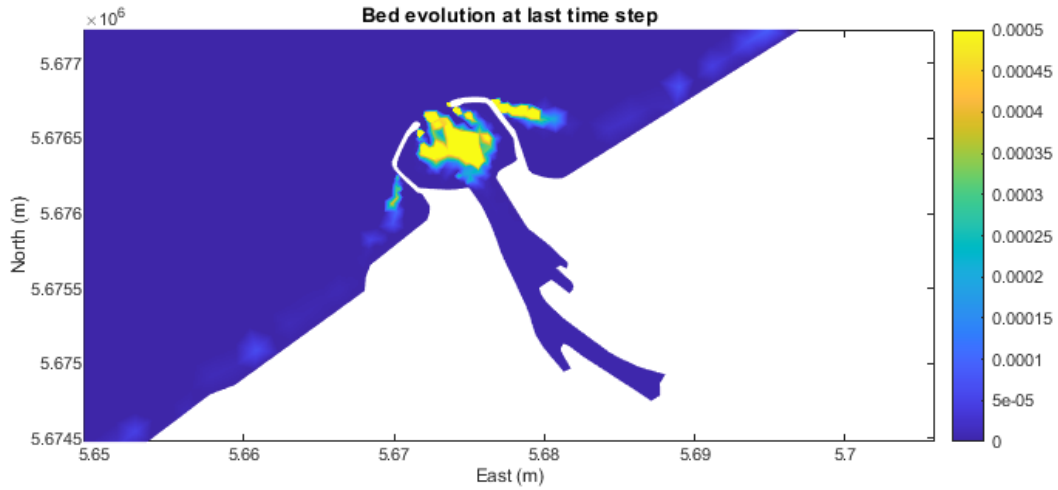
Bed evolution at last time step
×10^6
5.677
5.6765
5.676
5.6755
5.675
5.6745
North (m)
5.65
5.66
5.67
5.68
5.69
5.7
East (m)
0.0005
0.00045
0.0004
0.00035
0.0003
0.00025
0.0002
0.00015
0.0001
5e-05
0

f)

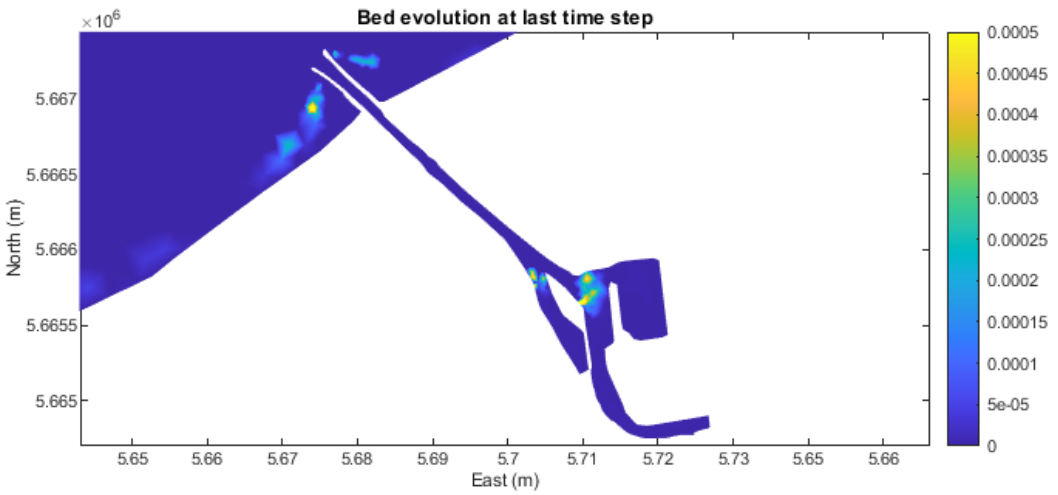

Fig. 32 Bed evolution [m] at the end of the model run with initially imposed plastic concentration = 1 particle/m^3 Figures show the zoomed-in area of a) Antwerp, b) Terneuzen, c) Vlissingen, d) Zeebrugge, e) Ostend, f) Nieuwpoort.

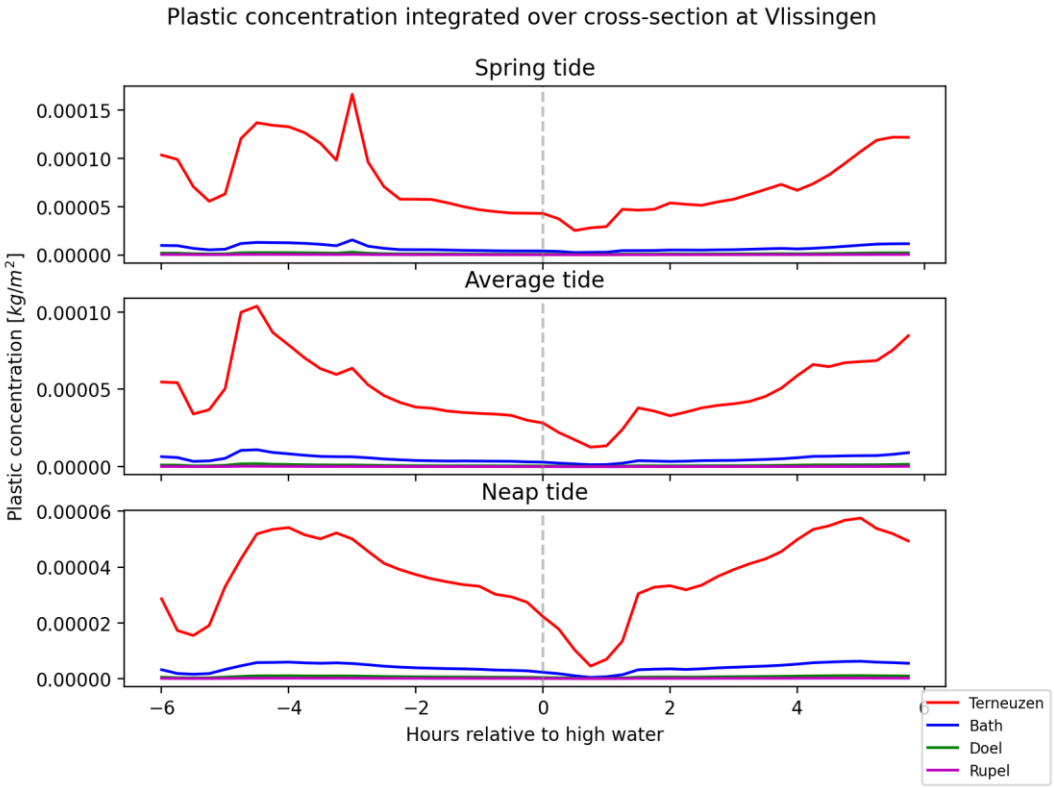

Fig. 33 Plastic concentration integrated over the cross-section at Vlissingen over the last spring-neap cycle. Each line plot shows the median concentration over the flood-ebb period across the cross-section when injected at four different locations, i.e., Terneuzen, Bath, Doel and Rupel.

Results: Scenario 2

A constant flux of particles (1 particle/m^2/s) is injected as a point source at four selected locations. The four locations are Terneuzen, BE-NL border point (close to Bath), Doel and Rupel confluence. The transport of injected particles is analysed.

In Fig. 33, the median plastic concentration over several flood-ebb cycles which are integrated over the cross-section at Vlissingen is shown for different tidal conditions. The flood-ebb cycles for the last spring-ebb cycle (15-11-2020 to 30-11-2020) are considered in the analysis. The plastics injected from Terneuzen alone is the dominant plastic concentration. However, the other locations, i.e. Bath, Doel and the Rupel confluence contribute significantly lower concentrations at the mouth of the estuary. In the other words, plastic injected at these three locations seldom reaches the mouth of the estuary. We can conclude, the source points of plastic upstream of Bath has very little contribution to the plastic concentration that reaches the sea.

a)

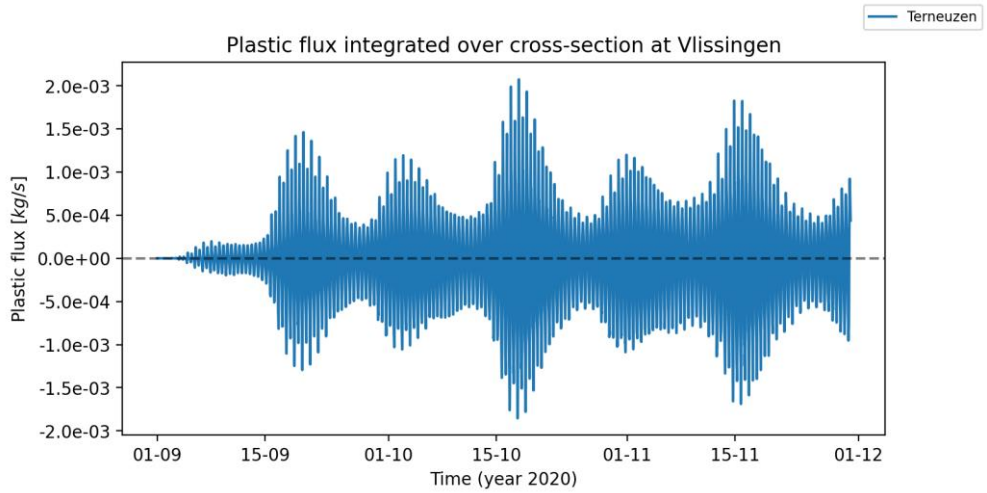

b)

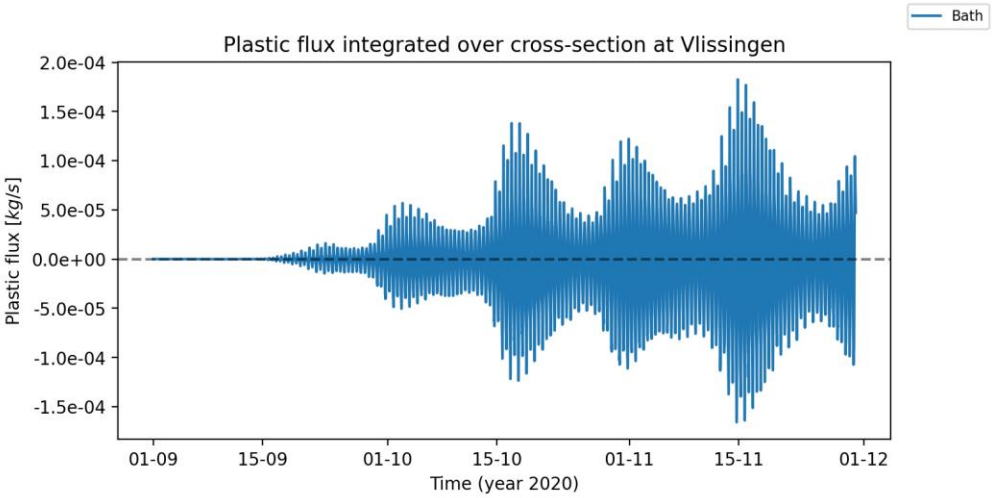

c)

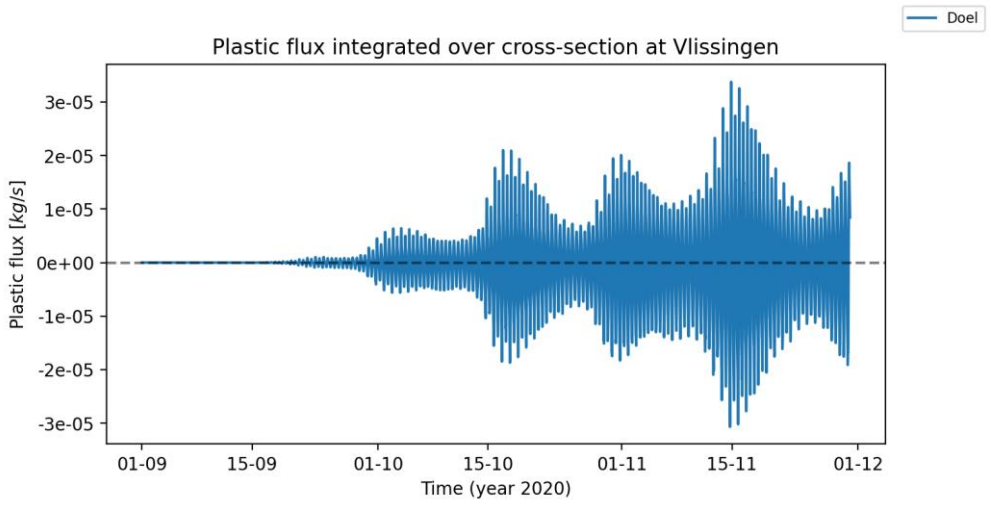

d)

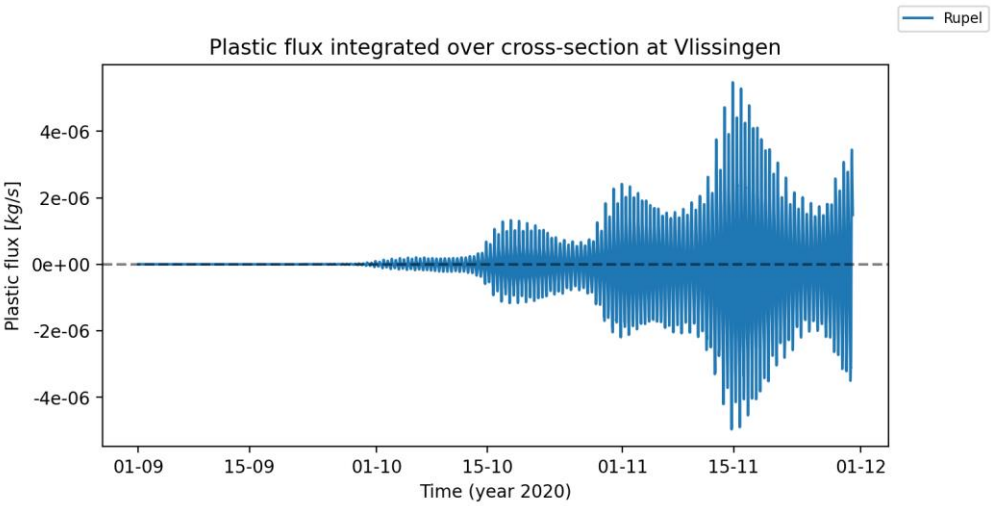

Fig. 34 Plastic flux integrated over the cross-section at Vlissingen for the three months of model run. Figures for point source at a) Terneuzen, b) Bath, c) Doel, d) Rupel confluence. Model run with point sources at a constant rate 1 particle/second. Notice the different vertical scales.

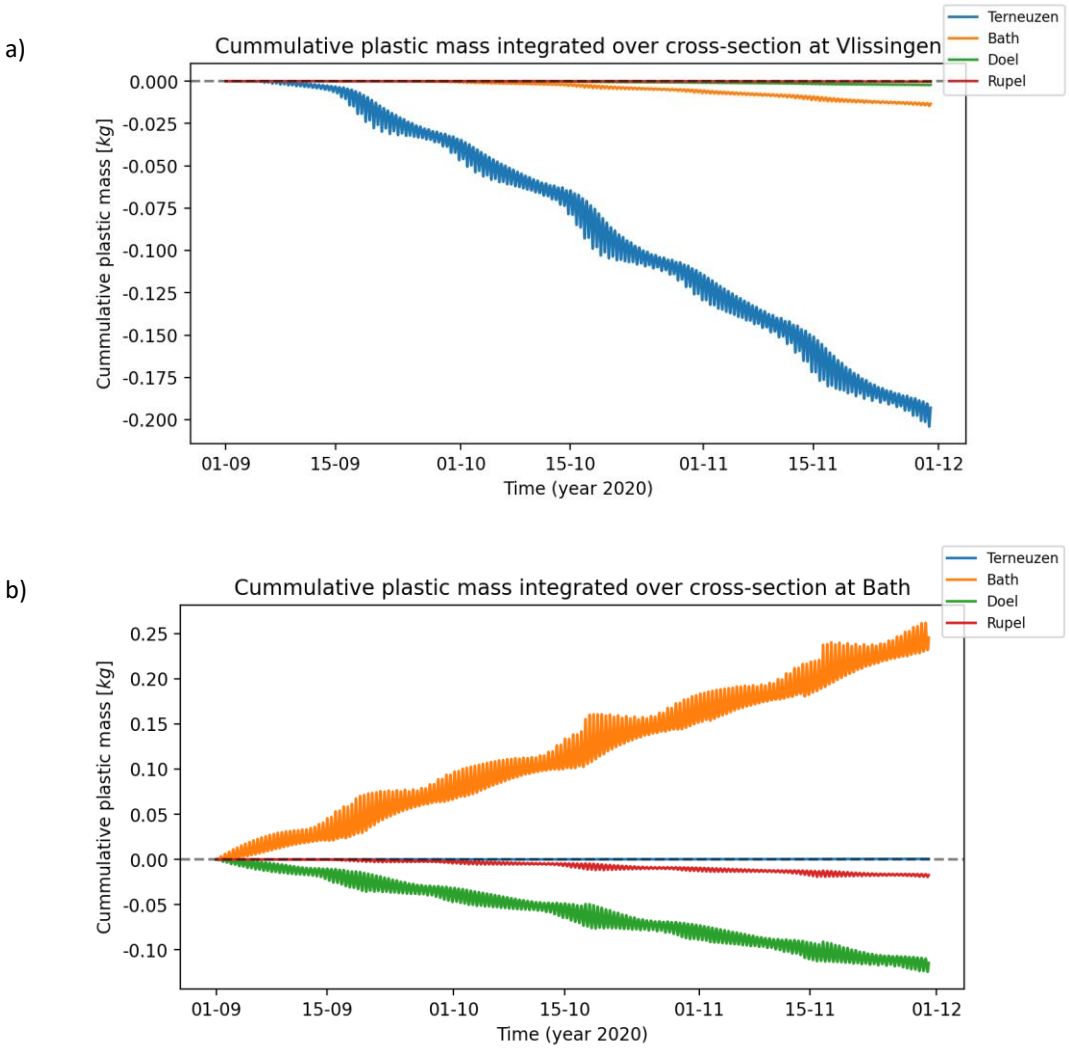

Fig. 35 Cumulative plastic flux across the cross-sections at a) Vlissingen and b) Bath for the three months of model run with four sources of plastics i.e., Terneuzen, Bath, Doel and Rupel confluence. The positive and negative values indicate the landward and seaward directions respectively.

In Fig. 34, the time evolution of the plastic flux across the Vlissingen cross-section is shown for the four injection points. The flux is considered positive if it is entering the estuary and negative if it is entering the sea. The magnitude of the flux reaching the estuary mouth from source points Terneuzen, Bath, Doel and Rupel are in a decreasing order of magnitude 10 i.e., 2.e-03, 2.e-04, 3.e-05 and 5.e-06 [kg/s] respectively. However these quantities are negligible in comparison to the total plastic quantity injected at each of the four locations i.e., 575 kg. The positive and negative fluxes seem to be mirroring each other, implying that the net flux is close to zero or in other words, the plastic injected from the 4 points of the estuary is trapped within the estuary during the period of model investigation. The time scale of the plastic transport from these injection points is also revealed in the flux plots in Fig. 34. A significant number of plastic items

from the Terneuzen point source reaches the mouth of the estuary within 3 days, from Bath within 15 days, from Doel within 17 days and from the Rupel confluence within 28 days.

In Fig. 35 the cumulative values from Fig. 34 are presented over the model run period for two cross sections at Vlissingen and Bath. At the Vlissingen cross-section (Fig. 35a), the plastic flux from the Terneuzen source point is the predominant one, with marginal flux also reaching from Bath. Both of these masses are negligible in comparison to the total quantity of plastic injected from individual sources. However the net flux is towards the sea for all 4 source locations. This actually reflects the net diffusive transport resulting from the concentration gradient, which is negative towards the sea. At the Bath cross-section (Fig. 35b), the cumulative flux of the Bath source point is the only significant positive value, though the absolute value of this cumulative flux is negligible to the total quantity injected at the source point. The primary explanation from this apparent different trend again is net diffusive dispersal.

a)

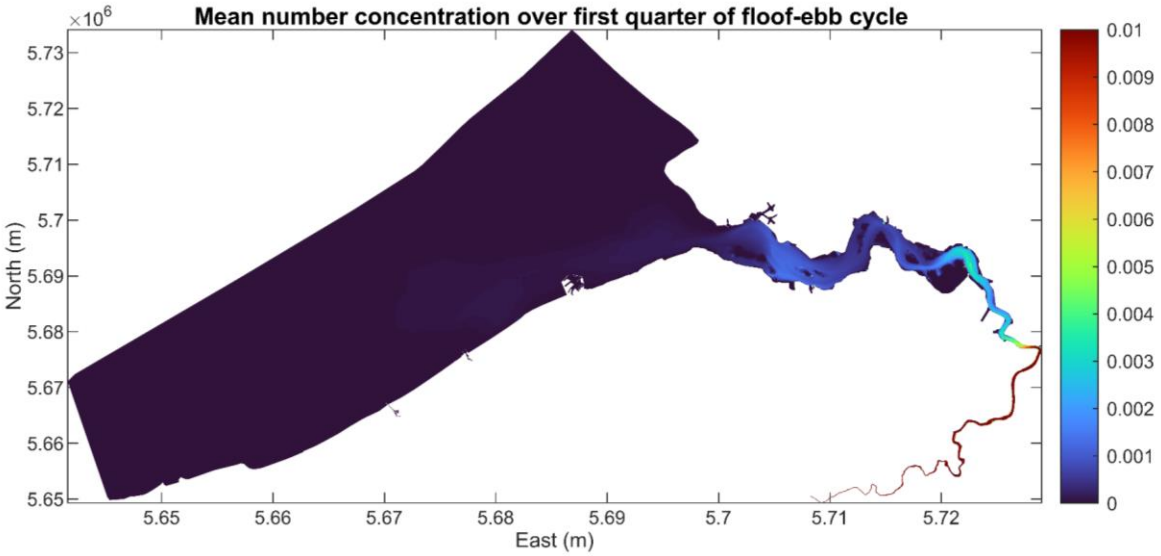

b)

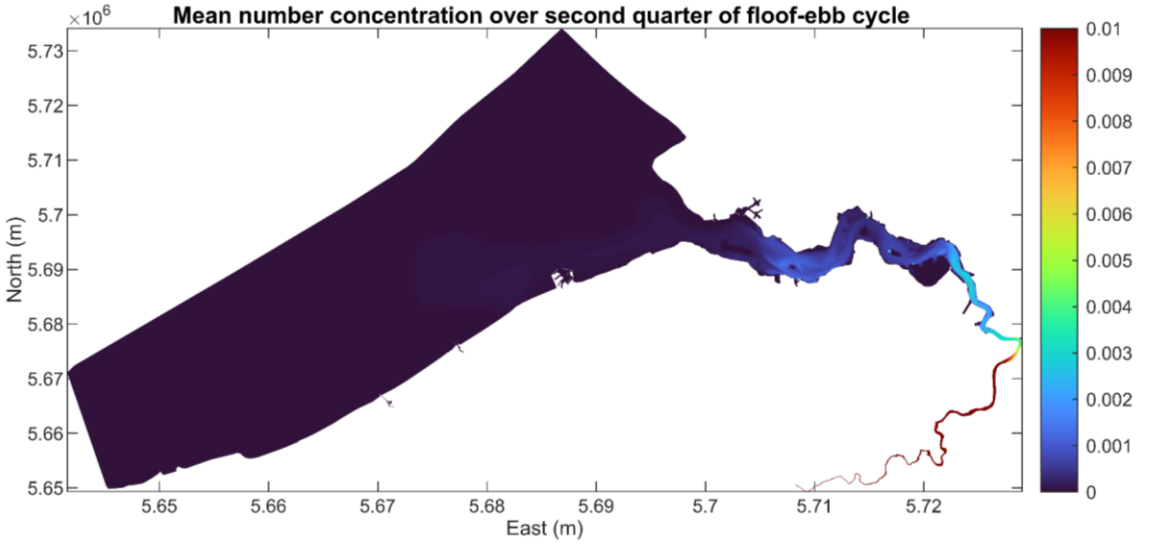

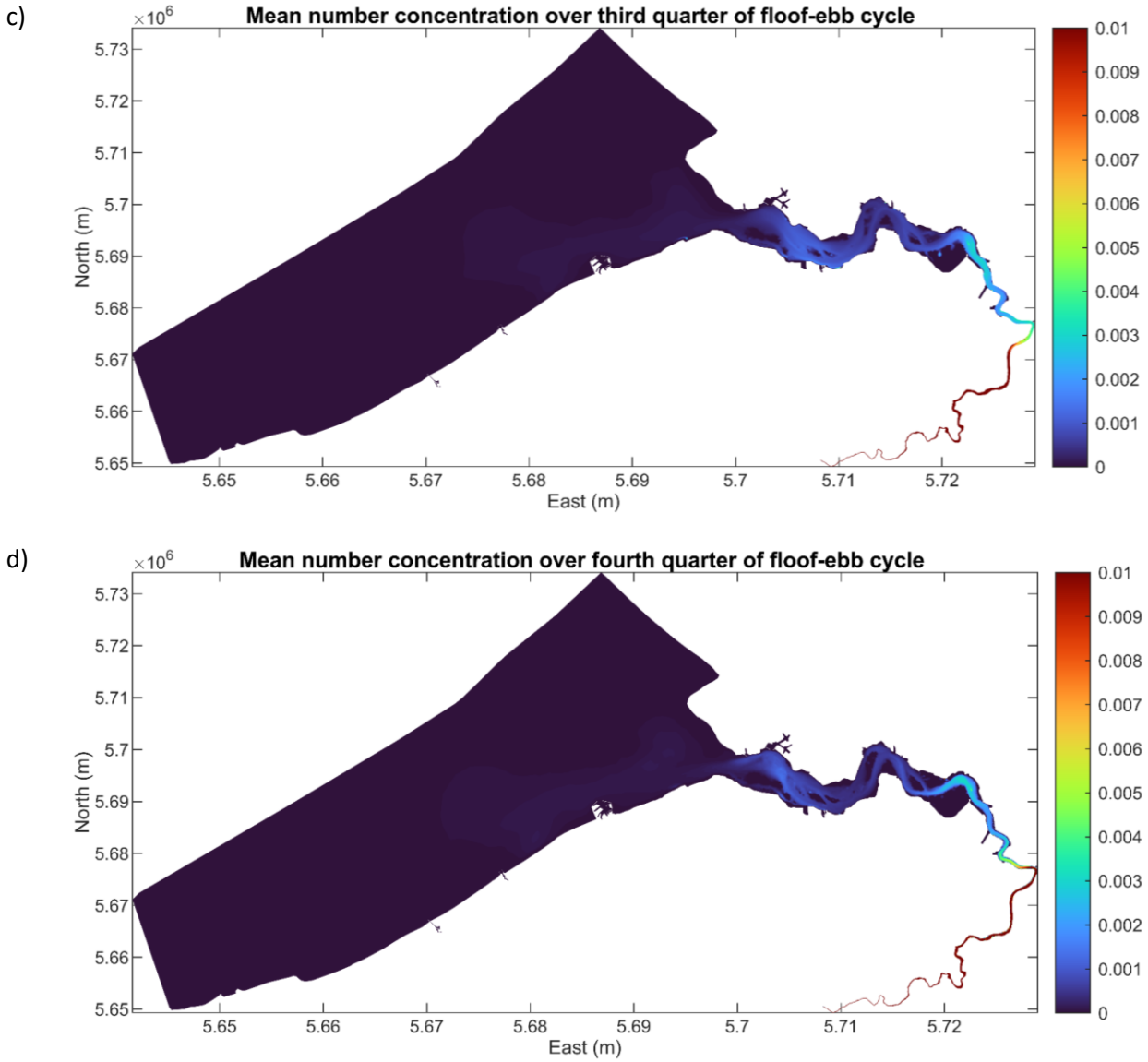

Fig. 36 Mean number concentration [number/m^3] of the plastic particles for the model run with point sources at a constant rate 1 particle/s. Figures show the total number concentration averaged over each quarter (3 hours each) of the last flood-ebb cycle (from 29 Nov 08:45 to 29 Nov 20:45) of the model result.

The Doel and Rupel source points have marginal negative cumulative flux indicating very little net flux towards the intertidal area. The plastic flux from the Terneuzen point source is not significant at the Bath cross-section. In other words, at this cross-section very few plastics from Bath location will move upstream (landward) and very few plastics from Doel and Rupel move towards the intertidal areas (seaward).

In Fig. 36, the plastic number concentrations averaged over each quarter of a flood-ebb cycle are shown. Here plastic from all the source points is combined. It is noted that the plastic concentrations are much higher in the narrow river sections upstream of Doel as compared to the intertidal area. This is likely due

to the large tidal water volume that is available in the intertidal area leading to dilution of particles in large water volumes. In contrast to the estuary, very low plastic concentrations can be seen in the sea. This reinforces the observation from other scenario investigations that the estuary acts as a trap for the plastic particles.

a)

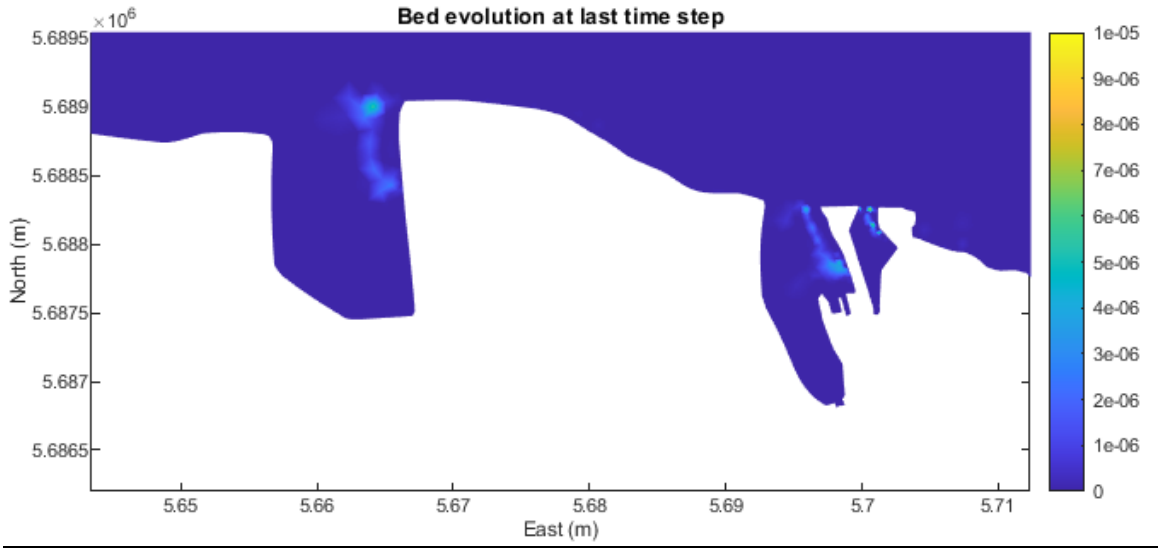

b)

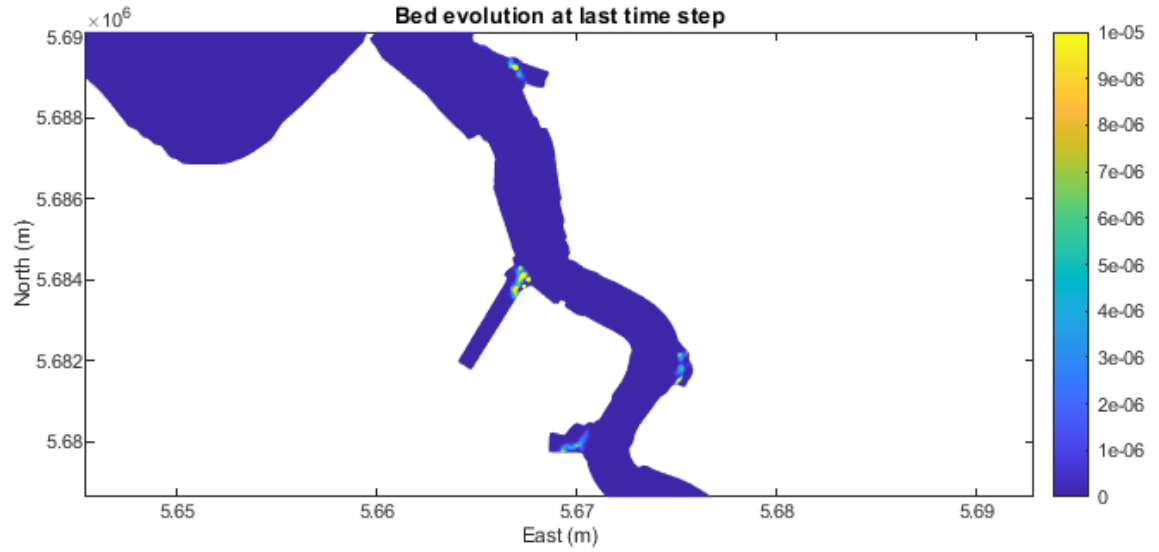

Fig. 37 Bed evolution [m] at the end of the model run with point sources at a constant rate 1 particle/s. Figures showing a)Terneuzen b) Antwerpen

In Fig. 37, the bed evolution at the last time step of the model (30-11-2020 00:00) is shown. The bed evolution is a combined effect of all the 4 point sources of plastic. The highest bed evolution occurs on the sharp curves of the bank of the river upstream of Bath and around the locks in the Doel / Antwerpen area. Slightly lower bed evolution can also be seen in the Terneuzen area. These are the locations very

close to the point sources of plastic used in the model. These locations of high depositions are characterised by port infrastructures (sluices/locks and docks) which generate low-energy environments. As they tend to form a pool of water, seldom disturbed, the deposition process is enabled. However, it is important to note that the actual flow across these infrastructures is not included in the model. The deposition forms could be significantly different if there are high velocity flows occurring in these areas as part of the operation of the sluices and locks.

Results: Scenario 3

A constant flux of particles (1 particle/m^3) is injected at the off-shore sea boundary for the entire time duration of the model run.

> ***Remark:*** *It should be noted that this condition is the least realistic among the 3 scenarios, and most likely overpredicts the real conditions. A uniform concentration along the boundary is unlikely. Moreover, it is known from the literature that the amounts of suspended plastics in offshore waters are low. It would be more realistic to run this case again in the future with boundary fluxes computed by a larger North Sea model.*

This scenario reveals the transport timescales and paths that plastic entering the domain from the sea boundary would take. In Fig. 38, the plastic flux is shown for the model run time, integrated across the cross-section at the Vlissingen and Bath. The plastic flux peaks at the same time as the highest amplitude of the spring tide (16-11-2020) at the Vlissingen cross-section. However, the peak positive flux is slightly greater (> 3 kg/s) than the negative flux (< 3 kg/s), indicating that the net flux is transported towards the estuary. The flux that reaches the cross-section at the Bath, is 1000 times less than that of at the Vlissingen cross-section. These observations imply the significant part of net plastic flux reaching the estuary from the sea does not move upstream of the Bath and is trapped within the wider estuary region.

Figure 39 shows the average number concentration of plastic particles during each quarter of a flood-ebb cycle. It is observed that plastic concentration in the range 1-2 particles/m^3 crosses the Vlissingen area to reach the estuary but does not travel beyond ~20 km into the upstream. During the second and third quarter, the plastic travels the most into the estuary as compared to the first and fourth quarter. A highly concentrated zone is formed around the Ostend port, as observed also in scenario 1.

a)

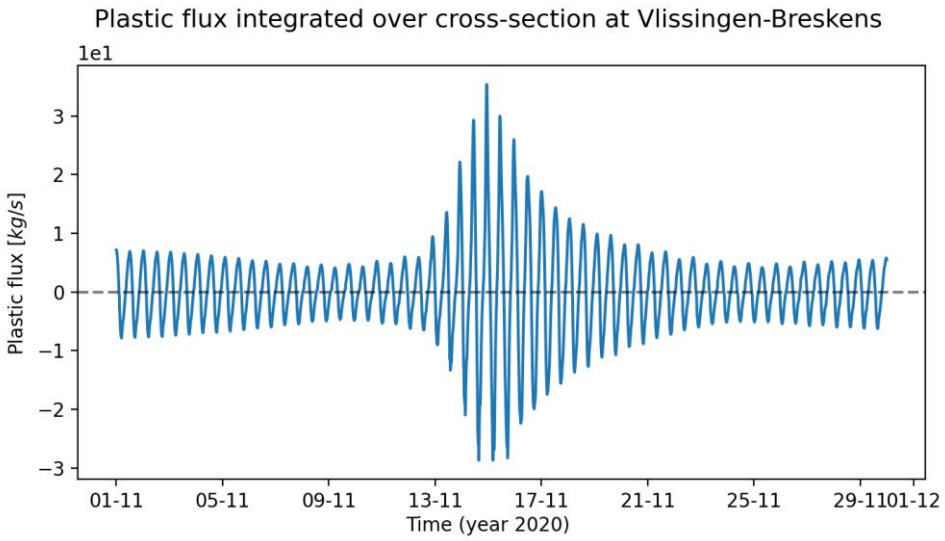

b)

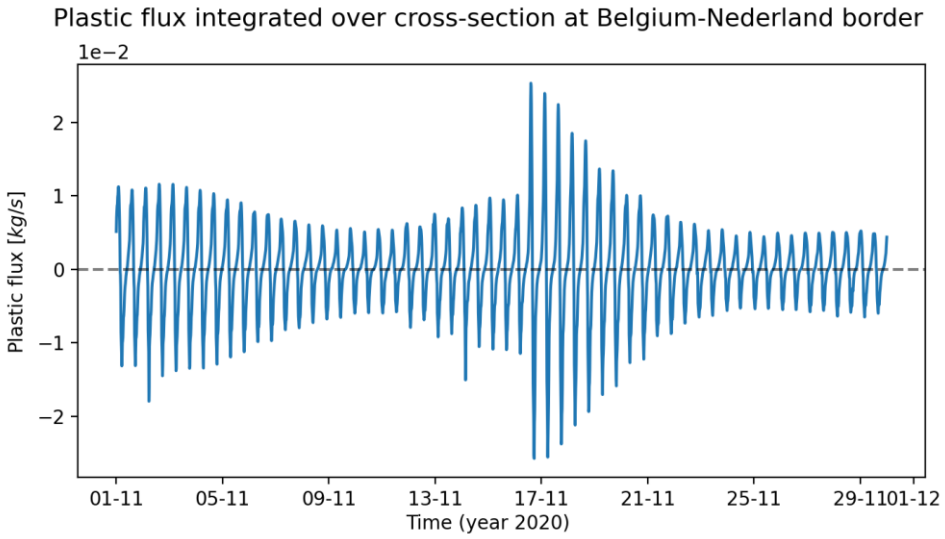

Fig. 38 Plastic flux integrated over the cross-section at Vlissingen for the November month of model run with sea boundary concentration imposed at 1 particle/m^3

a)

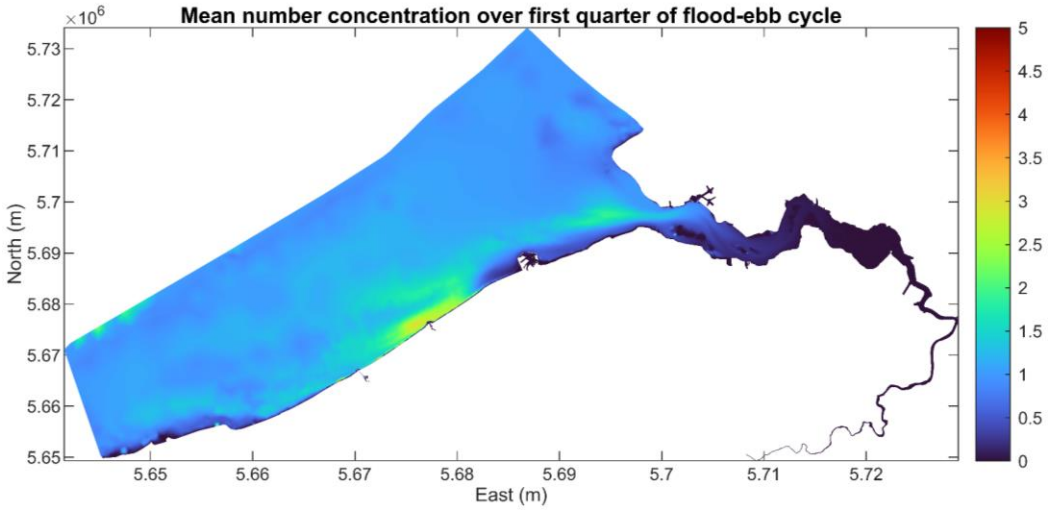
Mean number concentration over first quarter of flood-ebb cycle
×10^6
North (m)
East (m)
5.65
5.66
5.67
5.68
5.69
5.7
5.71
5.72
5.73
0
0.5
1
1.5
2
2.5
3
3.5
4
4.5
5

b)

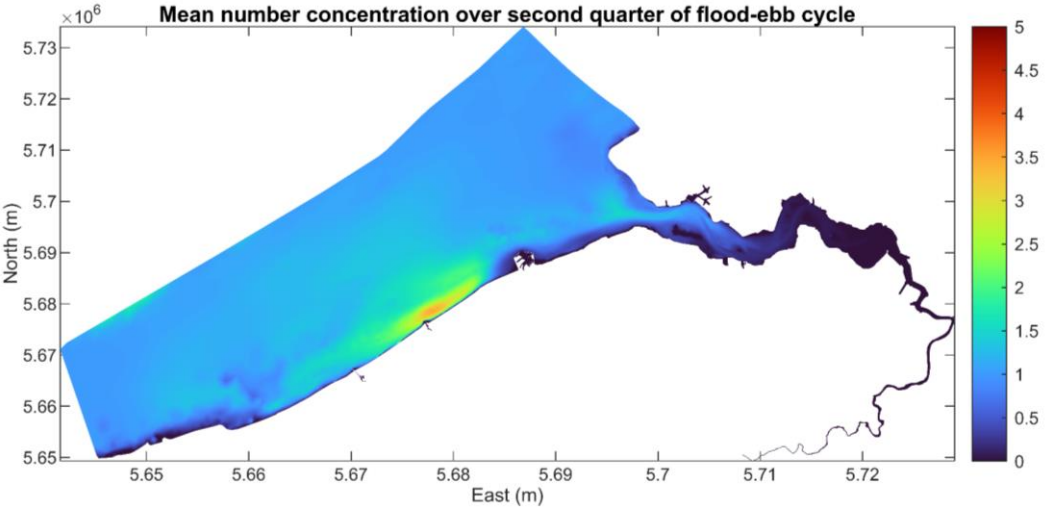
Mean number concentration over second quarter of flood-ebb cycle
×10^6
North (m)
East (m)
5.65
5.66
5.67
5.68
5.69
5.7
5.71
5.72
5.73
0
0.5
1
1.5
2
2.5
3
3.5
4
4.5
5

c)

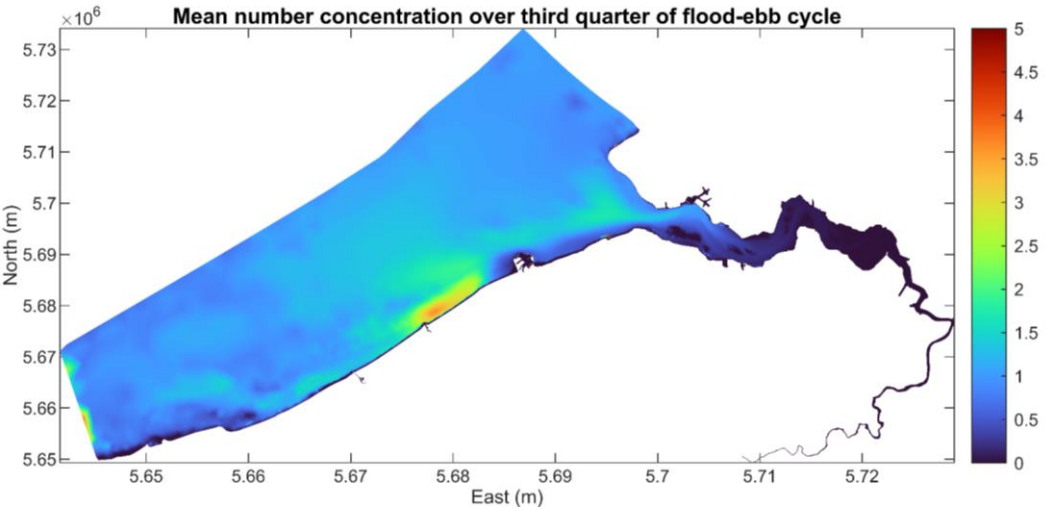
Mean number concentration over third quarter of flood-ebb cycle
×10^6
North (m)
East (m)
5.65
5.66
5.67
5.68
5.69
5.7
5.71
5.72
5.73
0
0.5
1
1.5
2
2.5
3
3.5
4
4.5
5

d)

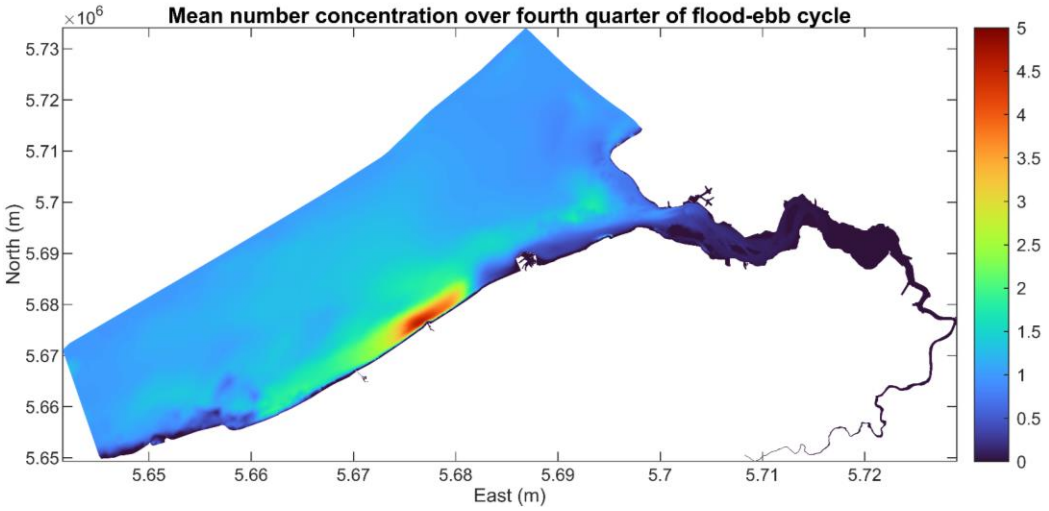

Fig. 39 Mean number concentration of the plastic particles for the model run with off-shore boundary imposed concentration = 1 particle/m^3. Figures show the average number concentration over 4 quarters (3 hours each) of the last flood-ebb cycle (from 29 Nov 08:45 to 29 Nov 20:45) of the model result.

In Fig. 40, the bed evolutions are shown for the last time step of the model run (30-11-2020 00:00). Only the areas where significant bed deposition is observed are shown here. The highest bed deposition occurs at the Vlissingen-Oost port. The ports of Zeebrugge and Ostend show a similar range of deposition, while Nieuwpoort shows considerably low depositions. It is interesting to note that, even though the concentrated accumulation zone occurs around the Port of Ostend, the deposition quantities do not reflect this fact. One of the explanations could be that the rate of deposition is largely cancelled out by the rate of erosion, leading to overall lesser bed evolution. Again, it should be noted that the deposition forms could be significantly different if there are high velocity flows occurring in these areas as part of the operation of the sluices and lock of the port.

a)

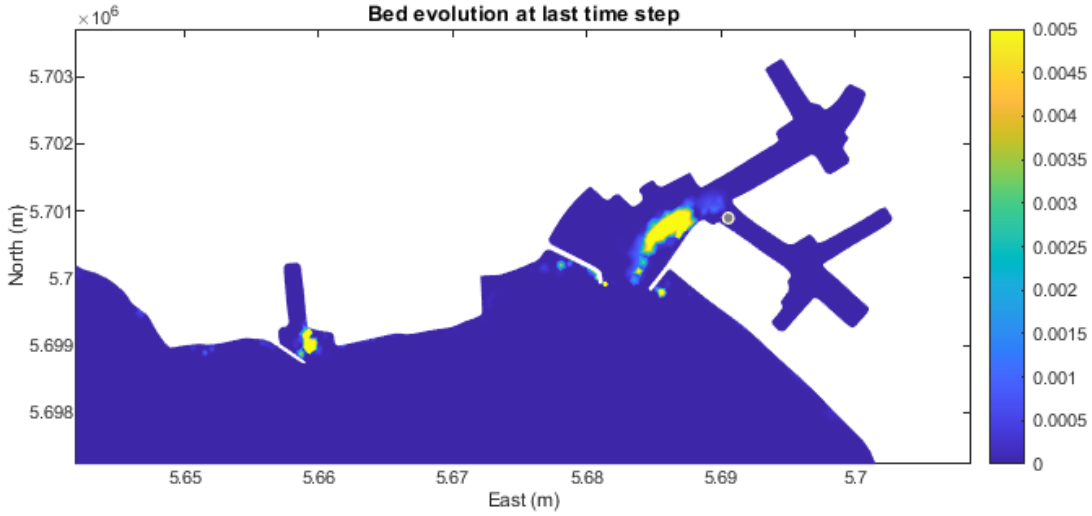
Bed evolution at last time step
×10^6
5.703
5.702
5.701
5.7
5.699
5.698
North (m)
5.65
5.66
5.67
5.68
5.69
5.7
East (m)
0.005
0.0045
0.004
0.0035
0.003
0.0025
0.002
0.0015
0.001
0.0005
0

b)

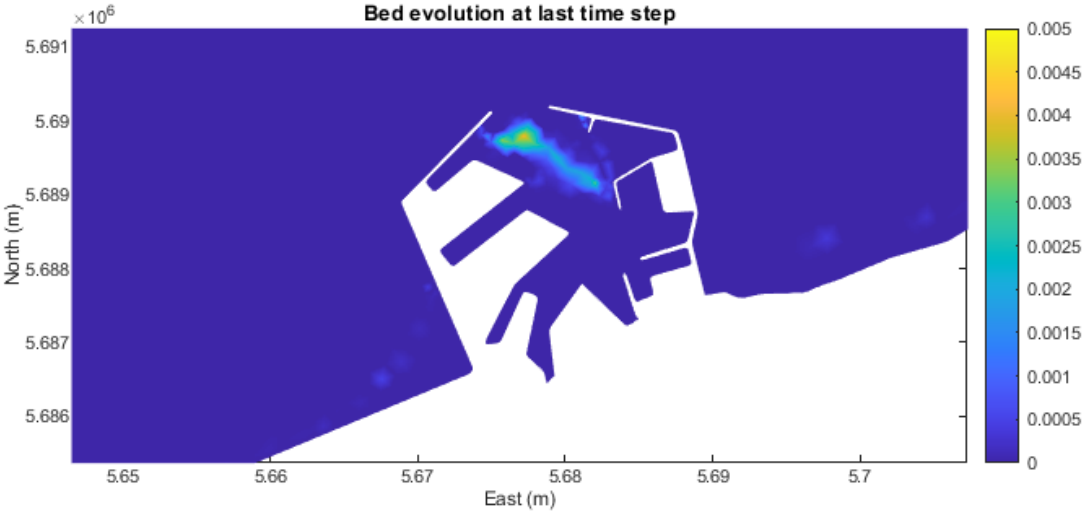
Bed evolution at last time step
×10^6
5.691
5.69
5.689
5.688
5.687
5.686
North (m)
5.65
5.66
5.67
5.68
5.69
5.7
East (m)
0.005
0.0045
0.004
0.0035
0.003
0.0025
0.002
0.0015
0.001
0.0005
0

c)

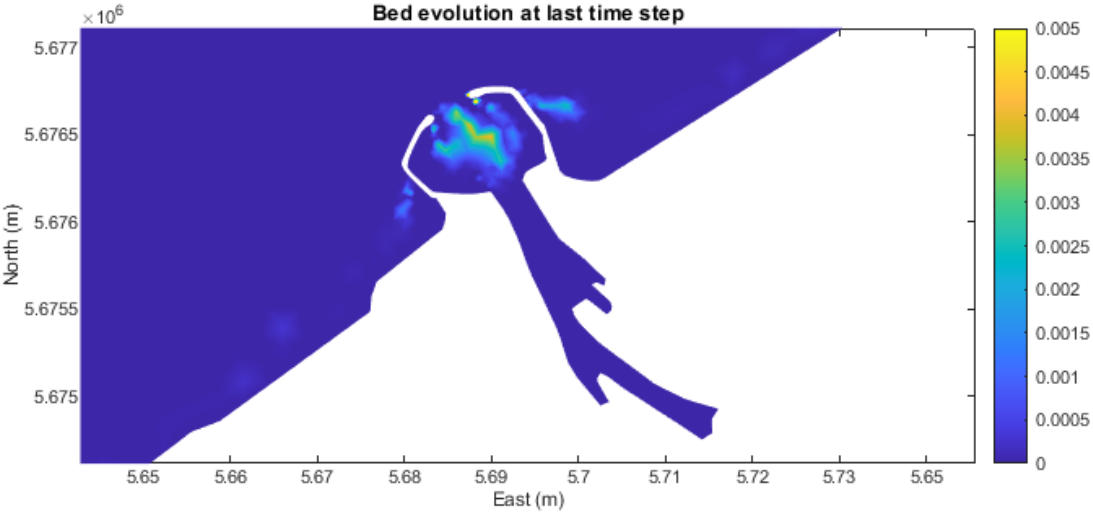
Bed evolution at last time step
×10^6
5.677
5.6765
5.676
5.6755
5.675
North (m)
5.65
5.66
5.67
5.68
5.69
5.7
5.71
5.72
5.73
5.65
East (m)
0.005
0.0045
0.004
0.0035
0.003
0.0025
0.002
0.0015
0.001
0.0005
0

d)

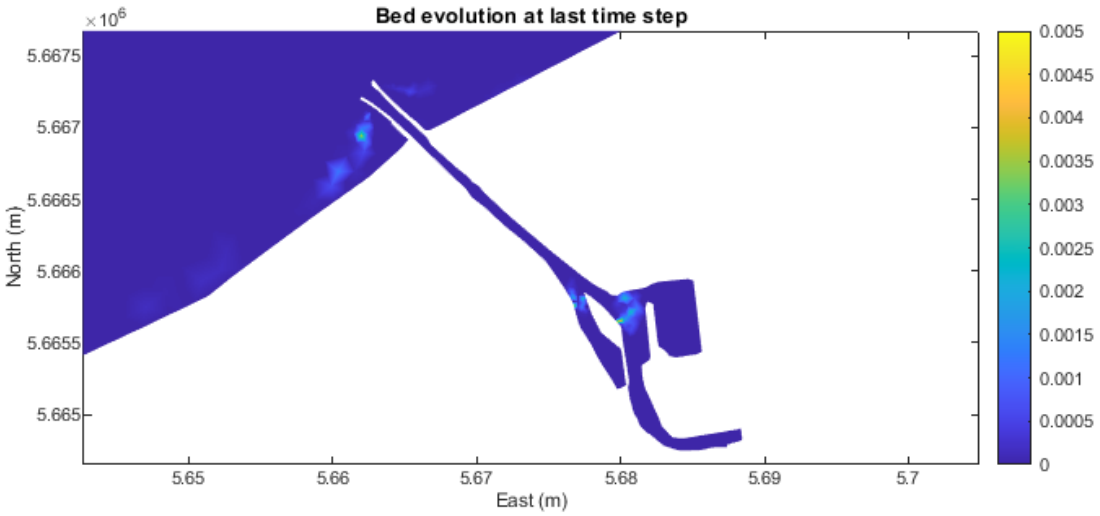

Fig. 40 Bed evolution at the end of the model run with off-shore boundary imposed concentration of 1 particle/m^3. Figures show zoomed-in on the areas of a) Vlissingen, b) Zeebrugge, c) Ostend, and d) Nieuwpoort.

Interpretation of model results for different polymer types

The model results are obtained for a selected *reference* plastic particle with density 1131 kg/m3 and size of 5 mm (one of the particles investigated in the study of Khatmullina and Isachenko (2017), which has a corresponding settling velocity of 0.127 m/s.

In order to interpret the model results correctly for other non-buoyant (i.e. sinking) particles, taken into account that boundary conditions are defined in terms of mass concentration or mass flux, one has to replace 1 particle of the reference material by another number of particles (*N*) of another size (*d*) in order to guarantee the same setting velocity and the same mass balance.

The procedure to compute these parameters is presented in Annex D and yields the following table for the most common polymer with density higher than that of water.

Polymer	Density (kg/m^3)	*N* (# particles)	Size *d* (mm)
PS	1040	0.5	13.5
reference	1131	1	5.0
PET	1350	8	2.3
PVC	1425	12	2.0

11. Conclusions on the model results

The following *qualitative* results are obtained:

- Plastic particles in suspension move up and down with the tide in the estuary, but their travel does not extend beyond 20 km. The particles from Terneuzen up to the Bath do reach the estuary mouth but are brought back landwards with the next flood. The majority of particles from upstream of the Bath do not cross the Vlissingen section. The tested scenarios suggest that the Scheldt estuary is a major sink for plastics.
- The small net dispersive fluxes over spring-neap cycles at different cross-sections can be explained by the concentration gradients resulting from not considering background concentrations of historical plastic sources for which no data are available. Concentration gradients induce diffusion-like transport in the opposite direction of the gradient.
- The particles from the uniform initial concentration show the tendency to accumulate at the edge of the water on intertidal areas. This suggests that beaching is a very important process, more important than accumulation on the bottom. However, one has to bear in mind that aggregation with cohesive sediment aggregates has not yet been taken into account. The latter process is expected to greatly enhance the deposition of microplastics, reducing its dispersal even further.

The simulations need to be repeated after the model has been upgraded to a much improved version that can handle additional processes, which currently are neglected. By that time additional data, that will be collected in the meantime, will also be incorporated in the validation of the model, which should allow to generate some confidence in the actual estimated values.

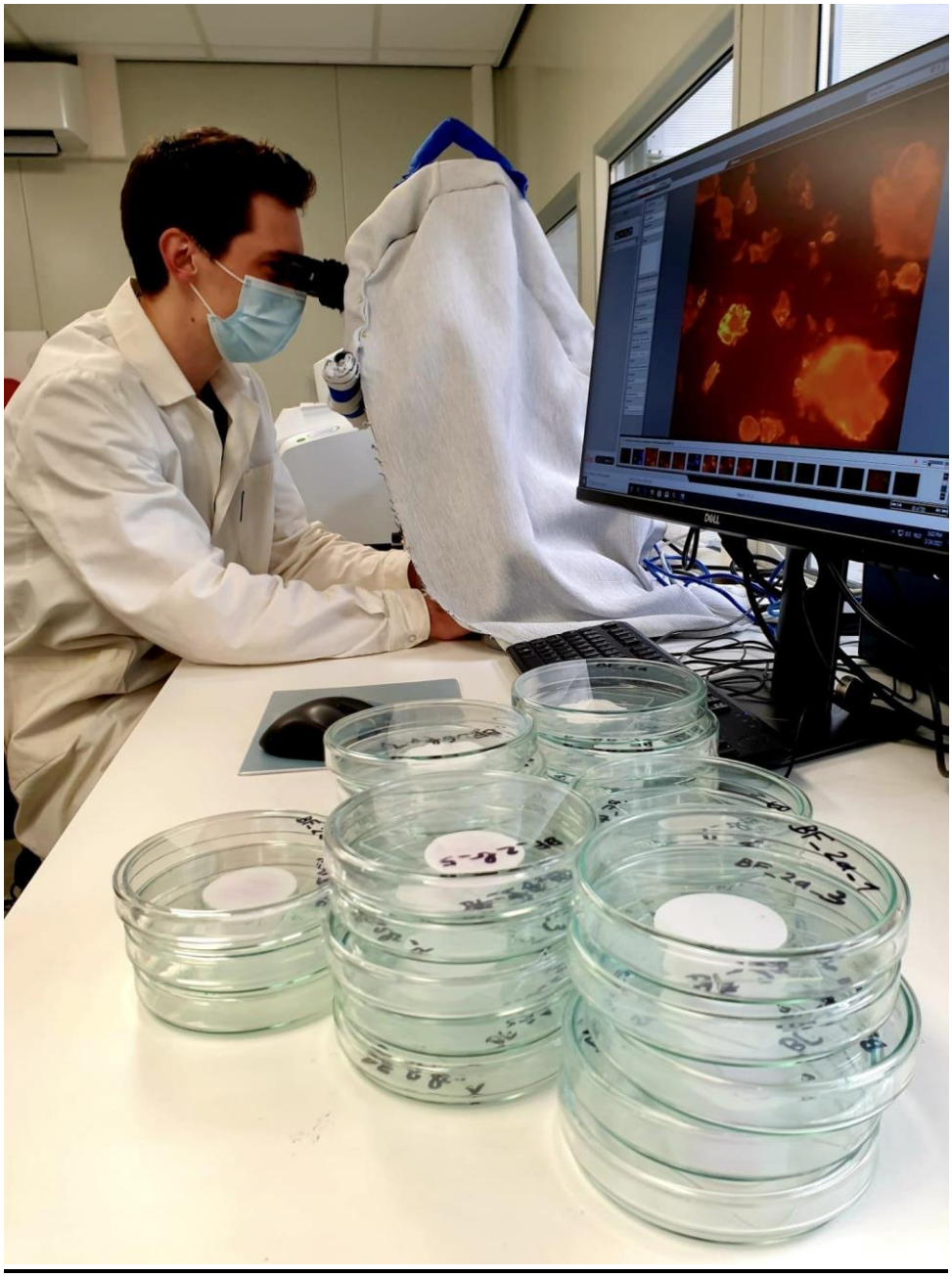

Chapter 5
Discussion and conclusions

Discussion

Plastics have been detected in all selected sampling locations, i.e. in the river Yser in Nieuwpoort, in the port of Ostend and in the river Scheldt downstream from Antwerp, in the Ghent-Terneuzen canal, and in the port of Antwerp (Belgium; Fig. 2-6). Micro- and macroplastics have been observed in the sediment and aqueous compartments at all sampling sites. In two samples, in the Insteekdok in Zelzate, of in total 346 samples no macroplastic have been observed. The results indicated that plastic is an abundant pollutant in riverine and estuarine ecosystems in Flanders. The results of the sampling campaigns in 2020 and 2021 generally support the statement that plastic is ubiquitous in the environment (Fahrenkamp-Uppenbrink, 2008).

Based on the current consortium's experience with sampling for plastic and our involvement in multiple past and ongoing European projects, we presented state of the art sampling protocols and laboratory procedures in the 2020 report. The detailed sampling protocols are open for consultation in the annexes of the 2020 report, and available in short versions in Annex B of the present report, to enable the same protocols to be applied in the 2024-2025 evaluation projects, and thus to allow a fair and honest comparison with the data and fluxes calculated to date. Although plastic is ubiquitous in the aquatic environment, the volumes sampled (i.e. the volume of water passing through a sampling net, or the weight of sediment collected) need to be substantial to account for the 'natural' spatiotemporal variability of plastic pollution. This recommendation as well as other guidelines are integrated in our detailed protocols. The need for a substantial sampling weight is the main reason why in the present report no macroplastic sediment concentrations are being reported for the river Yser in Nieuwpoort, in the port of Ostend, in the Ghent-Terneuzen canal, and in the port of Antwerp. The weight and volume of sediment collected with the Van Veen grab was too small to accurately quantify the macroplastic pollution. Although the developed protocols result in reliable and accurate quantification of the plastic pollution, the manual field sampling and laboratory processing of the samples remains labor-intensive (Annex B and C). Also, the use of a research vessel to sample for plastic is expensive. In the coming years, to be able to feed the plastic dispersion model with an increasing series of data, further investments are needed to develop an automated and cost-efficient sampling and laboratory preocedure. In this project, because of the mutual interest of the plastic data for the PLUXIN project, all ship time and part of the laboratory work was regarded as an in kind contribution by the project consortium. In case that large volumes of water need to be sampled, other trustworthy sampling devices such as a automated size-fractionation Ferrybox system modified for plastic sampling as developed in the ANDROMEDA project and that can be operated also from ships of opportunity can be a possible alternative.

The plastic concentrations vary spatially, and the highest microplastic concentrations have been observed in the river Scheldt. On average, the surface water of the river Scheldt contained 42.9 ± 70.6 particles/m³ microplastics (Table 3a). In surface water of the port of Ostend (8.6 ± 13.2 part/m³; Table 4a) and in the river Yser in Nieuwpoort (6.8 ± 7.5 particles/m³; Table 5a) the number of microplastic was five- to tenfold lower than the microplastic concentrations observed in the river Scheldt. These concentrations are in line with microplastic concentrations reported in other European rivers, estuaries and ports. Although not the goal of the current project, these observed concentrations have been compared with preliminary science-

based safe concentrations (i.e. Everaert et al., 2018; Besseling et al., 2019; Everaert et al., 2020) that are regarded as threshold above which negative effects for the estuarine ecosystem can potentially happen. It was found that the microplastic concentrations observed remained orders of magnitude below the safe environmental thresholds of $7.99 * 10^3 – 1.49 * 10^6$ part/m³ (Everaert et al., 2018), but in the present research only micropastic > 100µm have been considered.

In terms of macroplastic, we observed a high spatial variation with port areas being more polluted than estuarine environments. On average, the surface water of the river Scheldt contained 14.2 ± 59.5 g/1000 m³ macroplastic (Table 3b). In the port of Ostend on average 8.8 ± 35.2 g/1000 m³ macroplastic have been observed (Table 4b). As such, the mass of macroplastic in the surface water of the river Scheldt is comparable to the mass of macroplastic observed in the port of Ostend. The mass of macroplastics observed in the river Yser (0.6 ± 2.4 g/1000 m³) is about one order of magnitude lower than the concentration observed in Ostend (Table 5b). Inside the port of Antwerp and in the Ghent-Terneuzen canal the mass of macroplastics is 727 ± 2056 g/1000 m³ and 841 ± 2440 g/1000 m³, respectively (Table 6 and 7). The port of Antwerp and in the Ghent-Terneuzen canal are considered to be hotspots of pollution of buoyant macroplastic. However, also inside the port there are large spatial differences (Table 6 and 7).

All sediment samples contained microplastics, and the concentrations ranged on average from 4301.6 ± 4926.8 part kg DW^{-1} in Wintam to 1214.7 ± 849.9 part kg DW^{-1} in Doel. On average, the Scheldt estuary downstream from Temse Bridge contained 2757.7 ± 3559.7 part kg DW^{-1} (Table 3a). The sediment in the Tijdok in the port of Ostend did contain 4058.1 ± 6590.4 part kg DW^{-1} (Table 4a), a concentration comparable to the sediment microplastic concentrations observed in Wintam. In the sediment of the river Yser, close to Portus Novus, microplastics were present at a concentration of 2824.8 ± 5660.5 part kg DW^{-1}. Overall, all sediment compartments appeared to be heavily polluted with the microplastics, even at levels that exceed the preliminary science-based safe threshold of 540 part kg DW^{-1} as defined in Everaert et al. (2018), but still one order of magnitude lower than a more recent safe threshold of $2.2 * 10^5$ part kg DW^{-1} (Besseling et al., 2019). Note, that this risk estimate was not the goal of the present research and should be interpreted with caution.

Besides the large inter-region variability of plastic concentrations, an interesting intra-region gradient of variability of plastic concentrations has been suggested. In the river Scheldt, decreasing plastic concentration from the inland sampling location towards the coastal sampling location for both micro- and macroplastics were observed. In the river Scheldt, the macroplastic concentration at sampling location Doel was about a factor ten lower than the mass of macroplastics observed at sampling location Wintam (Table 3b). Interestingly, in the river Yser, an inverse trend was observed, i.e. highest plastic concentrations in the coastal sampling locations and lower concentration close to the Ganzepoot (Table 5b). This inverse trend in the river Yser was likely to be attributable to the tidal cycle regime (see further). The decreasing levels of plastics from the hinterland towards the marine environment that was observed in the river Scheldt corroborates with other European studies (Scherer et al., 2020; Van Emmerik et al., 2022). To allow a fair and honest comparison in 2024-2025 with the present data, it is important to take into account the spatial variability we detected. We recommend selecting multiple sampling locations in

one region, and not to rely on single spot sampling campaigns. As such, for the evaluation project it will be essential to predefine the sampling locations based on the present study and include tidal regimes, to account for the 'natural' variability of plastic pollution.

The plastic concentrations vary temporally as observed based on our tidal cycle campaigns (Fig. 20-22) and bimonthly spot samples. However, based on the current data it is not possible to make overall conclusions on the location-specific impact of the tidal cycle on the plastic concentrations. It is however, obvious that the tidal cycle data are a crucial component of the plastic flux model. A simple spot sampling campaign is insufficient to correctly quantify plastic concentrations and fluxes. To correctly estimate plastic concentrations a range of different sampling strategies are needed, amongst which tidal cycle campaigns, frequent spot samplings and seasonal samplings. As for the spatial variability (cfr. paragraph above), it is important to integrate this temporal variability in the plastic t_0 flux quantification, in order to normalize for the natural variability of the plastic concentrations.

In chapter 3 of this report, unprocessed plastic concentrations were presened and these have been used as an input to quantify the actual plastic flux in chapter 4. In chapter 3, the plastic concentrations were reported as the number of particles and fibres (i.e. part m^{-3}) for microplastics, and mass-based concentrations (i.e. g per $1000m^3$) for macroplastics. Before proceeding towards the actual modelling step, these units have been aligned. To do so, for each plastic item detected, its size dimensions, shape and polymer type were measured. The size frequency distributions clearly indicated that smaller sized plastics are more abundant than large plastics. This is a non-surprising (exponential) relation that has been reported earlier in literature (Kooi and Koelmans, 2019). From the size frequency distributions (Fig. 14 - 17), one can see that macroplastics are detected in low absolute numbers, and that microplastics are detected in high absolute numbers. Despite being very abundant, microplastics do not contribute a lot to the mass of plastics. To convert the individual plastic count data to a mass-based unit, we used particle size dimensions, shape, polymer type, and reported densities.

The actual plastic flux will be expressed in a mass-based unit. In theory, plastic concentrations could either be based on the number of particles and fibres detected (i.e. the counts), or alternatively expressed in mass-based units (cfr. previous paragraph). Regardless of the nature of the unit (i.e. numbers or masses), there is an absolute necessity to normalize the results for the volume of water (e.g. m^3) or sediment (kg DW) in which the plastic has been detected. Having in mind that: 1) larger plastics proportionally contribute more to the mass of plastic; 2) macroplastics are very often at the basis of the microplastic pollution; 3) macroplastics are more easily visually detected; and 4) large plastic are more easily manually removed from the aquatic environments, we would recommend to use a mass-based unit to report on the goals and achievements of the Flemish Integral Action Plan on Marine Litter. A common denominator used to normalize for plastics detected in water samples could be m^3. For plastics observed in the sediment, we would recommend normalizing for kg DW.

We detected clear spatial differences in the most dominant polymers. Polymers less dense than estuarine and coastal water (1.02-1.03 g cm^{-3}) such as PP (0.90 - 0.92 g cm^{-3}), PE (0.86 - 0.98 g cm^{-3}) and PS (0.96–

1.05 g cm^{-3}) dominated the samples taken at the water surface (Fig. 7-9; Table 8). In the surface water of the river Scheldt and in the port of Ostend, PP and PS were most often encountered, and this is in line with other international studies. In the port of Nieuwpoort however, we detected a high amount of PP, PET and PAM in the surface water (Fig. 9). PAM is a non-expected polymer type that is often used in agriculture, contact lenses and thickener for paints. The FTIR-spectrum of PAM is quite difficult to differentiate from the spectrum of water due to a broad peak between 3500 cm^{-1} and 2500 cm^{-1} (Fig. 10). The signal of water has a similar peak in that wavelength region. As such, it may be possible that some plastic particles (e.g. being of PP, PS or PP nature) that were still wet may have been misidentified as being PAM. This broad peak, either from water or PAM, is quite prominent and can cause mis-identification of particles. Therefore, the results on PAM should be interpreted with caution, and it requires further investigation whether PAM is indeed a polymer present is the samples. More than 90% of the buoyant macroplastics observed was of PP, PE, or PS origin (Table 8).
Sediment samples were dominated by dense polymers such as PET (1.38 g cm^{-3}), PAM (1.19 g cm^{-3}), and PS (0.96– 1.05 g cm^{-3}) (Fig. 11 - 13). In the sediment of the river Scheldt, PET contributed to 85% of the plastic pollution. In the port of Ostend, in more than two third (71%) of the cases we detected PS, and in one fifth of the cases (17%) we observed PAM. In the river Yser, PS was most prevalent (67%), next to PAM (25%). Overall, in terms of partitioning of the polymers in the aquatic environment, the physical-chemical expectations have been fulfilled. Light-weighted polymers are often observed at the water surface, whereas polymers denser than the ambient water sink to the sediment. Information of the polymer type is important to unravel the sources of pollution. If the focus is on macroplastic, stakeholders panels can be used to match the plastics items that were found with their original use.

For unravelling the plastic flux towards the marine environment, a hydrodynamic plastic dispersion model was used. This model consisted of an ensemble analysis, a flood-ebb cycle analysis, a flux analysis, and a residual mass flux analysis. By doing so, we were able to convert the mass-based plastic concentrations to a plastic flux and indicate the direction of flow at a given point in time. The hydrodynamic model was calibrated and validated and a general circulation pattern of the plastic transport was inferred. Three scenarios have been initiated to understand the whereabouts of the particles in time and space. **A first scenario** was run assuming a uniform particle concentration of 1 part m^{-3} (= 74 * 10^{-6} kg m^{-3}) in the entire study area at t_0. In this first scenario, it was calculated that the plastic concentration drops quickly after flood due to low flow velocities which enables the vertical downward movement and settling of particles. It was modelled that one major accumulation zone is located in the coastal nearshore area between the port of Ostend and the port of Zeebrugge (Fig. 30). In the Scheldt estuary, two distinct zones with higher than average plastic concentrations were identified, i.e. between Vlissingen and Bath, and upstream of Antwerp. Based on the residual plastic mass flux, the plastic transported towards the sea was mainly following ebb channels (Fig. 31). Plastic moving into the estuary mainly made use of flood channels. In the estuary, there are small-scale circulation patterns which suggest that plastic particles can be trapped and do not leave the estuarine region. It was suggested that some areas such as the port of Ostend have a net positive erosion-deposition rate, indicating that the flow hydrodynamic regime at that location is most favorable for plastic deposition (Fig. 32). A **second scenario** was run assuming a constant flux of particles of 1 part s^{-1} at four selected locations in the estuary during the entire simulation period. The simulated

injection of particles in the Scheldt estuary happened in Terneuzen, at the Dutch-Belgian border, in Doel and at the Rupel confluence. It was observed that only a fraction of the plastics from Terneuzen would contribute to the flux of plastic outside the Scheldt estuary into the North Sea (Fig. 33). A plastic source in Bath, Doel or close to the confluence of the Rupel would seldom reach the mouth of the estuary, i.e. would only to a very limited extent contribute to a plastic flux from the estuary to the North Sea. As such, sources of plastic upstream of the Dutch-Belgain border contributed little to the mass of plastic that reaches the North Sea. Therefore, the Flemish estuary of the river Scheldt is considered to function as a plastic reservoir (Fig. 34 and Fig. 35), with a plastic plume that moves around the plastic injection points (Fig. 36). A **third scenario** assumed a constant flux of 1 particle m^{-3} s^{-1} was imposed at the boundaries of the study area (Fig. 26) throughout the simulation period. This scenario indicated a net plastic flux towards the estuary, and the simulation implied that a significant part of the net plastic flux reaching the estuary does not move upstream of the Dutch-Belgian border, and is thus trapped in the estuary (Fig. 38). It was simulated that plastic particles entering the estuary typically travel about 20 km upstream. Also in this third scenario, a highly concentrated zone with plastic was formed around the port of Ostend (Fig. 39). **Overall**, plastic particles in suspension are expected to move up and down with the tide in the estuary, but their travel does not extend beyond 20 km. The simualtions indicated that plastic particles with point sources between Terneuzen and Bath did reach the estuary mouth but are brought back landwards with the next flood. The majority of particles from upstream of the Dutch-Belgian border did not cross the mouth of the estuary at the Vlissingen intersection. The tested scenarios suggested that the Scheldt estuary is a major sink for plastics. This finding is in line with recent international research (e.g. Van Emmerick et al., 2020). Plastic particles had the tendency to accumulate in intertidal areas, suggesting that beaching is a very important process, and may even be more important than accumulation on the river bed. Integration of some other key processes that affect the hydrodynamic behavior such as wave regimes, biofouling, and aggregation of small sized plastic with cohesive sediment aggregates may still alter the simulated patterns. The latter process is expected to enhance the deposition of microplastics, reducing its dispersal even further. As beaching is considered an important process, dedicated monitoring campaigns can be initiated to quantify the number and mass of plastic littered on the banks of the estuary. To do so, the hydrodynamic model be applied to select expected hotspots of pollution and the data obtained can be used to further validate the model. In future, citizen science initiatives could be a suitable tool to enable detection and quantification of the amount of plastic that is beaching in the estuary and in other parts of the study area.

In the present study, our primary focus was on collecting data at locations close to and in direct contact with the marine environment, i.e. in ports and river estuaries. The sampling locations selected in the 2020-2021 projects are those that are minimally required to have a first quantification of the plastic flux towards the marine environment. In the second order, the current project consortium recommended to enlarge the number of sampling locations, and take samples in the Flemish hinterland. As such, it would be able to quantify the plastic load coming from the hinterland through streams and rivers. In this context, citizen science campaigns (e.g. in cooperation with schools in the scope of their STEM education) could greatly contribute to a more advanced insight in the plastic flux. Protocols on how to take the samples and knowledge about the sampling devices and consumable have been made available (Annex B and C). For

these citizen science projects going down to 100 µm might be too ambitious, but with a focus on plastics > 1 mm could be sufficient to provide insights in the spatial distribution of plastic pollution. Now that we have strong indications that estuaries trap plastic and act as plastic reservoirs, the need to stop plastic pollution at the source is even more prominent.

Conclusion

In this joint 2020-2021 report about the plastic t_0 measurement in the scope of the Flemish Integral Action Plan on Marine Litter, the first insights have been presented. Plastic concentrations covering the Yser estuary, the Scheldt estuary, and four harbors have been quantified. New knowledge about the spatial and temporal variability of the plastic pollution in Flanders is provided. The patterns (concentrations, polymer composition, size frequency distributions, etc) that are presented in this report corroborate often with results and conclusions taken in other European rivers and streams. The data presented in this report (and available on the MDA) have been integrated in the plastic flux model. The Scheldt estuary is considered a major sink for plastics. Most plastic moves up and down following the tidal cycles, and often settles down about 20 km from its point source. Due to the asymmetric tidal regime, plastic particles coming from the marine environment move landwards. Plastic particles have the tendency to accumulate at the edge of the water in intertidal areas. This suggests that beaching is a very important process, and may even be more important than accumulation on the river bed. The protocols developed, the results obtained and simulations made with the hydrodynamic model are transparent and do allow a fair and honest evaluation of the measures taken at policy level to combat the plastic pollution problem at the evaluation moment in 2024-2025.

Chapter 6
Highlights & Perspectives

Key Highlights of the plastic t_0 study 2020-2021

- Transparent **state of the art protocols** have been developed prior to going into the field to ensure high quality data
- Sampling protocols and laboratory procedures align with the most recent methodological development in plastic research
- **346 samples** have been collected from June 2020 to July 2021 to quantify the plastic pollution in Flemish rivers, estuaries and harbors.
- **Twenty locations** have been sampled for plastic, some in tidal cycle measurements, some in bi-monthly spot samples, some in seasonal multiple day campaigns.
- **Expert knowledge and stakeholders opinions** such as harbor authorities and river managers have been consulted to identify suitable and interesting sampling locations.
- Focus was on both **microplastic (100 µm - 5 mm) and macroplastic (> 5mm)** pollution. The integration of both size fractions is unprecedented.
- The presence of microplastics is widespread in the environment. Microplastics have been **detected on all locations** in the study area.
- Microplastic concentrations **vary spatially**, and the highest concentrations have been observed in the river Scheldt.
- On average, the surface water of the **River Scheldt** contains **42.9 particles/m³**, the surface water in **Oostende and Nieuwpoort** contains smaller numbers of plastics items with averages of **8.6 and 6.8 microplastics/m³.**
- Macroplastic concentrations **vary spatially**, and the highest concentrations have been observed in the port of Antwerp and in the Ghent-Terneuzen canal.
- On average, the surface water of the **River Scheldt** contains **14.2 g macroplastic/1000 m³**, the surface water in **Oostende and Nieuwpoort** contains smaller numbers of plastics with averages of **8.8 and 0.6 microplastics/m³**. The **port of Antwerp** and the **Ghent-Terneuzen canal** contain on average **727 g macroplastic/1000 m³**and **841 g macroplastic/1000 m³**, respectively.
- The **sediment** in three locations has average **microplastic concentrations of 2757.7 microplastics kg DW^{-1} in the River Scheldt, 4058.1 microplastics kg DW^{-1} in Oostende and 2824.8 microplastics kg DW^{-1} in Nieuwpoort**.
- Microplastic concentrations in sediment are high, **indicating sediment to be sinks of microplastics.**
- The **variability** between samples taken at the same location, but with a short time interval **can be substantial**.
- Light-weighted polymers such as **polypropylene** are most prominent **in surface waters**, whereas polymers denser than the ambient water**,** such as **PET**, are more prominent **in the sediment. Polystyrene is very common** in both surface waters and sediment.
- **Smaller sized plastics are more abundant than large plastics** based on the size frequency distributions.
- Based on the relatively small number of samples, it is difficult to infer a **tidal influence** from the microplastic concentrations, but it is an important factor to be integrated in the hydrodynamic model.

- An **innovative hydrodynamic model** has been set-up, following the same methodology as used for sediment transport.
- Qualitatively it is observed that most **plastics stay in the estuary**.
- The Scheldt estuary appears to function as a **sink** for plastic
- Accumulation of plastic occurs at locations with high fine-grained sediment (i.e. mud) deposition.
- The quantified total mass-based plastic depositions remains low, but there is no time integration component implemented yet.
- Although small in absolute mass, over time there could be a large number of small plastic being deposited at the sediment or beaching which can potentially lead to adverse ecological effects.

Recommendations

The start of a new monitoring programme in Flanders to detect trends in plastic flux to the sea requires a value at time 0. In that respect, a hydrodynamic based plastic dispersion model has been developed in order to quantify this baseline (t_0 flux). This model provides first valuable insights into the whereabouts of plastic in the aquatic environment. In order to make more accurate predictions in future, and being able to integrate more complex processes influencing the movement of plastic in the aquatic environment, some data gaps and challenges need to be overcome.

- No 'one-fits-all-solution' is possible in terms of sampling and laboratory techniques. The search for a cost-effective method to detect, identify and quantify microplastic should be continued in order to enable less expensive but equally accurate observations of microplastic.
- Estuaries are regarded as reservoirs for plastic, and a net land inwards flux of plastic is to be expected based on the scenario-analysis with the plastic dispersion model. Additional data in the current study area would be beneficial to validate these predictions. Besides, offshore coastal plastic concentration data could further improve the model fit, and confirm the net land inwards plastic flux.
- To quantify the plastic load coming from the hinterland through streams and rivers, the project consortium suggests integrating samples from the hinterland in Flanders. Including citizen science campaigns (e.g. in cooperation with STEM education programmes) could contribute to a more advanced insight in the plastic flux. These data could also validate the model-based finding that plastic rather tends to beach than sink to the sediment.
- An increasing number of plastic removal infrastructures are being deployed in ports and rivers. To date, we have no knowledge about the influence of these infrastructures on the plastic load. Quantification of the number and mass of plastic items removed via these infrastructure, and sharing this information would be valuable and partly representative for the plastic load originating from the Flemish hinterland.
- The plastic dispersion model at this stage does not include the potential influence of waves on the movement of plastic in the aquatic environment. An additional module to the model to enable the integration of potential wave effects would be beneficial. Also adding information about the potential formation of plastic aggregates and biofilm formation would be beneficial. These influencing factors are being considered in the final PLUXIN model.

- The current model can only be run for one settling velocity at a time, which is suboptimal. Inclusion of the settling velocities of diverse plastic particles and different shapes would advance the representativeness of the model for field conditions.
- Storm surges are expected to lead to higher land-inward flux because the asymmetric tides propagate further land inwards with a higher amplitude. Coupling to a North Sea model could further provide insights about the effect of storm surges on the plastic flux.
- There is insufficient detailed information to identify sources of plastics, i.e. tides are moving plastic up- and downstream, but the net flux remains low. Polymer identification can help to identify important sectors, but does not provide sufficient details. Setting up a stakeholder panel can help identifying the right sources of plastic pollution based on their expert knowledge

In this report crucial information is shared to allow a fair and honest evaluation of the current situation and establish a solid knowledge base, allowing policy measures and actions to be formulated in a targeted manner to tackle the plastic litter problem.

References

Besseling, E., Redondo-Hasselerharm, P., Foekema, E.M., Koelmans, A.A., 2019. Quantifying ecological risks of aquatic micro- and nanoplastic. Crit. Rev. Environ. Sci. Technol. 49, 32e80. https://doi.org/10.1080/10643389.2018.1531688

Bi, Q.; Toorman, E.A. (2015). Mixed-sediment transport modelling in Scheldt estuary with a physics based bottom friction law. Ocean Dynamics, 65:555-587.

Breugem, B.A.; Fonias, E.; Wang, L.; Bolle, A.; Kolokythas, G.; De Maerschalck, B. (2019). TEL2TOM: Coupling TELEMAC2D and TOMAWAC on arbitrary meshes, Proc. XXVth TELEMAC-MASCARET User Conference, Toulouse, 15-17 October 2019.

Carbery, M.; O'Connor, W.; Palanisami, T. (2018). Trophic transfer of microplastics and mixed contaminants in the marine food web and implications for human health, Environment International, 115: 400-409.

De Backer, 2017. Action Plan on Marine Litter. DG EnvironmentMarine Environment Service

De Maerschalck, B.; Kolokythas, G.; Breugem, A.; Vanlede, J.; Mostaert, F. (2020). Modelling Belgian Coastal zone and Scheldt mouth area: Subreport 10 – Summary of the 2D TELEMAC morphodynamic model ScaldisCoast: version 2020 developed for the Complex Projects Coastal Vision and Extra Container Capacity Antwerp. Version 5.0. FHR Reports, 15_068_10. Flanders Hydraulics Research: Antwerp.

Devriese, L.I.; Janssen, C.R. (2020). Overzicht van het onderzoekslandschap en de wetenschappelijke informatie inzake (marien) zwerfvuil en microplastics in België. VLIZ Beleidsinformerende Nota's, 2020_001. Vlaams Instituut voor de Zee (VLIZ): Oostende. ISBN 9789492043887. 45 pp.

Dris, R., Imhof, H., Sanchez, W., Gasperi, J., Galgani, F., Tassin, B., Laforsch, C., 2015b. Beyond the ocean: contamination of freshwater ecosystems with (micro-) plastic particles. Environ. Chem. 12 (5), 539–550. https://doi.org/10.1071/EN14172.

Escobar, J.S. (2022). Mud and sand transport under current-and-wave action in coastal areas. PhD thesis, Dept. of Civil Engineering, KU Leuven (in preparation).

Everaert, G., Asselman, J., Bouwens, J., Catarino, A.I., Janssen, C.R., Shettigar, N.A., Teunkens, B., Toorman, E., Van Damme, S., Vercauteren, M., Devriese, L. Plastic baseline (t_0) measurement in the scope Flemish Integral Action Plan on Marine Litter (OVAM). Report 2020. Flanders Marine Institute, Ostend, Belgium. https://www.vliz.be/en/imis?module=ref&refid=338341.

Everaert, G., Cauwenberghe, L. Van, Rijcke, M. De, Koelmans, A.A., Mees, J., Vandegehuchte, M., Janssen, C.R., 2018. Risk assessment of microplastics in the ocean : modelling approach and fi rst conclusions *. Environ. Pollut. 242, 1930e1938. https://doi.org/10.1016/j.envpol.2018.07.069

Fahrenkamp-Uppenbrink, J., 2018. Microplastics everywhere. Science 360 (44), 17e46. https://doi.org/10.1126/science.360.6384.44-q

Kooi, M., Koelmans, A.A., 2019. Simplifying microplastic via continuous probability distributions for size, shape, and density. Environ. Sci. Technol. Lett. 6, 551e557. https://doi.org/10.1021/acs.estlett.9b00379.

Leslie, H.A., Brandsma, S.H., van Velzen, M.J.M., Vethaak, A.D., 2017. Microplastics en route: field measurements in the Dutch river delta and Amsterdam canals, wastewater treatment plants, North Sea sediments and biota. Environ. Int. 101, 133–142. https://doi.org/10.1016/j.envint.2017.01.018.

Mani, T., Blarer, P., Storck, F.R., Pittroff, M., Wernicke, T., Burkhardt-Holm, P., 2019. Repeated detection of polystyrene microbeads in the lower Rhine River. Environ. Pollut. 245, 634–641. https://doi.org/10.1016/j.envpol.2018.11.036

Mani, T., Hauk, A., Walter, U., Burkhardt-Holm, P., 2015. Microplastics profile along the Rhine River. Sci. Rep. 5, 17988. https://doi.org/10.1038/srep17988. Nelms, S.E; Galloway, T.S.; Godley, B.J.; Jarvis, D.S.; Lindeque, P.K. (2018). Investigating microplastic trophic transfer in marine top predators, Environmental Pollution, 238: 999-1007.

OVAM, 2017. Vlaams Integraal Actieplan Marien Zwerfvuil Regeerakkoord van de Vlaamse Regering 2019-2024. Vlaamse Regering: Brussel. 303 pp.

Scherer, C. et al. Comparative assessment of microplastics in water and sediment of a large European river. Sci. Total. Environ. 738, 139866 (2020).

Toorman, E.A.; Shettigar N.A.; Escobar, J.S. (2021). Numerical simulation of plastic fluxes within the Scheldt Estuary and the Belgian Coastal Zone. Interim report HYD/PLUXIN/21.01, Hydraulics & Geotechnics Section, Dept. of Civil Engineering, KU Leuven (in preparation).

van Emmerik, T., Mellink, Y., Hauk, R., Waldschläger, K., Schreyers, L., 2022. Rivers as Plastic Reservoirs. Front. Water, https://doi.org/10.3389/frwa.2021.786936.

Van Quickenborne, V. (2020). Exposé d'orientation politique Mer du Nord = Beleidsverklaringen Noordzee. DOC 55 1610/005. Chambre des Représentants de Belgique = Belgische Kamer van volksvertegenwoordigers: Brussel. 11 pp

Vanlede, J. (2022). Mud dynamics in the Belgian coastal zone and siltation in the harbor of Zeebrugge. PhD thesis, TU Delft.

Vereecke, E.E. (2019). Simulation of shallow overland flow with a physics-based bottom friction law for rain-induced soil erosion modelling. MSc thesis, Dept. of Civil Engineering, KU Leuven, 122 pp.

Station list

Table 9 Overview of the geographical positions of all sampling locations

#	Station	Location	Coordinates
1	(A) Harbour mouth	Port of Ostend	51.23507, 2.92326
2	(B) Tijdok / Zeewezendok (VLIZ)	Port of Ostend	51.23185, 2.92918
3	(C) RYCO (yacht club)	Port of Ostend	51.22376, 2.94068
4	(A) Harbour mouth	Port of Nieuwpoort (river Yser)	51.15031, 2.72755
5	(B) Portus Novus (yacht club)	Port of Nieuwpoort (river Yser)	51.14347, 2.74517
6	(C) Ganzepoot	Port of Nieuwpoort (river Yser)	51.13499, 2.75576
7	Doel	River Scheldt	51.31778, 4.27622
8	Antwerp (Galgenweel)	River Scheldt	51.20886, 4.37783
9	Wintam	River Scheldt	51.1263, 4.31411
10	Temse	River Scheldt	51.12069, 4.22426
11	Schelde Rijn Kanaal (Noordlandbrug)	Port of Antwerp	51.36797, 4.301
12	Kanaaldok (Lillobrug)	Port of Antwerp	51.30817, 4.32289
13	Doeldok	Port of Antwerp	51.29008, 4.23676
14	Vijfde Havendok (Noordkasteelbrug)	Port of Antwerp	51.24631, 4.38489

15	Grootdok	North Sea Port (canal Ghent-Terneuzen)	51.07693, 3.7371
16	Ringvaart	North Sea Port (canal Ghent-Terneuzen)	51.10199, 3.73163
17	Sifferdok	North Sea Port (canal Ghent-Terneuzen)	51.09161, 3.75365
18	Mercatordok	North Sea Port (canal Ghent-Terneuzen)	51.11184, 3.759
19	Kluizendok	North Sea Port (canal Ghent-Terneuzen)	51.16147, 3.76628
20	Zelzate Insteekdok	North Sea Port (canal Ghent-Terneuzen)	51.18964, 3.80486

Data management and archiving

All environmental samples that are to be taken receive a predefined code during the planning phase of the sampling cruises. This predefined code is 'activated' from the moment of collecting the sample in the field. This code is used to temporarily store the samples, is used to report the results of the samples, and is archived together with the metadata of the cruise in the Marine Data Archive (MDA). As such, one sample is traceable from the beginning until the end of the activities in the scope of this project, and can even be traced back in case that is needed for use by third parties. All information on samples is carefully noted and acquired photos are stored in the VLIZ-servers, and their names are saved using the sample coding. All final data have been archived in the MDA that is a password-protected archive hosted by the ISCU certified data centre of VLIZ (Fig. 21).

The Marine Data Archive (MDA) will be used as an online repository specifically developed to archive sampling results in a fully documented manner in a dedicated project folder. The MDA enables the project consortium to manage its data files and file versions, and will serve as a back-up system and repository for data publication.

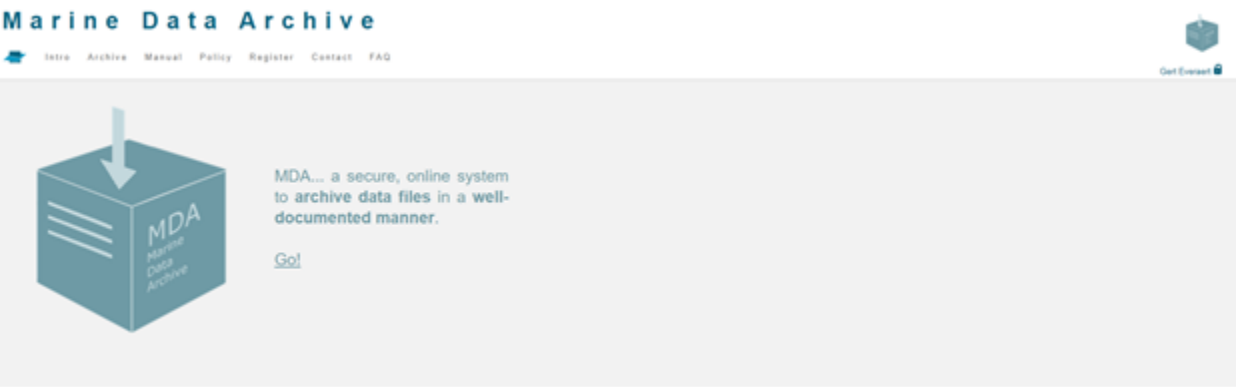

Fig. 40 Interface of the Marine Data Archive (MDA) hosted by VLIZ. This infrastructure is used to archive all the data and protocols used to support this report. Accessible through: http://mda.vliz.be

Annex A: Cruise planning

Table 10 Overview of all plastic sampling campaigns between July 2020 and July 2021

Date (DD/MM/YYYY)	Type campaign	Location
09/07/2020	Tidal cycle measurement	Port of Ostend
10/07/2020	Spotsampling	Port of Ostend
22/09/2020	Spotsampling	Port of Nieuwpoort
23/09/2020	Tidal cycle measurement	Port of Nieuwpoort
24/09/2020	Spotsampling	Port of Ostend
07/10/2020	Spotsampling	Port of Nieuwpoort
14/10/2020 – 16/10/2020	Seasonal	River Scheldt (Doel – Wintam – Antwerp)
17/11/2020	Spotsampling	Port of Ostend
18/11/2020	Spotsampling	Port of Nieuwpoort
19/11/2020	Spotsampling	Port of Antwerp
08/12/2020 – 10/12/2020	Seasonal	River Scheldt (Doel – Wintam – Antwerp)
26/01/2021 – 28/01/2021	Seasonal	River Scheldt (Doel – Wintam – Antwerp)
03/02/2021	Spotsampling	River Scheldt (Temse)

15/02/2021	Spotsampling	Port of Ostend
12/03/2021	Spotsampling	Port of Nieuwpoort
31/03/2021	Tidal cycle measurement	Port of Ostend
20/04/2021 – 22/04/2021	Seasonal	River Scheldt (Doel – Wintam – Antwerp)
27/04/2021	Spotsampling	Port of Ostend
28/04/2021	Spotsampling	Port of Nieuwpoort
17/05/2021	Spotsampling	North Sea Port
18/05/2021	Spotsampling	North Sea Port
15/06/2021	Spotsampling	Port of Antwerp
16/06/2021	Spotsampling	Port of Antwerp
28/06/2021	Spotsampling	Port of Nieuwpoort
29/06/2021	Tidal cycle measurement	Port of Nieuwpoort
30/06/2021	Spotsampling	Port of Ostend

Annex B: Sampling protocols in brief

Sampling protocol for water samples

Microplastics (100 µm - 5 mm)

Principle

The collection of surface water samples is performed using a Mantanet with a mesh size of 100 µm (Fig. B.1). The Manta net is deployed and is towed at the water surface during minimum 5 to maximum 10 minutes. The exact sampling duration depends on the amount of debris that is accumulating in the net end. The manufacturers rate the maximum speed 3 knots (5.6 km/h). Note that in the river Scheldt peak water currents are possible up to 4 knots.

Fig. B.1 Manta net sampling for microplastic in the river Scheldt in the vicinity of Antwerp

Step 1 Preparation in the lab

The sample recipients (i.e. 1 L glass bottles with metal caps) are rinsed threefold with MilliQ water in the lab prior to the sampling campaign, for microplastics decontamination purposes. When dry, the glass bottles are filled with about 500 ml MilliQ water. Next, they are given an extra aluminium foil seal (between bottle and cap) and are closed using their metal caps. The bottles are labelled two-fold (on the cap and the bottle itself) with sticker labels and/or alcohol marker.

Step 2 Prior deployment

The Manta net (including the net ring) is thoroughly rinsed by towing it for 1 minute through the surface seawater, without the net end. A metal bucket and funnel are rinsed with seawater. The net end (100 µm) is rinsed with seawater separately in the pre-rinsed metal bucket. The flowmeter start value and the time are noted and/or photographed after rinsing (right before deployment of the Manta net). Collect an equipment blank to quantify the background seawater microplastic contamination.

Step 3 Deployment

The net end (100 µm) is reattached to the Mantanet, using the net ring. The metal top of the net opening should remain slightly above the water surface during sampling. The flowmeter should be on the bottom of the net opening during sampling.

Step 4 Retrieval

The net end is transferred to a precleaned metal bucket. The net end is turned inside out manually in the metal bucket. The MilliQ water present in the prepared sample recipient (glass bottle) is used to pre-rinse the net end in the metal bucket. The total volume of MilliQ water used needs to remain below 1 L, so the sample can still be collected in the glass bottle (1 L).

Step 5 Transfer

The metal bucket is rinsed with MilliQ water, via the funnel - into the sample recipients. The funnel is rinsed with MilliQ water, into the glass bottle.

Step 6 Preservation and metadata

Preservation of the sample: The samples are preserved in the fridge (4°C) max. 24 hours following the sampling campaign. The start- and end-time (date, hour) of towing the net is noted, alongside the start- and end-values (number of rotations) of the flowmeter. The location/trajectories (coordinates) of the samples are noted. Other data recorded are: weather conditions, passage of -dredging- vessels, visual observations of macroplastics, and sluices in the vicinity (open/closed).

Macroplastic using a suspension sampler and bedload sampler

Principle

The collection of water samples at different depths is performed using a custom-made Suspension sampler with a mesh size of 12 mm (Fig. B.2); and a custom-made Bedload sampler with a mesh size of 6.35 mm (Fig. B.3). Both the suspension sampler and the bed-load sampler are designed to sample water volumes upwards of a 1000m^3.

The suspension sampler

The suspension sampler is deployed using the large crane. This specially designed sampler consists of three frames hanging underneath each other. Each frame has a height of 50 cm and a width of 100 cm. Each of these frames has a 2.4 m long removable net. The upper net samples the water surface; the other

two frames can be set at various depths. The nets are deployed at the beginning of the tide and are left until the tide turns once more. This type of sampler can only be used for static sampling, meaning the RV Simon Stevin is anchored during sampling (or using dynamic positioning). The suspension sampler is equipped with two flowmeters. A mechanical flowmeter is installed in the upper net and an electronic flowmeter is installed underneath the lower net. The latter is required to monitor whether the lower net is positioned at the proper depth.

Fig. B.2. Suspension sampler used to perform observations at different depths in the water column

The bed-load sampler

The bed-load sampler is specially designed to sample macroplastics near the riverbed (moving as bed-load). The opening of the sampler is 70 cm high and 1.40 m wide. The cage is deployed at the beginning of the tide and is left until the tide turns once more. This type of sampler can only be used for static sampling, meaning the RV is anchored during sampling (or using dynamic positioning). Additionally, a mechanical flowmeter is installed in the cage.

Fig. B.3. The bed-load sampler is taken on board of the RV Simon Stevin

After deployment, the samplers are taken out of the water and living biota such fish and shrimp are to be removed. The samples, containing macroplastics and organic matter, are then taken to the campus for further analysis.

Macroplastic (>5 mm) using a Bongonet

The principle and the steps taken are identical to the protocol for microplastics sampling (cfr. microplastics: 100 µm - 5 mm). The only essential differences is that the Bongonet has a mesh size of 500 µm, is rinsed using the deck wash and/or with tap water, and is towed for a duration of minimum 30 minutes to maximum 90 minutes.

Sampling protocol for sediment samples

Microplastics (100 µm - 5 mm) & Macroplastic (> 5 mm)

Principle

The collection of sediment samples is performed with a Van Veen grab (Fig. B.4). Depending on the availability of a crane, one can use a large or small grab sampler.

Fig. B.4 A Van Veen grab is a simple instrument to collect sediment samples

Step 1 Preparation in the lab

The sample recipients (i.e. 800 mL metal containers) for are rinsed threefold with tap water in the lab prior to the sampling campaign, for macroplastics decontamination purposes

Step 2 Prior to deployment

The sieving table is thoroughly rinsed with water using the deck hose on board. A metal bucket needs to be rinsed threefold on beforehand. Collect an equipment blank to quantify the background water macroplastic contamination.

Step 3 Deployment

Repeated deployments can be necessary to obtain a grab filled with sediment. This depends on the surface of the bottom, the water current and the depth at which you aim to take a sample.

Step 4 Retrieval

The Van Veen grab is emptied on the sieving table or in a metal bucket depending on the size of the grab

Step 5 Storage and metadata recording

The collected sediment is transferred by hand (after washing) into the metal containers. The exterior of the container is rinsed to remove excess sediment, before preservation of the sample in the freezer. The depth at which the sample was taken is noted, alongside the type of sediment collected (e.g. sand, sludge, etc.), the time (date, hour and tide) and place (coordinates) of collection.

Annex C: Laboratory procedures and protocols in brief

Macroplastics (> 5 mm) after Bongonet sampling
Macroplastics (> 5 mm) after Bedload and suspension sampling
Identification and quantification of plastics in sediment samples

Macroplastics (> 5 mm)

Identification and quantification of plastics in water samples

Microplastics (100 µm - 5 mm)

All materials used during the laboratory processing were rinsed thoroughly using deionized water and were kept in a dust-free environment. Microplastics were extracted from the water using consecutive digestion, filtration and density separation steps. All extracted microplastics were collected on a polytetrafluoroethylene (PTFE) filter (pore size 10 µm, diameter 25 mm). In case of heavily loaded samples, solutions were sieved and distributed over multiple filters to allow reliable analysis. Filters were analyzed using Fourier-Transform infrared spectroscopy. Collected data was processed using R-Studio. A more detailed description of the extraction protocol can be found in the previous report (2020).

Macroplastics (> 5 mm) after Bongonet sampling

Step 1 Sieving

Sieves used: 5 mm and 1 mm on top of each other.

Pour the contents of the bottle into the 5 mm sieve on top. Rinse the sample through the sieves with tap water.

Step 2 Retrieving + counting

Use tweezers to transfer macroplastics from both sieves into the sample recipients (e.g. petri dishes). Count all macroplastics, including pieces of which you are uncertain that they are plastic.

Step 3 Weighing

Use a balance to weigh each macroplastic piece individually.

Step 4 Measuring size

Use a ruler to measure the longest length of each individual piece of macroplastic.

Step 5 Characterizing

Note the colour, shape (round, square, fiber, etc.) and type (foil, hard plastic, etc.) for each individual piece of macroplastic. Take a picture of each piece of macroplastic, including the label of the sample.

Step 6 Identifying the polymer

Use the µFTIR to determine the polymers type

If needed, use a knife to cutoff a small piece of the macroplastic, to study it with the µFTIR.

Step 7 Provide metadata

The sampled volume of water is calculated, to quantify the concentration of macroplastics in environmental samples.

Macroplastics (> 5 mm) after Bedload and suspension sampling

Step 1 Rinsing and drying

After a quick rinse, samples are stored in a greenhouse and left to dry.

Step 2 Sieving

Dried samples are placed on a sorting table with a 6.35 mm mesh. As the dry organic matter falls apart and through the mesh, only the plastic items stay behind.

Step 3 Separating foils

In the first stage of the analysis, foil-like plastics are separated from the rest.

Step 4 Categorization

Foil-like plastics are then separated based on their size:

2.5 cm – 5.0 cm, 5.0 – 10.0 cm, 10.0 cm – 20.0 cm, 20.0 cm – 30.0 cm, > 30.0 cm.

Other plastics are categorized as a rest fraction.

Step 5 Counting and weighing

All items are counted and weight per category.

Step 6 Identifying the macroplastics

Use the µFTIR to determine the polymers type

If needed, use a scalpel to cutoff a small piece of the macroplastic, to study it with the µFTIR.

Step 7 Provide metadata

The sampled volume of water is calculated, to quantify the concentration of macroplastics in environmental samples. Metadata includes the volume of water which passed through the nets during sampling, to determine a concentration of plastic items per 1000 m^3 of water.

Identification and quantification of plastics in sediment samples

Microplastics (100 µm - 5 mm)

Sediment samples were kept frozen (-20°C) upon analysis. The sample was homogenized thoroughly using a metal spoon. To create 3 replicates, approximately 60 g of wet weight was collected three times and put in a conical centrifuge tube. Sodium Iodide was added, the tubes were shaken well and centrifuged at 3500 rpm for 5 minutes. The supernatants were filtered using a cellulose nitrate filter (pore size 8,0 µm, diameter 47 mm; Whatman, VWR, Leuven, Belgium). This was repeated three times to remove all microplastics present in the sediment. The cellulose nitrate filters were digested using KOH for 24h after which the solution was filtered on a PTFE-filter (pore size 10,0 µm, diameter 25 mm). The PTFE-filters were dried for at least 24h before analysis using Fourier-transformation infrared (FTIR) spectroscopy. Collected data was processed using R-studio.

Macroplastics (> 5 mm)

Step 1 Drying

Dry the sediment sample in the oven at 60°C during 6 days.

Step 2 Weighing

Weigh the container including the dry sediment (= total weight). Weigh the container separately after processing (= container weight). The weight of the dry sediment = Total weight – container weight

Step 3 Sieving

Sieves used: 5 mm and 1 mm on top of each other. Transfer the contents of the container into the 5 mm sieve on top, and rinse the sediment through the sieves with tap water

Step 4 Retrieving + counting

Use tweezers to transfer macroplastics from both sieves into the sample recipients (e.g. glass vials or petri dishes). Count all macroplastics, including pieces of which you are uncertain they are made of plastic.

Step 5 Weighing

Use the balance to measure each macroplastic piece individually.

Step 6 Sizing

Use a ruler to measure the longest length of all pieces of macroplastic in your sample.

Step 7 Characterizing

Note the colour, shape (round, square, fibre, etc.) and type (foil, hard plastic, etc.) for each individual piece of macroplastic. Take a picture of each piece of macroplastic, including the label of the sample.

Step 8 Identifying the macroplastics

Use the µFTIR to determine the polymers type

If needed, use a scalpel to cut off a small piece of the macroplastic, to study it with the µFTIR.

Annex D: Methodology to convert model results to other polymers

Conversion table for different plastics

The model results are obtained for a selected *reference* plastic particle with density 1131 kg/m3 and size of 5 mm (one of the particles investigated in the study of Khatmullina and Isachenko (2017), which has a corresponding settling velocity of 0.127 m/s.

In order to interpret the model results correctly for other non-buoyant (i.e. sinking) particles, taken into account that boundary conditions are defined in terms of mass concentration or mass flux, one has to replace 1 particle of the reference material by another number of particles (*N*) of another size (*d*) in order to guarantee the same setting velocity and the same mass balance.

The procedure is as follows:

- The size *d* for an equivalent particle is obtained by tuning its value to obtain the same settling velocity as for the reference particle, using a new settling velocity formula for spherical particles which corrects the Stokes settling velocity for turbulence boundary layer and wake generation at high-Reynolds numbers (Toorman, 2021).
- The mass of a single particle = polymer density x volume of a spherical particle with the computed diameter *d*.
- The equivalent number of particles to generate the same mass is obtained by dividing the mass of one reference particle by the mass of one equivalent particle.

This procedure yields the following table for the most common polymer with density higher than that of water.

Polymer	Density (kg/m^3)	# particles	Size (mm)
PS	1040	0.5	13.5
reference	1131	1	5.0
PET	1350	8	2.3
PVC	1425	12	2.0

The calculation procedure is available in an Excel sheet, which can be obtained from the KUL Leuven contributors.

Reference:

Toorman, E.A. (2021). Modification of the Dietrich (1982) formula and a new closure for the terminal settling velocity of spherical particles. Internal technical note. Hydraulics & Geotechnics Section, Dept. of Civil Engineering , KU Leuven.